

# 1 **European pollen-based REVEALS land-cover reconstructions for the** 2 **Holocene: methodology, mapping and potentials**

3  
4 Esther Githumbi<sup>1,2</sup>, Ralph Fyfe<sup>3</sup>, Marie-Jose Gaillard<sup>2</sup>, Anna-Kari Trondman<sup>2,4</sup>, Florence Mazier<sup>5</sup>, Anne-  
5 Birgitte Nielsen<sup>6</sup>, Anneli Poska<sup>1,7</sup>, Shinya Sugita<sup>8</sup>, Jessie Woodbridge<sup>3</sup>, Julien Azuara<sup>9</sup>, Angelica  
6 Feurdean<sup>10,11</sup>, Roxana Grindean<sup>11,12</sup>, Vincent Lebreton<sup>9</sup>, Laurent Marquer<sup>13</sup>, Nathalie Nebout-  
7 Combourieu<sup>9</sup>, Miglè Stančikaitė<sup>14</sup>, Ioan Tanțău<sup>11</sup>, Spassimir Tonkov<sup>15</sup>, Lyudmila Shumilovskikh<sup>16</sup>, and  
8 LandClimII data contributors<sup>17+</sup>.

9  
10 <sup>1</sup>Department of Physical Geography and Ecosystem Science, University of Lund, 22362 Lund, Sweden

11 <sup>2</sup>Department of Biology and Environmental Science, Linnaeus University, 39182 Kalmar, Sweden

12 <sup>3</sup>School of Geography, Earth and Environmental Sciences, University of Plymouth, PL4 8AA Plymouth, United Kingdom

13 <sup>4</sup>Division of Education Affairs, Swedish University of Agricultural Science (SLU), 23456 Alnarp, Sweden

14 <sup>5</sup>Environmental Geography Laboratory, GEODE UMR 5602 CNRS, Université de Toulouse Jean Jaurès, 31058 Toulouse,  
15 France

16 <sup>6</sup>Department of Geology, Lund University, 22100 Lund, Sweden

17 <sup>7</sup>Department of Geology, Tallinn University of Technology, 19086 Tallinn, Estonia

18 <sup>8</sup>Institute of Ecology, Tallinn University of Technology, 10120 Tallinn, Estonia

19 <sup>9</sup>Département Homme et Environnement, UMR 7194 Histoire Naturelle de l'Homme Préhistorique, 75013 Paris, France

20 <sup>10</sup>Senckenberg Biodiversity and Climate Research Centre (BiK-F), 60325 Frankfurt am Main, Germany

21 <sup>11</sup>Department of Geology, Faculty of Biology and Geology, Babeş-Bolyai University, 400084 Cluj-Napoca, Romania

22 <sup>12</sup> Institute of Archaeology and History of Arts, Romanian Academy, Cluj-Napoca, 400015, Romania

23 <sup>13</sup>Department of Botany, University of Innsbruck, 6020 Innsbruck, Austria

24 <sup>14</sup>Institute of Geology and Geography, Vilnius University, Vilnius, LT-03101 Vilnius, Lithuania

25 <sup>15</sup>Department of Botany, Sofia University St. Kliment Ohridski, 1164 Sofia, Bulgaria

26 <sup>16</sup>Department of Palynology and Climate Dynamics, Georg-August-University, 37073 Göttingen, Germany

27 <sup>17+</sup>Team list

28 +A full list of authors appears at the end of the paper.

29

30 *Correspondence to:* Esther Githumbi (esther.githumbi@lnu.se)

31 **Abstract.** Quantitative reconstructions of past land-cover are necessary to determine the processes involved in climate-human-  
32 land interactions. We present the first temporally continuous and most spatially extensive pollen-based land-cover  
33 reconstruction for Europe over the Holocene (last 11,700 cal yr BP). We describe how vegetation cover has been quantified  
34 from pollen records at a 1°x1° spatial scale using the ‘Regional Estimates of VEgetation Abundance from Large Sites’  
35 (REVEALS) model. REVEALS calculates estimates of past regional vegetation cover in proportions or percentages.  
36 REVEALS has been applied to 1128 pollen records across Europe and part of the Eastern Mediterranean-Black Sea-Caspian-  
37 Corridor (30°-75°N, 25°W-50°E) to reconstruct the percentage cover of 31 plant taxa assigned to 12 plant functional types  
38 (PFTs) and 3 land-cover types (LCTs). A new synthesis of relative pollen productivities (RPPs) for European plant taxa was  
39 performed for this reconstruction. It includes multiple RPP values ( $\geq 2$  values) for 39 taxa, and single values for 15 taxa (total  
40 of 54 taxa). To illustrate this, we present distribution maps for five taxa (*Calluna vulgaris*, *Cerealia-t*, *Picea abies*, deciduous  
41 *Quercus* t. and evergreen *Quercus* t.) and three land-cover types (open land-OL, evergreen trees-ET and summer-green trees-  
42 ST) for eight selected time windows. The reliability of the REVEALS reconstructions and issues related to the interpretation  
43 of the results in terms of landscape openness and human-induced vegetation change are discussed. This is followed by a review  
44 of the current use of this reconstruction and its future potential utility and development. REVEALS data quality are primarily  
45 determined by pollen count data (pollen count/sample, pollen identification and chronology) and site type/number (lake or  
46 bog, large or small, 1 site vs multiple sites) used for REVEALS analysis (for each grid cell). A large number of sites with high  
47 quality pollen count data will produce more reliable land-cover estimates with lower standard errors compared to a low number  
48 of sites with lower quality pollen count data. The REVEALS data presented here can be downloaded from  
49 <https://doi.pangaea.de/10.1594/PANGAEA.937075>.

50

## 51 **1 Introduction**

52 The reconstruction of past land cover at global, continental and sub-continental scales is essential for the evaluation of climate  
53 models, land-use scenarios and the study of past climate – land cover interactions. Vegetation plays a significant role within  
54 the climate system through biogeochemical and biogeophysical feedbacks and forcings (Foley, 2005; Gaillard et al., 2015,  
55 2010b, 2018; Strandberg et al., 2014). Land use has modified the land cover of Europe over Holocene timescales at local,  
56 regional and continental scales (Roberts et al., 2018; Trondman et al., 2015; Woodbridge et al., 2018). Concerted efforts have  
57 been made to model land-use and land-cover change (LULCC) over Holocene time scales (e.g. HYDE 3.2 (Klein Goldewijk  
58 et al., 2017) and KK10 (Kaplan et al., 2011)). KK10 has been used to assess the impact of the scale of deforestation between  
59 6000 and 200 cal yr BP in Europe on regional climate in the modelling study of Strandberg et al (2014). The KK10-inferred  
60 land-cover change resulted in cooling or warming of regional climate by 1° to 2° depending on the season (winter or summer)  
61 and/or geographical location. Major changes in the forest cover of Europe over the Holocene may therefore have had a  
62 significant impact on past regional climate, particularly those driven by deforestation since the start of agriculture during the  
63 Neolithic period, the timing of which varies in different parts of Europe (Fyfe et al., 2015; Gaillard et al., 2015; Hofman-  
64 Kamińska et al., 2019; Nosova et al., 2018; Pinhasi et al., 2005; de Vareilles et al., 2021). Estimating past land-cover change  
65 can enable quantification of the scale at which human impact on terrestrial ecosystems perturbed the climate system. This in  
66 turn allows us to consider when environmental changes moved beyond the envelope of natural variability (Ruddiman, 2003;  
67 Ruddiman et al., 2016). We focus here on the role of LULCC in the climate system; anthropogenic land-cover change can  
68 have broader consequences for other processes and lead to changes in erosion and fluvial systems (Downs and Piégay, 2019),  
69 biodiversity (Barnosky et al., 2012), nutrient cycling (Guiry et al., 2018; McLauchlan et al., 2013), habitat exploitation by  
70 megafauna (Hofman-Kamińska et al., 2019), and wider ecosystem functioning (Ellis, 2015; Stephens et al., 2019).

71 The Earth System Modelling (ESM) community use LULCC model scenarios, along with dynamic vegetation models, to  
72 understand interactions between different components of the earth system in the past (Gilgen et al., 2019; He et al., 2014;  
73 Hibbard et al., 2010; Smith et al., 2016). Disagreement between LULCC scenarios suggests that their evaluation is needed  
74 using independent, empirical datasets (Gaillard et al., 2010a). Pollen-based reconstruction of past land cover represents  
75 probably the best empirical data for this purpose, as fossil pollen is a direct proxy for past vegetation, and fossil pollen records  
76 are ubiquitous across the continent of Europe (Gaillard et al., 2010a, 2018). The Landscape Reconstruction Algorithm (LRA)  
77 with its two models Regional Estimates of VEgetation Abundance from Large Sites (REVEALS) (Sugita, 2007a) and Local  
78 VEgetation Estimates (LOVE) (Sugita, 2007b) is the only current land-cover reconstruction approach based on pollen data that  
79 effectively reduces the biases caused by the non-linear pollen-vegetation relationship due to differences in sedimentary  
80 archives, basin size, inter-taxonomic differences in pollen productivity and dispersal characteristics, and spatial scales.  
81 REVEALS and LOVE are mechanistic models that transform pollen count data to produce quantitative reconstructions of  
82 regional (spatial scale  $\geq 10^4$  km<sup>2</sup>) and local (spatial scale = relevant source area of pollen *sensu* Sugita (1993),  $\geq$  ca. 1-5 km  
83 radius) vegetation cover, respectively (Sugita, 2007a; 2007b). The REVEALS model was first tested and validated in southern

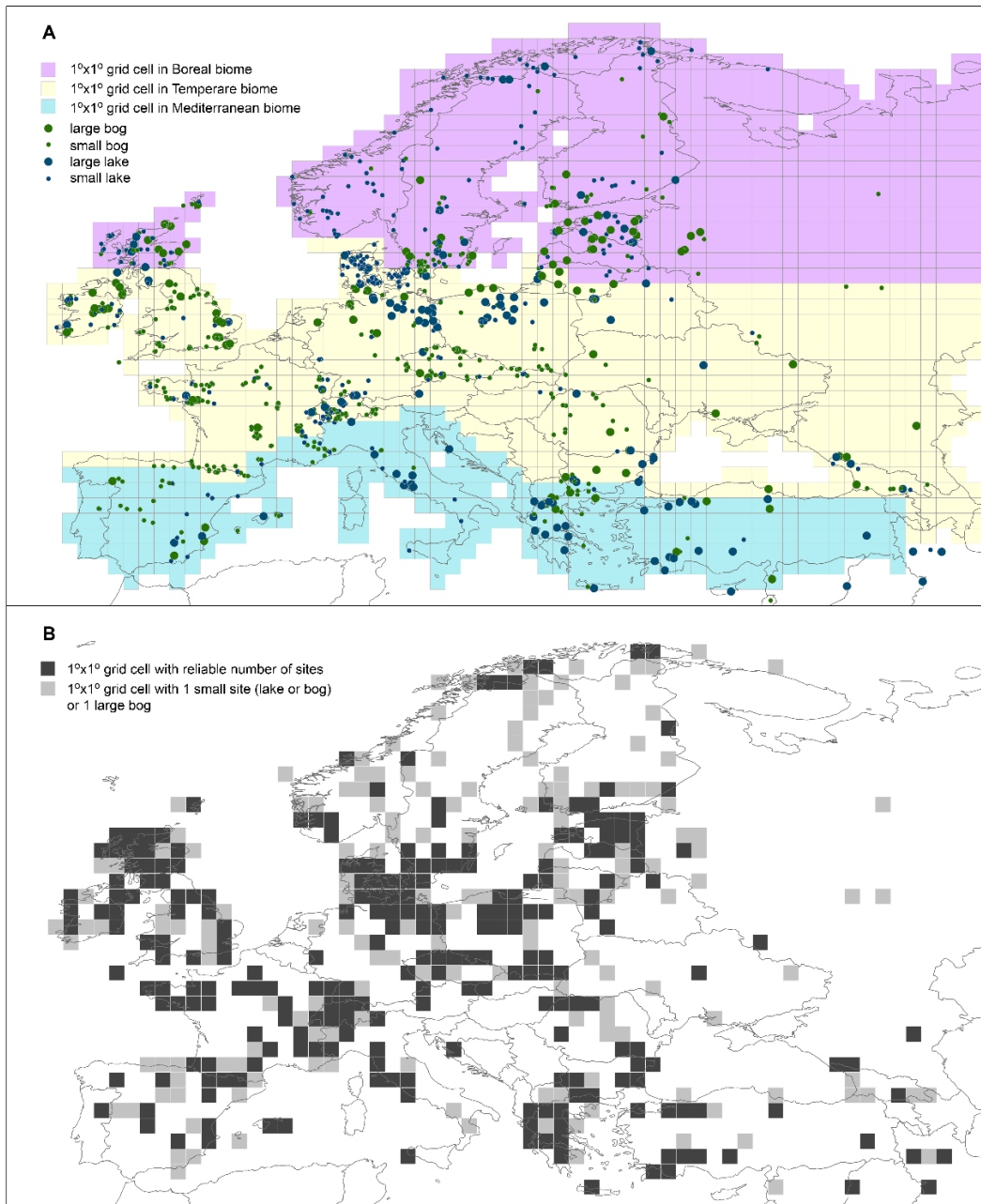
84 Sweden (Hellman et al., 2008a, 2008b) and later in other parts of Europe and the world (Mazier et al., 2012; Soepboer et al.,  
85 2010; Sugita et al., 2010).

86 The first pollen-based REVEALS reconstruction of plant cover over the Holocene covering a large part of Europe (Trondman  
87 et al., 2015) was used for the assessment of LULCC scenarios (Kaplan et al., 2017), and helped to evaluate climate model  
88 simulations using LULCC scenarios (Strandberg et al., 2014). A comparison between REVEALS-based open land cover from  
89 pollen records and Holocene deforestation simulated by HYDE 3.1 and KK10 showed that the REVEALS reconstructions  
90 were more similar to KK10 than HYDE 3.1 scenarios (Kaplan et al., 2017). Therefore, estimates of past plant cover from fossil  
91 pollen assemblages are essential to both test and constrain LULCC models, and also provide alternative inputs to Earth System  
92 Models (ESMs), Regional Climate Models (RCMs) and ecosystem models (Gaillard et al., 2018; Harrison et al., 2020). This  
93 allows improved assessments of biogeophysical and biogeochemical forcings on climate due to LULCC over the Holocene  
94 (Gaillard et al., 2010; Harrison et al., 2020; Ruddiman et al., 2016; Strandberg et al., 2014).

95 Europe is of particular interest as one of the global regions that has experienced major human-induced land-cover  
96 transformations. Europe has large N-S and W-E gradients in modern and historical climate and land use (Marquer et al., 2014,  
97 2017). Early agriculture dates from the start of the Holocene in the SE Mediterranean region (Palmisano et al., 2019; Roberts  
98 et al., 2019; Shennan, 2018), and human impact on vegetation across most of Europe is characterized by early land-cover  
99 changes through agriculture and the use of fire (Feurdean et al., 2020; Marquer et al., 2014; Strandberg et al., 2014; Trondman  
100 et al., 2015). There is therefore a clear need to extend quantitative vegetation reconstruction to the whole of Europe, including  
101 for the first time the Mediterranean region and additional areas of eastern Europe. The increase in the spatial coverage of sites  
102 and temporal scale to the entire Holocene to capture transient vegetation change at sub-millennial time scales is vital to capture  
103 information on the transformation of the biosphere by human actions. Europe has a deep history of pollen data production  
104 (Edwards et al., 2017) and an open-access repository for pollen records (the European Pollen Database (EPD)) as well as  
105 regional pollen repositories (list of databases and access links in section 2.2 and the Data Availability section). These data  
106 repositories result in abundant pollen records that can be used for data-driven reconstructions of past vegetation patterns at  
107 continental scales. Pollen based vegetation reconstructions for Europe have used community-level approaches (Huntley, 1990),  
108 biomization methods (Davis et al., 2015; Prentice et al., 1996), modern analogue techniques (MAT; Zanon et al., 2018), and  
109 pseudobiomization (Fyfe et al., 2010, 2015; Woodbridge et al., 2014). These approaches capture the major trends in vegetation  
110 patterns over the course of the Holocene (Roberts et al., 2018; Sun et al., 2020) and biomization methods have proved useful  
111 for evaluation of climate model results (Prentice and Webb III, 1998). The results of these forms of pollen data manipulation  
112 either classify pollen data into discrete classes (e.g. biomization, pseudobiomization) or are semi-quantitative, capturing  
113 relative change through time based on all pollen taxa within a sample. They cannot achieve reconstructions of the cover of  
114 evergreen versus summer-green trees, for example, or the cover of individual tree and herb taxa. Although useful in  
115 summarising palynological change over time based on entire pollen assemblages, such outputs are of limited use when  
116 differentiation of plant functional types (PFTs) is necessary (Strandberg et al., 2014). Forest cover over the Holocene inferred  
117 from pollen records using these approaches differs from forest cover obtained with REVEALS (Hellman et al., 2008a; Roberts

118 et al., 2018); these differences confirm that REVEALS corrects biases resulting from the non-linearity of the pollen-vegetation  
119 relationship.

120 In this paper we present the results of the second generation of REVEALS-based reconstruction of plant cover over the  
121 Holocene in Europe, after the first reconstruction published by Trondman et al. (2015). This second generation reconstruction  
122 is, to date, the most spatially and temporally complete estimate of plant cover for Europe across the Holocene. As with the  
123 Trondman et al. (2015) reconstruction, this new dataset is specifically designed to be used in climate modelling. It is performed  
124 at a spatial scale of  $1^{\circ} \times 1^{\circ}$  (ca. 100 km  $\times$  100 km) across  $30^{\circ}$ - $75^{\circ}$ N,  $25^{\circ}$ W- $50^{\circ}$ E (Europe and part of the Eastern Mediterranean-  
125 Black Sea-Caspian-Corridor) (Fig. 1). The number of pollen records used (1128), the area covered and time length (entire  
126 Holocene) are a significant advance on the results presented in Trondman et al. (2015), which used 636 pollen records covering  
127 NW Europe (including Poland and the Czech Republic but excluding western Russia and the Mediterranean area), and  
128 produced estimates for five time windows (in cal yr BP, hereafter abbreviated BP): 6200-5700, 4200-3700, 700-350, 350-100  
129 BP and 100 BP to present. Marquer et al. (2014, 2017) produced continuous REVEALS reconstructions over the entire  
130 Holocene, however, only for transects of individual sites (19 pollen records) and groups of grid cells around them.



131

132 **Figure 1: Study region showing site coverage, A.) Colours represent different modern biomes (purple = boreal, yellow = temperate,**  
 133 **blue = Mediterranean) while size and colour of circle represents site type and size (see caption in panel A). B.) Grid cell reliability**  
 134 **dependent on number of pollen records, black grid cells =reliable results, grey grid cells = less reliable results. Reliable =  $\geq 1$  large**  
 135 **lake (s),  $\geq 2$  small lake(s) or/and small bog(s), mix of  $\geq 1$  large lake (s) and  $\geq 1$  small lake(s) or/and small bog(s); less reliable = 1 bog**  
 136 **(large or small) or 1 small lake. See section 4.1 for details and discussion on reliability of REVEALS results.**

137 The  $1^\circ \times 1^\circ$  scale corresponds approximatively to the spatial extent of pollen-based REVEALS reconstructions as evaluated  
 138 by empirical studies in Europe (Hellman et al., 2008b; Soepboer et al., 2010): the REVEALS estimated abundances of plant  
 139 taxa (in percentage cover) correspond most closely to the plant abundances in an area of ca. 100 km x 100 km or larger (see  
 140 Li et al., 2020 for further discussion of the spatial scale of REVEALS reconstructions). This spatial scale is appropriate for  
 141 climate models that typically use spatial scales of  $0.25^\circ$  to  $1^\circ$  (Gaillard et al., 2010a).

## 142 2 Methods

### 143 2.1 REVEALS model and parameters

144 The REVEALS model (Sugita, 2007a) is a generalized version of the R-Value model of Davis (Davis, 1963). The development  
 145 of pollen-vegetation modelling from the R-Value model, via the ERV models of Andersen (Andersen, 1970) and Parsons and  
 146 Prentice (Parsons and Prentice, 1981) through to the REVEALS model is described in detail in numerous earlier papers  
 147 (Broström et al., 2004; Bunting et al., 2013b; Sugita, 1993, 2007a).

148 Using simulations, Sugita (2007a) showed that “large lakes” represent regional vegetation, i.e. between-lake differences in  
 149 pollen assemblages are very small, which was the case for lakes  $\geq 50$ ha in the simulations (Sugita, 2007a). Tests using modern  
 150 pollen data from surface lake sediments have shown that pollen assemblages from lakes  $\geq 50$ ha are appropriate to estimate  
 151 regional plant cover using the REVEALS model (e.g. tests by Hellman et al. (2008a and b) in southern Sweden and by Sugita  
 152 et al. (2010) in northern America).

153 The REVEALS model (equation 1) calculates estimates of regional vegetation abundance in proportions or percentage cover  
 154 using fossil pollen counts from “large lakes” (Sugita, 2007a).

$$155 \hat{V}_i = \frac{n_{i,k} / \hat{\alpha}_i \int_R^{Z^{\max}} g_i(z) dz}{\sum_{j=1}^m \left( \frac{n_{j,k}}{\hat{\alpha}_j \int_R^{Z^{\max}} g_j(z) dz} \right)} = \frac{n_{i,k} / \hat{\alpha}_i K_i}{\sum_{j=1}^m (n_{j,k} / \hat{\alpha}_j K_j)} \quad (1)$$

- 156 •  $\hat{V}_i$  is the estimate of the regional vegetation abundance for taxon  $i$  (proportion or percentage).
- 157 •  $n_{i,k}$  is the pollen count of taxon  $i$  at site  $k$ .
- 158 •  $\hat{\alpha}_i$  is the estimate of pollen productivity (relative pollen productivity, RPP) for taxon  $i$ .
- 159 •  $z$  is the distance between the centre of the sedimentary basin and the pollen source.
- 160 •  $g_i(z)$  is the pollen dispersal/deposition function for taxon  $i$  expressed as a function of distance  $z$ . Fall speed of pollen  
 161 (FSP), wind speed and atmospheric conditions are parameters needed to calculate this function.

- 162 •  $R$  is the radius of the sedimentary basin.
- 163 •  $Z_{\max}$  is the maximum distance within which most pollen originates (i.e. the maximum spatial extent of the regional
- 164 vegetation).
- 165 •  $m$  is the total number of taxa included,
- 166 •  $K_i = \int_R^{Z_{\max}} g_i(z) dz$  is the “pollen dispersal-deposition coefficient” of taxon  $i$  from the border of the study site
- 167 (distance from the pollen sample corresponding to the radius  $R$  of the lake) to  $Z_{\max}$ .

168

169 The assumptions of the REVEALS model are listed in Sugita (2007a). Using simulations Sugita (2007a) demonstrated that, in  
 170 theory, the model can also be applied to pollen records from multiple “small lakes” (< 50 ha), i.e. lakes for which between lake  
 171 differences in pollen assemblages can be large. However, the REVEALS estimates using pollen records from “small lakes”  
 172 generally have larger standard errors (SE) than those based on pollen data from large lakes. The latter was demonstrated for  
 173 empirical pollen records from large lakes versus small sites (lakes and bogs) by Trondman et al. (2016) in southern Sweden  
 174 and Mazier et al. (2012) in the Czech Republic. Although the application of the model to pollen data from bogs violates the  
 175 model assumption that no plants grow on the basin, REVEALS can be applied using models of pollen dispersal and deposition  
 176 for lakes or bogs. The Prentice model (Prentice, 1985; 1988) describes deposition of pollen at a single point in a deposition  
 177 basin and is suitable for pollen records from bogs. Sugita (1993) developed the “Prentice-Sugita model” that describes pollen  
 178 deposition in a lake, i.e. on its entire surface with subsequent mixing in the water body before deposition at the lake bottom.  
 179 The original versions of both models use the Sutton model of pollen dispersal, i.e. a Gaussian plume model from a ground-  
 180 level source under neutral atmospheric conditions (Sutton, 1953). A Lagrangian stochastic model of dispersion has also been  
 181 introduced as an alternative for the description of pollen dispersal in models of the pollen-vegetation relationship in general,  
 182 and in the REVEALS model in particular (Theuerkauf et al., 2012, 2016). It is difficult, in both theory and practice, to eliminate  
 183 the effects of pollen coming from plants growing on sedimentary basins (e.g. Poaceae and Cyperaceae in bogs) on regional  
 184 vegetation reconstruction. Previous studies have assessed the impacts of the violation of this assumption on REVEALS  
 185 outcomes (Mazier et al., 2012; Sugita et al., 2010; Trondman et al., 2016, 2015). An empirical study in southern Sweden  
 186 (Trondman et al., 2016) indicated that REVEALS estimates based on pollen records from multiple small sites (lakes and/or  
 187 bogs) are similar to the REVEALS estimates based on pollen records from large lakes in the same region. The results also  
 188 suggested that increasing the number of pollen records significantly decreased the standard error of the REVEALS estimates,  
 189 as expected based on simulations (Sugita, 2007a). It is therefore appropriate to use pollen records from small bogs to increase  
 190 the number of pollen records included in a REVEALS reconstruction, following the protocol of the first generation REVEALS  
 191 reconstruction for Europe (Mazier et al., 2012; Trondman et al., 2015). However, REVEALS estimates of plant cover using  
 192 pollen assemblages from large bogs only should be interpreted with great caution (Mazier et al., 2012; see also section 4,  
 193 Discussion).



194 The inputs needed to run the REVEALS model are: original pollen counts; relative pollen productivity estimates (RPPs) and  
195 their standard deviation; fall speed of pollen (FSP); basin type (lake or bog); size of basin (radius); maximum extent of regional  
196 vegetation; wind speed (m/s); and atmospheric conditions. FSP can be calculated using measurements of the pollen grains and  
197 Stokes' law (Gregory, 1973). RPPs of major plant taxa can be estimated using datasets of modern pollen assemblages and  
198 related vegetation, and the Extended R-Value model (e.g. Mazier et al., 2008). RPPs exist for a large number of European  
199 plant taxa, and syntheses of FSPs and RPPs were published earlier by Broström et al. (2008) and Mazier et al. (2012). The  
200 latter was used in the “first generation” REVEALS reconstruction (Trondman et al., 2015). A new synthesis of European RPPs  
201 was performed for this “second generation” reconstruction (Appendices A, B, and C). Preparation of data from individual  
202 pollen records, and the values of model parameters used, are described below (sections 2.2 and 2.3).

## 203 **2.2 Pollen records – data compilation and preparation**

204 1143 pollen records from 29 European countries and the Eastern Mediterranean-Black Sea-Caspian-Corridor were obtained  
205 from databases and individual data contributors. The contributing databases include: the European Pollen Database (Fyfe et  
206 al., 2009; Giesecke et al., 2014); the Alpine Palynological database (ALPADABA; Institute of Plant Sciences, University of  
207 Bern; now also archived in EPD); the Czech Quaternary palynological database (PALYCZ; Kuneš et al., 2009); PALEOPYR  
208 (Lerigoleur et al., 2015); and datasets compiled within synthesis projects from the Mediterranean region (Fyfe et al., 2018;  
209 Roberts et al., 2019) and the Eastern Mediterranean-Black Sea-Caspian-Corridor (EMBSecBIO project; Marinova et al., 2018)  
210 (see Fig. 1 for map and Data availability section for data location and team list for individual pollen data contributors). We  
211 followed the protocols and criteria published in Mazier et al. (2012) and Trondman et al. (2015) for selection of pollen records  
212 and application of the REVEALS model. Available pollen records were filtered based on criteria including basin type (to  
213 exclude archaeological sites and marine records) and quality of chronological control (excluding sites with poor age-depth  
214 models or fewer than three radiocarbon dates). This resulted in 1128 pollen records from lakes and bogs, both small and large.  
215 The rationale behind the use of pollen records from small sites is based on the knowledge that REVEALS estimates based on  
216 pollen records from multiple sites provide statistically validated approximations of the regional cover of plant taxa (e.g.  
217 Trondman et al., 2016; see details under section 2.1 on the REVEALS model).

218 The taxonomy and nomenclature of pollen morphological types from the 1128 pollen records were harmonised. The pollen  
219 morphological types were then consistently assigned to one of 31 RPP taxa (Table 1; see section 2.3 and Appendices A-C for  
220 details on the RPP dataset used in this study), following the protocol outlined in Trondman et al. (2015: SI-2 with examples of  
221 harmonization between pollen-morphological types and RPP taxa). This process takes into account plant morphology, biology,  
222 and ecology of the species that are included in each pollen morphological type. Consequently, RPP-harmonized pollen count  
223 data were produced for each of the 1128 pollen records. It should be noted that the EMBSecBIO data does not contain pollen  
224 counts from cultivars, i.e. pollen from cereals and cultivated trees were deleted from the pollen records (Marinova et al., 2018).  
225 Therefore, the cover of agricultural land (represented by cereals in this reconstruction) will always be zero in the Eastern

226 Mediterranean-Black Sea-Caspian-Corridor in grid cells with only pollen records from EMBSecBIO, even though agriculture  
227 did occur in the region from the early Neolithic.

228 For the application of REVEALS, an age-depth model (in cal yr BP) is required for each pollen record. We used the author's  
229 original published model, the model available in the contributing database or, where necessary, a new age-depth model was  
230 constructed following the approach in Trondman et al. (2015). The age-depth model for each pollen record is used to aggregate  
231 RPP-harmonised pollen count data into 25 time windows throughout the Holocene following a standard time division used in  
232 Mazier et al. (2012) and Trondman et al. (2015), which were later adopted by the Past Global Changes (PAGES) LandCover6k  
233 working group (Gaillard et al., 2018). The first three time windows (present–100 BP (where present is the year of coring), 100-  
234 350 BP; 350-700 BP) capture the major human-induced land-cover changes since the Early Middle Ages. Subsequent time  
235 windows are contiguous 500-year long intervals (e.g. 700-1200 BP, 1200-1700 BP, 1700-2200 BP, etc.) with the oldest interval  
236 representing the start of the Holocene (11200-11700 BP). The use of 500-year long time windows is motivated by the necessity  
237 to obtain sufficiently large pollen counts for reliable REVEALS reconstructions. Since the size of the error on the REVEALS  
238 estimate partly depends on the size of the pollen count (Sugita, 2007a), the length of the time window should be a reasonable  
239 compromise to ensure both a useful time resolution of the reconstruction and an acceptable reliability of the REVEALS  
240 estimate of plant cover (Trondman et al., 2015).

241 **Table 1: Land-cover types (LCTs) and Plant Functional Types (PFTs) according to Wolf et al. (2008) and their corresponding pollen**  
 242 **morphological types. Fall speed of pollen (FSP) and the mean relative pollen productivity (RPP) estimates from the new RPP**  
 243 **synthesis (see section 2.3 and Appendices A-C for details) with their standard errors in brackets (see text for more explanations).**  
 244 **\*The FSP values of evergreen *Quercus t.* and Mediterranean Ericaceae according to the original study (Mazier, unpublished) are**  
 245 **0.015 and 0.051, respectively (see Appendix B, Table B.3). The value of 0.035 (FSP of deciduous *Quercus t.*) and 0.038 (FSP of boreal-**  
 246 **temperate Ericaceae) were used instead (see discussion in section 4.2 for explanation). , t = type e.g. evergreen *Quercus t.* RPP used**  
 247 **in this study are relative to grass pollen productivity where Poaceae = 1 (indicated in bold).**

Land-cover types (LCTs)	PFT	PFT definition	Plant taxa/Pollen-morphological types	FSP (m/s)	RPP (SD)
Evergreen trees (ET)	TBE1	Shade-tolerant evergreen trees	<i>Picea abies</i>	0.056	5.437 (0.097)
	TBE2	Shade-tolerant evergreen trees	<i>Abies alba</i>	0.12	6.875 (1.442)
	IBE	Shade-intolerant evergreen trees	<i>Pinus sylvestris</i>	0.031	6.058 (0.237)
	MTBE	Mediterranean shade-tolerant broadleaved evergreen trees	<i>Phillyrea</i>	0.015	0.512 (0.076)
			<i>Pistacia</i>	0.03	0.755 (0.201)
			Evergreen <i>Quercus t.</i>	0.035*	11.043 (0.261)
	TSE	Tall shrub, evergreen	<i>Juniperus communis</i>	0.016	2.07 (0.04)
	MTSE	Mediterranean broadleaved tall shrubs, evergreen	Ericaceae	0.038*	4.265 (0.094)
<i>Buxus sempervirens</i>			0.032	1.89 (0.068)	
Summer green trees (ST)	IBS	Shade-intolerant summer-green trees	<i>Alnus glutinosa</i>	0.021	13.562 (0.293)
			<i>Betula</i>	0.024	5.106 (0.303)
	TBS	Shade-tolerant summer-green trees	<i>Carpinus betulus</i>	0.042	4.52 (0.425)
			<i>Carpinus orientalis</i>	0.042	0.24 (0.07)
			<i>Castanea sativa</i>	0.01	3.258 (0.059)
			<i>Corylus avellana</i>	0.025	1.71 (0.1)
			<i>Fagus sylvatica</i>	0.057	5.863 (0.176)
			<i>Fraxinus</i>	0.022	1.044 (0.048)
			Deciduous <i>Quercus t.</i>	0.035	4.537 (0.086)
			<i>Tilia</i>	0.032	1.21 (0.116)
	<i>Ulmus</i>	0.032	1.27 (0.05)		
TSD	Tall shrub, summer-green	<i>Salix</i>	0.022	1.182 (0.077)	
Open land (OL)	LSE	Low shrub, evergreen	<i>Calluna vulgaris</i>	0.038	1.085 (0.029)
	GL	Grassland - all herbs	<i>Artemisia</i>	0.025	3.937 (0.146)
			Amaranthaceae/Chenopodiaceae	0.019	4.28 (0.27)
			Cyperaceae	0.035	0.962 (0.05)
			<i>Filipendula</i>	0.006	3 (0.285)
			<b>Poaceae</b>	<b>0.035</b>	<b>1 (0)</b>
			<i>Plantago lanceolata</i>	0.029	2.33 (0.201)
			<i>Rumex acetosa-t</i>	0.018	3.02 (0.278)
	AL	Agricultural land - cereals	Cerealia-t	0.06	1.85 (0.380)
			<i>Secale cereale</i>	0.06	3.99 (0.320)

248

## 249 2.3 Model parameter setting

250 For the purpose of this study, a new synthesis of the RPP values available for European plant taxa was performed in 2018-  
251 2019 based on the latest synthesis by Mazier et al. (2012) and additional RPP studies published since then (Appendix A-C).  
252 This synthesis provides new alternative RPP datasets for Europe, including or excluding plant taxa with dominant entomophily,  
253 and with the important addition of plant taxa from the Mediterranean area (Appendix A, Table A1). The selection of RPP  
254 studies, RPP values (shown in Appendix B, Tables B1 and B2) and calculation of mean RPP and their standard error (SD) for  
255 Europe are explained in Appendix C. The location of studies included in the RPP synthesis is shown in Fig. C1 and related  
256 information is provided in Table C1. The synthesis includes a total of 54 taxa for which RPP values are available (Tables B1  
257 and B2), 39 taxa from studies in boreal and temperate Europe, and 15 taxa from studies in Mediterranean Europe of which  
258 seven include exclusively sub-Mediterranean and Mediterranean taxa: *Buxus sempervirens*, *Carpinus orientalis*, *Castanea*  
259 *sativa*, Ericaceae (Mediterranean species), *Phillyrea*, *Pistacia* and evergreen *Quercus* type. RPP values are available from both  
260 boreal/temperate and Mediterranean Europe for seven taxa: i.e. Poaceae (reference taxon), *Acer*, *Corylus avellana*, Apiaceae,  
261 *Artemisia*, *Plantago lanceolata* and Rubiaceae (Table B2). Table A1 presents the new RPP dataset for the 54 plant taxa and,  
262 for comparison, the mean RPP values from Mazier et al. (2012) and from the recent synthesis by Wieczorek & Herzs Schuh  
263 (2020). Moreover, comparison with the RPP values of three studies not used in our synthesis is shown in Table A2. For the  
264 REVEALS reconstructions presented in this paper, we excluded strictly entomophilous taxa, which resulted in a total of 31  
265 taxa (Table 1). The excluded taxa are Compositae (Asteraceae) SF Cichorioideae, *Leucanthemum (Anthemis)-t.*, *Potentilla-t.*,  
266 *Ranunculus acris-t.*, and Rubiaceae. We included entomophilous taxa that are known to be characterised by some anemophily,  
267 e.g. *Artemisia*, Amaranthaceae/Chenopodiaceae, Rubiaceae, and *Plantago lanceolata*. We excluded plant taxa with only one  
268 RPP value except Chenopodiaceae, *Urtica*, *Juniperus*, and *Ulmus*, and the seven exclusively sub-Mediterranean and  
269 Mediterranean taxa mentioned above.

270 The FSP values (Tables 1 and A1) for boreal and temperate plant taxa were obtained from the literature (Broström et al., 2008;  
271 Mazier et al., 2012); these values were in turn extracted from Gregory (1973) for trees, and calculated based on pollen  
272 measurements and Stokes' law for herbs (Broström et al., 2004). FSPs for Mediterranean taxa (*Buxus sempervirens*, *Castanea*  
273 *sativa*, Ericaceae (Mediterranean species), *Phillyrea*, *Pistacia*, and *Quercus* evergreen type) were obtained by using pollen  
274 measurements and Stokes' law (Mazier et al., unpublished); the FSP of *Carpinus betulus* (Mazier et al., 2012) was used for  
275 *Carpinus orientalis* (Grindean et al., 2019).

276 The site radius was obtained from original publications where possible. Sites in the EMBSeCBIO were classified as small  
277 (0.01-1 km<sup>2</sup>), medium (1.1-50 km<sup>2</sup>) or large (50.1-500 km<sup>2</sup>). These were assigned radii of 399m, 2921m and 10000 m,  
278 respectively. Where a site's radius could not be determined from publication, it was geolocated in Google Earth and the area  
279 of the site was measured. A radius value was extracted assuming that a site shape is circular (Mazier et al., 2012). A constant  
280 wind speed of 3 m/s, assumed to correspond approximatively to the modern mean annual wind speed in Europe, was used  
281 following Trondman et al. (2015).  $Z_{\max}$  (maximum extent of the regional vegetation) was set to 100 km.  $Z_{\max}$  and wind speed

282 influence on REVEALS estimates has been evaluated earlier in simulation and empirical studies (Gaillard et al., 2008; Mazier  
283 et al., 2012; Sugita, 2007a), which support the values used for these parameters. Atmospheric conditions are assumed to be  
284 neutral (Sugita, 2007a).

## 285 **2.4 Implementation of REVEALS**

286 REVEALS was implemented using the REVEALS function within the LRA R-package of Abraham et al. (2014) (see Code  
287 availability, section 6). The function enables the use of deposition models for bogs (Prentice's model) and lakes (Sugita's  
288 model), and two dispersal models (a Gaussian plume model, and a Lagrangian stochastic model taken from the DISCOVER  
289 package (Theuerkauf et al., 2016)). Within this study, the Gaussian plume model was applied. The REVEALS model was run  
290 on all pollen records within each  $1^\circ \times 1^\circ$  grid cell across Europe. The REVEALS function is applied to lake and bog sites  
291 separately within each  $1^\circ \times 1^\circ$  grid cell, and combines results (if there is more than one pollen record per cell) to produce a  
292 single mean cover estimate (in proportion) and mean standard error (SE) for each taxon. The formulation of the SE is found  
293 in Appendix A of Sugita (2007a). The REVEALS SE accounts for the standard deviations on the relative pollen productivities  
294 for the individual pollen taxa (Table 1) and the number of pollen grains counted in the sample (Sugita, 2007a). The uncertainties  
295 of the averaged REVEALS estimates of plant taxa for a grid cell are calculated using the delta method (Stuart and Ord., 1994),  
296 and expressed as the SEs derived from the sum of the within- and between-site variations of the REVEALS results in the grid  
297 cell. The delta method is a mathematical solution to the problem of calculating the mean of individual SEs (see Li et al., 2020,  
298 Appendix C, for formula and further details). Results of the REVEALS function are extracted by time window, producing 25  
299 matrices of mean REVEALS land-cover estimates and 25 matrices of corresponding mean SEs for each of the 31 RPP taxa  
300 and each grid cell. The 31 RPP taxa are also assigned to 12 plant functional types (PFTs) and three land-cover types (LCTs)  
301 (Table 1), and their mean REVEALS estimates calculated. These PFTs follow Trondman et al. (2015), with the addition of  
302 two PFTs for Mediterranean vegetation not reconstructed in earlier studies: Mediterranean shade-tolerant broadleaved  
303 evergreen trees (MTBE) and Mediterranean broadleaved tall shrubs, evergreen (MTSE). The mean SE for LCTs and PFTs  
304 including more than one plant taxon are calculated using the delta method (Stuart and Ord., 1994), as described above.

## 305 **2.5 Mapping of the REVEALS estimates**

306 To illustrate the information that the new REVEALS reconstruction provides, we present and describe (section 3) maps of the  
307 REVEALS estimates (% cover) and their associated SEs for the three LCTs (Fig. 2 to 4) and five taxa for eight selected time  
308 windows: the five taxa are *Cerealia-t* and *Picea abies* (Fig. 5 and 6), *Calluna vulgaris*, deciduous *Quercus* type (t.), and  
309 evergreen *Quercus* t. (Fig. D1-D3). The selection of the five taxa and eight time windows is motivated essentially by notable  
310 changes in the spatial distribution of these taxa through time, with higher resolution for recent times characterised by the largest  
311 and most rapid human-induced changes in vegetation cover. For visualisation purposes, the estimates are mapped in nine %  
312 cover classes. These fractions are the same for the three LCTs (Figures 2-4), and the mapped output can therefore be directly  
313 compared. In contrast, the colour scales used for the five taxa vary between maps depending on the abundance of the PFT/taxon

314 (Fig. 5 and 6, D1-D3). Different taxa thus have different scales and maps cannot be directly compared. We visualise uncertainty  
315 in our data by plotting the SE as a circle inside each grid cell; it is the coefficient of variation (CV, i.e. the standard error  
316 divided by the REVEALS estimate). Circles are scaled to fill the grid cell if the SE is equal or greater than the mean REVEALS  
317 estimate (i.e.  $CV \geq 1$ ). Grid-based REVEALS results that are based on pollen records from just one large bog, or single small  
318 bogs or lakes, provide lower quality results (see section 2.1 on the REVEALS model, and discussion section 4.1). The quality  
319 of REVEALS land-cover estimates by grid cell and time window is provided in Table GC\_quality\_by\_TW (see section 5, Data  
320 availability). The percentage scale ranges we use here are different from those used in the maps of Trondman et al. (2015) and,  
321 therefore, the data visualisation cannot be directly compared.

## 322 **3 Results**

323 The complete REVEALS land cover reconstruction dataset includes mean REVEALS values (in proportions) and their related  
324 mean SE for 31 individual tree and herb taxa, twelve PFTs and three LCTs for each grid cell in 25 consecutive time windows  
325 of the Holocene (11.7 k BP to present). Here, results are illustrated by maps of the three LCTs (Fig. 2-4) and five taxa (Fig. 5-  
326 6, D1-D3). The presented maps are not part of the published dataset archived in the PANGAEA online public database (see  
327 Data availability, section 5), they are examples of how the data can be visually presented and what they can be used for.

### 328 **3.1 Land-cover types**

329 The three land-cover types are evergreen trees (ET), summer-green trees (ST) and open land (OL). ET includes six PFTs which  
330 are composed of nine pollen-morphological types (from here after referred to as taxa). ST includes three PFTs which are  
331 composed of twelve taxa while OL includes three PFTs that are in turn composed of ten taxa (Table 1).

#### 332 **3.1.1 Open Land (OL)**

333 At the start of the Holocene, open land (OL) (Fig. 2) has higher cover in western Europe where it generally exceeds 80%  
334 compared with central Europe where it is more typically ~60%. There is a general decline in OL cover through the early  
335 Holocene. At 5700-6200 BP most grid cells in central Europe have the lowest OL cover values between 10-50%. In western  
336 Europe, whilst OL is generally reduced, several grid cells on the Atlantic fringe of northern Scotland persistently maintain 80-  
337 90% OL cover. OL increases from the mid-Holocene, and by 2700-3200 BP the United Kingdom, France, Germany and the  
338 Mediterranean region have grid cells recording OL values >70%. In central, northern and eastern Europe grid cells OL values  
339 vary between 10 - 70% at 2700-3200 BP. Time windows from the last two millennia show a consistent increase in OL with  
340 values >60% across most of central, southern and western Europe and 20-70% in northern Europe.



342 **Figure 1. Grid-based REVEALS estimates of Open Land (OL) cover for eight Holocene time windows. Percentage cover of open**  
343 **land in 10% intervals represented by increasingly darker shades of green from 20%. Grey cells: cells without pollen data for the**  
344 **time window, but with pollen data in other time windows. Circles in grid cells represent the coefficient of variation (CV; the standard**  
345 **error divided by the REVEALS estimate). When  $SE \geq$  REVEALS estimate, the circle fills the entire grid cell and the REVEALS**  
346 **estimate is not different from zero. This occurs mainly where REVEALS estimates are low.**

### 347 **3.1.2 Evergreen Trees (ET)**

348 The cover of evergreen trees (ET) (Fig. 3) at 9700-10200 BP is <30% across Europe, and by 7700-8200 BP fewer than 30 grid  
349 cells show ET >50%. ET cover slowly increases through the early Holocene and at 5700-6200 BP groups of grid cells in  
350 southern Europe record >80%, while in northern Europe ET cover ranges between 10% and 60%. There is a consistent increase  
351 in ET cover over Europe during the mid- and late-Holocene with ET cover peaking at 2700-3200 BP before starting to decline.  
352 Across western parts of Europe, including the United Kingdom, western France, Denmark, and the Netherlands ET never  
353 exceeds 20% cover.



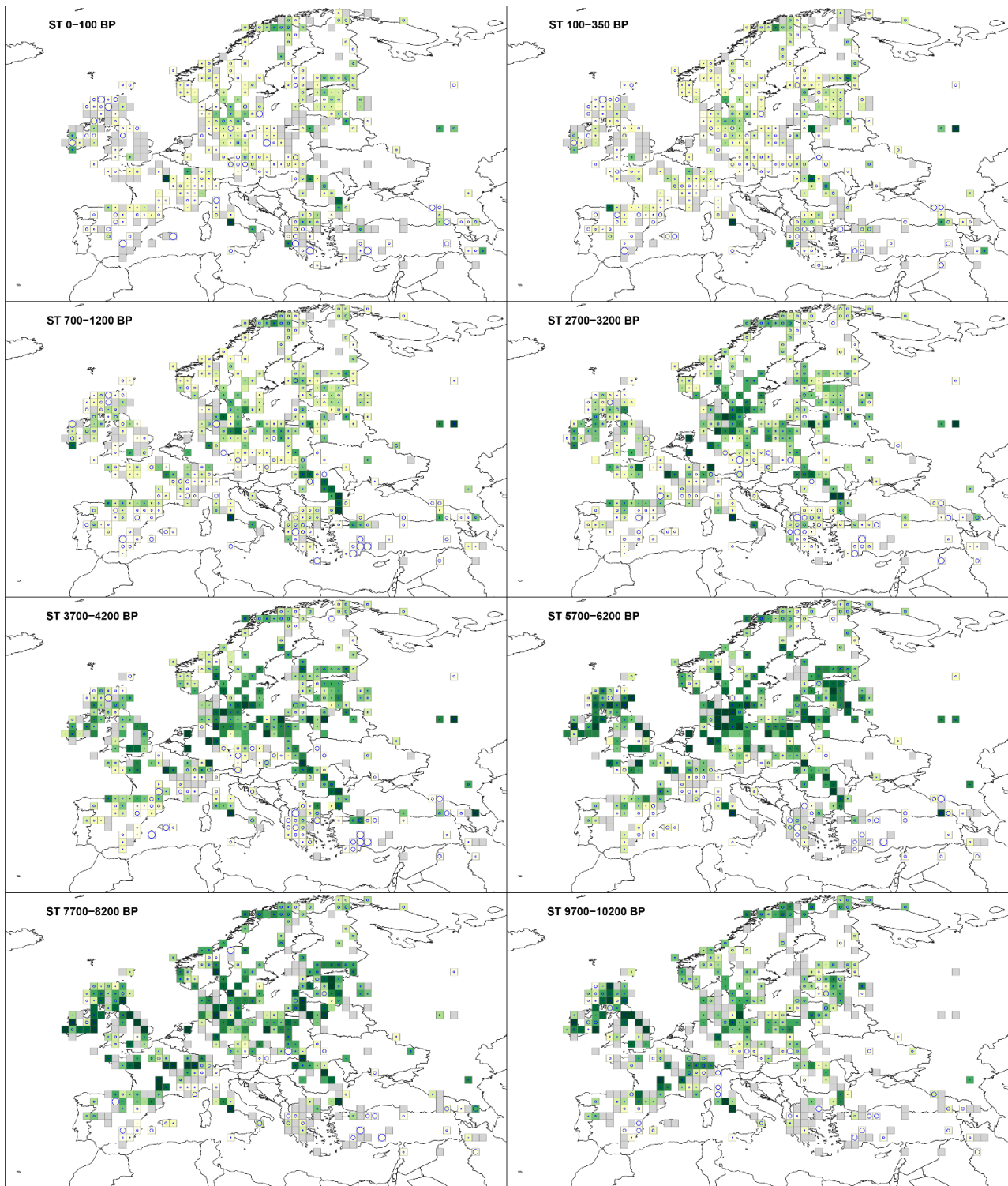


no data 0 10 20 30 40 50 60 70 80 90 % estimated regional vegetation cover

355 **Figure 2. Grid-based REVEALS estimates of Evergreen Tress (ET) cover for eight Holocene time windows. Percentage cover of**  
356 **Evergreen Trees in 10% intervals represented by increasingly darker shades of green from 20%. Grey cells: cells without pollen**  
357 **data for the time window, but with pollen data in other time windows. Circles in grid cells represent the coefficient of variation (CV;**  
358 **the standard error divided by the REVEALS estimate). When  $SE \geq$  REVEALS estimate, the circle fills the entire grid cell and the**  
359 **REVEALS estimate is not different from zero. This occurs mainly where REVEALS estimates are low.**

### 360 **3.1.3 Summer-green Trees (ST)**

361 The cover of summer-green trees (ST) (Fig. 4) in the early Holocene at 9700-10200 BP is >40% across Europe. A small  
362 number (<10) of grid cells in northern, western, central and southern Europe have cover >60%. This significantly increases  
363 towards 5700-6200 BP, at which time ST cover is >60% in central Europe, and 40-60% in northern Europe. ST cover remains  
364 <20% in southern Europe. From 5700-6200 BP there is a steady decline in ST cover across Europe. At 2700-3200 BP only  
365 central Europe has ST cover >50% while values are <50% for the rest of Europe. There is a consistent decline over the last  
366 two millennia BP. Most of Europe has ST cover <30% in the two last time windows (100-350 BP and 100 BP-present), except  
367 for a group of grid cells in the southern Baltic states and scattered records elsewhere.



no data 0 10 20 30 40 50 60 70 80 90 % estimated regional vegetation cover

369 **Figure 3. Grid-based REVEALS estimates of Summer-green Trees (ST) cover for eight Holocene time windows. Percentage cover**  
370 **of ST in 10% intervals represented by increasingly darker shades of green from 20%. Grey cells: cells without pollen data for the**  
371 **time window, but with pollen data in other time windows. Circles in grid cells represent the coefficient of variation (CV; the standard**  
372 **error divided by the REVEALS estimate). When  $SE \geq$  REVEALS estimate, the circle fills the entire grid cell and the REVEALS**  
373 **estimate is not different from zero. This occurs mainly where REVEALS estimates are low.**

### 374 **3.2 Selected taxa**

375 In terms of PFTs, Cerealia-type (t.) is assigned to agricultural land (AL), *Picea abies* to shade tolerant evergreen trees (TBE1:  
376 *Picea abies* is the only taxon in this PFT), *Calluna vulgaris* to low evergreen shrubs (LSE: *Calluna vulgaris* is the only taxon  
377 in this PFT), deciduous *Quercus* t. to shade tolerant summer-green trees (TBS), and evergreen *Quercus* t. to Mediterranean  
378 shade-tolerant broadleaved evergreen trees (MTBE) (Table 1).

#### 379 **3.2.1 Cerealia-type**

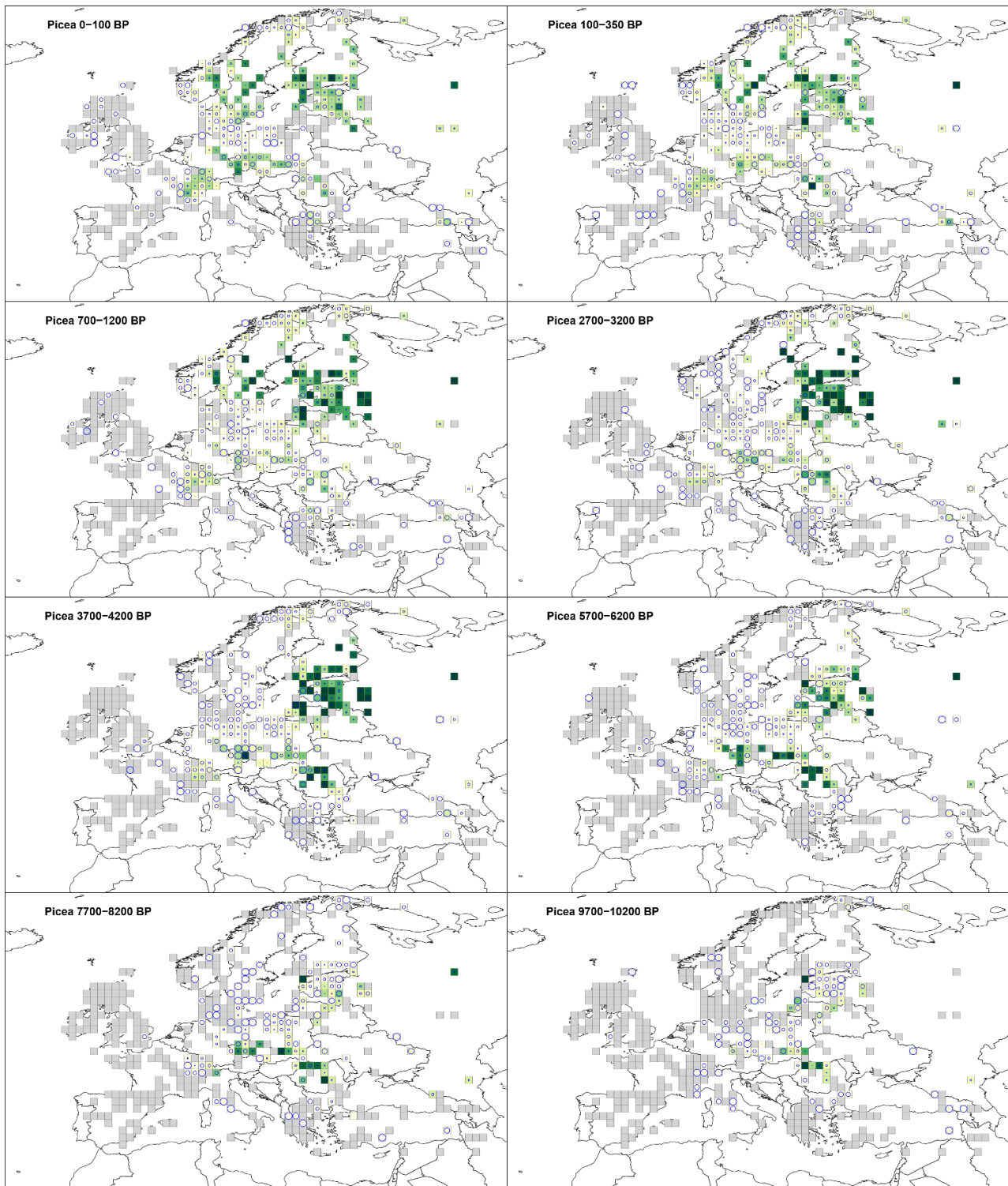
380 Cerealia-t. (Fig. 5) is recorded throughout the Holocene with 10-15% as the maximum cover. Cerealia-t. is present in southern  
381 Europe at 9700-10200 BP with several grid cells recording >5 to 10%. Whilst scattered grid cells in central and western Europe  
382 record the presence of Cerealia-t. at very low levels (0.5-1%), these values have high SE (greater than the REVEALS estimate)  
383 and are therefore not different from zero; they correspond to single findings of Cerealia-t. By 5700-6200 BP, grid cells in  
384 Estonia and France record 3-5% cover, and several regions within central and western Europe record 0-5% (0.5-1%), although  
385 with high SEs. At 2700-3200 BP, Cerealia-t. is recorded across central and western Europe in the United Kingdom, France,  
386 Germany, and Estonia with low values. In Norway, Sweden and Finland it has 0-1% cover with high SEs. The highest cover  
387 (>5%) is observed across Europe from 1200 BP.



389 **Figure 5. Grid-based REVEALS estimates of Cerealia – t. cover for eight Holocene time windows. Percentage cover in 0.5% intervals**  
390 **between 0 and 3%, 1% intervals between 3 and 5, and 5% interval between 5 and 10%. Intervals represented by increasingly darker**  
391 **shades of green from 1-1.5%. Grey cells: cells without pollen data for the time window, but with pollen data in other time windows.**  
392 **Circles in grid cells represent the coefficient of variation (CV; the standard error divided by the REVEALS estimate). When  $SE \geq$**   
393 **REVEALS estimate, the circle fills the entire grid cell and the REVEALS estimate is not different from zero. This occurs mainly**  
394 **where REVEALS estimates are low.**

### 395 **3.2.2 *Picea abies***

396 *Picea abies* cover (Fig. 6) is low (1-2%) at 9700-10200 BP, although a number of grid cells in central and eastern Europe  
397 record values between 30 and 50%. By 7700-8200 BP, grid cells recording 30-50% cover are observed in more regions of  
398 central and eastern Europe than earlier (Russia, Estonia, Romania, Slovakia and Austria). At 5700-6200 BP, almost all of  
399 central Europe has consistent but low cover of *Picea abies*; values are higher towards northeastern Europe (Russia, Estonia,  
400 Latvia, Belarus and Lithuania), up to 30-50%. By 2700-3200 BP the cover of *Picea abies* has increased across central (ca.  
401 10%) and northeastern Europe (>30%). From 1200 BP, *Picea abies* is recorded in northern Europe, particularly in Norway  
402 and Sweden with some grid cells recording 25-50% cover.



404 **Figure 6. Grid-based REVEALS estimates of *Picea* cover for eight Holocene time windows. Percentage cover in 1% interval between**  
405 **0 and 2%, 3% interval between 2 and 5%, 5% intervals between 5 and 30%, and 20% interval between 30 and 50%. Intervals**  
406 **represented by increasingly darker shades of green from 5-10%. Grey cells: cells without pollen data for the time window, but with**  
407 **pollen data in other time windows. Circles in grid cells represent the coefficient of variation (CV; the standard error divided by the**  
408 **REVEALS estimate). When  $SE \geq$  REVEALS estimate, the circle fills the entire grid cell and the REVEALS estimate is not different**  
409 **from zero. This occurs mainly where REVEALS estimates are low.**

### 410 **3.2.3 *Calluna vulgaris***

411 During the Holocene, *Calluna vulgaris* cover (Fig. D1) peaks at 50%, and is largely distributed in a central European belt from  
412 the United Kingdom across to the southern Baltic States. At 9700-10200 BP, it is recorded in only a few grid cells, mostly in  
413 central and western Europe, and at levels <10%. Cover slowly increases and by 7700-8200 BP, there are several grid cells with  
414 cover >25% within the United Kingdom, and with 10-20% cover within Denmark. At 5700-6200 BP, grid cells in coastal  
415 locations in northwestern Europe (particularly France, Germany and Denmark) have 50% *Calluna vulgaris* cover. Cover  
416 steadily increases within the same grid cells and by 2700-3200 BP, cover has increased in northern and eastern Europe e.g.  
417 Norway, Estonia, with values up to 20% cover. The highest cover of *Calluna vulgaris* is recorded in the last two millennia.  
418 Although some grid cells in southeast Europe record low cover values, these have high SE.

### 419 **3.2.4 Deciduous *Quercus* type (t.)**

420 Deciduous *Quercus* t. (Fig. D2) is recorded in central and western Europe at 9700-10200 BP at low levels (<10%), while in  
421 southern Europe (Italy) several grid cells recording >20% cover. By 7700-8200 BP, cover in central and western Europe is  
422 between 1-10% while in northern and eastern Europe grid cells it is <2% with high SEs. During the mid-Holocene (5700-6200  
423 BP) most of Europe, with the exception of some grid cells at the northern and southeast extremes, record deciduous *Quercus*  
424 t. cover values between 2-15%. By 2700-3200 BP, % cover in the same grid cells has decreased to values between 2-10%.  
425 Thereafter, the number of grid cells recording deciduous *Quercus* t. cover remains similar; however, the percentage cover  
426 slowly decreases and at 350-100 BP, the number of grid cells with deciduous *Quercus* t. cover above 5% is very low.

### 427 **3.2.5 Evergreen *Quercus* type (t.)**

428 The spatial distribution of evergreen *Quercus* t. (Fig. D3) remains the same throughout the Holocene. Cover of >30% is  
429 restricted to only a few grid cells and time windows. At the start of the Holocene, evergreen *Quercus* t. is recorded with values  
430 <15% in southern Europe (Spain, Italy, Greece and Turkey) with high SEs. Cover of evergreen *Quercus* t. does not exceed  
431 15% until 6700-7200 BP (not shown), in grid cells located in Turkey, Greece and Italy. From 6700-7200 BP there is an increase  
432 in the number of grid cells recording evergreen *Quercus* t. in southern Europe but most show low cover values (<15%), and  
433 have high SEs.



## 434 4 Discussion

435 The results presented here are the first full-Holocene grid-based REVEALS estimates of land-cover change for Europe  
436 spanning the Mediterranean, temperate and boreal biomes, which highlight the spatial and temporal dynamics of 31 plant taxa,  
437 12 PFTs and 3 LCTs across Europe over the last 11700 years. Previous studies have demonstrated major differences between  
438 REVEALS results and pollen percentages (Marquer et al., 2014; Trondman et al., 2015), and the differences between  
439 REVEALS results and other methods used to transform pollen data, including pseudobiomisation, and MAT (Roberts et al.  
440 2018). It is not the scope of this paper to evaluate the results in that context. This discussion focuses on the reliability and  
441 potential of this “second generation” of REVEALS land cover reconstruction for Europe for use by the wider science  
442 community.

### 443 4.1 Data reliability

444 The REVEALS results are reliant on the quality of the input datasets, namely pollen count data, chronological control for  
445 sequences, and the number and reliability of RPP estimates used (see discussion on RPPs under 4.2). The standard errors (SEs)  
446 can be considered a measure of the precision of the REVEALS results, and of reliability/quality (Trondman et al., 2015).  
447 Where SEs are equal or greater than the REVEALS estimates (represented in the maps of Fig. 2-6 and D1-D3 as a circle that  
448 fills the grid), caution should be applied in the use of the REVEALS estimates, as it implies that they are not different from  
449 zero when taking the SEs into account. Whilst this is possible within an algorithmic approach that includes estimates of  
450 uncertainty, it is conceptually impossible to have negative vegetation cover. If  $SEs \geq \text{mean REVEALS value}$  it is therefore  
451 uncertain whether the plant taxon has cover within the grid cell. Cover may either be very low or the taxon may be absent  
452 within the region (grid cell in this case).

453 The size of pollen counts impacts on the size of REVEALS SEs (Sugita, 2007a); larger counts result in smaller SEs.  
454 Aggregation of samples from pollen records to longer time windows results in larger count sizes and thus lower SEs (see  
455 sections 2.2 above and 4.2 below). Our input dataset includes more than 59 million individual pollen identifications, organised  
456 here into 16711 samples from 1128 sites, where a sample is an aggregated pollen count for RPP taxa for a time window at a  
457 site. Seventy-seven percent of samples have count sizes in excess of 1000 which is deemed most appropriate for REVEALS  
458 reconstructions (Sugita, 2007a). The mean count size across all samples is 3550. Samples with count sizes lower than 1000  
459 are still used, but result in higher SEs. More than half of the pollen records used in the study were sourced from databases (see  
460 section 2.2). Note that the EMBSeCBIO taxonomy has been pre-standardised, and the data compilers have removed *Cerealia-*  
461 *type* (t.). This means that for grid cells within the Eastern Mediterranean-Black Sea-Caspian-Corridor, caution is advised in  
462 the interpretation of *Cerealia-type*. Nevertheless, pollen from ruderals are often related to agriculture, for example, *Artemisia*,  
463 *Amaranthaceae/Chenopodiaceae*, and *Rumex acetosa* type are included in the land-cover type open land (OL); therefore,  
464 changes in OL cover in the Eastern Mediterranean-Black Sea-Caspian-Corridor may be related to changes in agricultural land  
465 (see also discussion below, re agricultural, section 4.3).

466 Aggregation of pollen counts to time windows depends on age-depth models. We have used the best age-depth models  
467 available to us, based on the chronologies presented in Giesecke et al. (2014) for EPD sites, and through liaison with data  
468 contributors. Nevertheless, future REVEALS runs may draw on improvements to age-depth modelling, which may result in  
469 some original pollen count data being assigned to different time windows.

470 The REVEALS results presented here are provided for  $1^\circ \times 1^\circ$  grid cells across Europe. The size and number of suitable pollen  
471 records is an important factor in the quality of the REVEALS estimates for each grid cell. The REVEALS model was developed  
472 for use with “large lakes” ( $\geq 50$  ha; Sugita, 2007a) that represent regional vegetation. Grid cells with multiple large lakes will  
473 thus provide results with the highest level of certainty and reflect the regional vegetation most accurately. These grid cell  
474 results comprised of one or more large lakes, or several small sites (lake or bog) or a mix of large site(s) and small sites, are  
475 considered “high quality” (dark grey grids in figure 1B). It has been shown both theoretically (Sugita, 2007a) and empirically  
476 (Fyfe et al., 2013; Trondman et al., 2016) that pollen records from multiple smaller ( $<50$  ha) lakes will also provide REVEALS  
477 estimates that reflect regional vegetation. However, SEs may be larger if there is high variability in pollen composition between  
478 records. We therefore also consider grid cells with multiple sites “high quality”. Application of REVEALS to pollen records  
479 from large bogs violates assumptions of the model (see section 2.1 above). Therefore, REVEALS estimates for grid cells  
480 including large bogs or single small sites (lake or bog) may not be representative of regional vegetation, particularly in areas  
481 characterised by heterogeneous vegetation. We consider such estimates as “lower quality” (light grey grids in figure 1B),  
482 although they may still provide first-order indications of vegetation cover, and represent an improvement on pollen percentage  
483 data (Marquer et al., 2014). Our results provide REVEALS estimates for a maximum of 420 grid cells per time window. The  
484 number and type of pollen records in a grid cell can change between time windows: not all pollen records cover the entire  
485 Holocene. To assess the reliability of individual results it is important to consider not just the number and type of pollen records  
486 in the total dataset, but how these changes between the time windows. Results for a maximum of 143 grid cells are based on  
487 three or more sites, 65 on two sites, and a minimum of 212 grid cells on a single site. The results of a maximum of 67 grid  
488 cells are based on single small bogs ( $<400$  m radius), 68 on single small lakes ( $<400$  m radius), and 82 on single large bogs.  
489 This implies that about half the grid cells with REVEALS results should be considered as “lower quality” results.

#### 490 **4.2 Role of RPPs and FSP in REVEALS results**

491 A key assumption of the REVEALS model is that RPP values are constant within the region of interest, and through time  
492 (Sugita, 2007a). Nevertheless, it has been suggested that RPPs may vary between regions, with the variation caused by  
493 environmental variability (climate, land use), vegetation structure, or methodological design differences (Broström et al., 2008;  
494 Hellman et al., 2008a; Mazier et al., 2012; Li et al., 2020; Wiczorek and Herzsuh, 2020). Wiczorek and Herzsuh (2020)  
495 have shown that inter-taxon variability in RPP values is generally lower than intra-taxon variability, lending support to  
496 application of the approach we used in the new synthesis of RPPs for Europe (Appendix A-C), i.e. calculation of mean RPPs  
497 using all available RPP values that can be considered as reliable. Nevertheless, some RPP taxa still present a challenge, for  
498 example, Ericaceae, where Mediterranean tree forms have a greater number of inflorescences and hence may have a higher

499 RPP than low-growth form Ericaceae in central and northern Europe. As we have only unique RPP values for Ericaceae in  
500 both boreal-temperate Europe and Mediterranean Europe, and therefore the large difference in RPP between the two biomes  
501 remains to be confirmed with more RPP studies.

502 Currently there is higher confidence in the boreal and temperate RPP values that are based on a wider set of studies increasing  
503 the spread of values and hence reliability of the mean RPP values used (Mazier et al., 2012; Wiczorek and Herschuh, 2020),  
504 whilst RPP values for Mediterranean taxa are based on fewer empirical RPP studies. The new RPP datasets for Europe  
505 produced for this study (Appendix A-C) can be used in different ways. The RPPs provided in Table A1 can be used for the  
506 entire European region, including or excluding entomophilous taxa, and including all values from the Mediterranean area or  
507 only the values for the strictly sub-Mediterranean and/or Mediterranean taxa. If one uses all RPPs from the Mediterranean  
508 area, there will be taxa for which there is both a RPP value obtained in boreal/temperate Europe and a RPP value obtained in  
509 Mediterranean Europe. Application of both RPP values in a single REVEALS reconstruction is not straightforward to achieve,  
510 because the border between the two regions has shifted over the Holocene. In the REVEALS reconstruction presented in this  
511 paper, we chose to use the RPPs from Mediterranean Europe only for the sub-Mediterranean and/or Mediterranean taxa  
512 (including Ericaceae) (Table 1 and A1), and for all other taxa we used the RPPs from boreal/ temperate Europe. The major  
513 issue with this choice is the RPP value of Ericaceae. Using only the large value from Mediterranean Europe may lead to an  
514 under-representation of Ericaceae (*Calluna* excluded), in particular in boreal Europe, but perhaps also in temperate Europe.  
515 Using only the small value from boreal/temperate Europe may lead to an over-representation of Ericaceae in Mediterranean  
516 Europe.

517 Until we have more RPP values for each taxon, it is not possible to disentangle the effect of all factors influencing the  
518 estimation of RPPs and to separate the effect of methodological factors from those of factors such as vegetation type, climate  
519 and land use. The only way to evaluate the reliability of RPP datasets is to test them with modern or historical pollen  
520 assemblages and related plant cover (Hellman et al., 2008a, 2008b). We argue that RPP values of certain taxa may not vary  
521 substantially within some plant families or genera, while they might be variable within others, depending on the characteristics  
522 of flowers and inflorescences that may be either very different or relatively constant within families or genera (see discussion  
523 in Li et al. (2018)). Therefore, we advise to use compilations of RPPs at continental or sub-continental scales rather than  
524 compilations at multi-continental scales as the northern Hemisphere dataset proposed by Wiczorek and Herzschuh (2020).  
525 We consider the RPP selection used within this work as the most suitable for Europe to date, but expect revised and improved  
526 RPP values as more RPP empirical studies are published. Moreover, experimentation in REVEALS applications will allow  
527 future studies to evaluate the effects of using different RPP datasets on land-cover reconstructions (e.g. Mazier et al., 2012).  
528 The role of FSP values in the pollen dispersal and deposition function ( $g_i(z)$  in equation (1) of the REVEALS model, section  
529 2.1) has been discussed by Theuerkauf et al. (2013). In this application of REVEALS we used the Gaussian Plume Model  
530 (GPM) of dispersion and deposition as most existing RPP values have been estimated using this model. The GPM approximates  
531 dispersal as a fast-declining curve with distance from the source plant, which implies short distances of transport for pollen  
532 grain with high FSP compared to other models of dispersion and deposition (Theuerkauf et al., 2012). We have used the FSP

533 values obtained for deciduous *Quercus* type (t.) (0.035 m/s) and boreal-temperate Ericaceae (0.037 m/s) for evergreen *Quercus*  
534 t. and Mediterranean Ericaceae, respectively, although the FSP values of those two taxa were estimated to 0.015 and 0.051 in  
535 the Mediterranean study (Table 1 and A1). Whether using a lower FSP for evergreen *Quercus* t. (0.015 m/s) and a higher FSP  
536 for Mediterranean Ericaceae (0.051 m/s) will have an effect on the REVEALS results is not known and requires further testing.

#### 537 **4.3 Use of the REVEALS land cover reconstructions results**

538 This second generation dataset of pollen-based REVEALS land cover in Europe over the Holocene is currently used in two  
539 major research projects: LandClim, and PAGES LandCover6k. LandClim is a Swedish Research Council project studying the  
540 difference in the biogeophysical effect of land-cover change on climate at 6000, 2500 and 200 BP (Fyfe et al., 2021; Githumbi  
541 et al., 2019; Strandberg et al., 2014; Trondman et al., 2015). PAGES LandCover6k focuses on providing datasets on past land-  
542 cover/land-use for climate modelling studies (Dawson et al., 2018; Gaillard et al., 2018; Harrison et al., 2020). The first  
543 generation REVEALS land-cover reconstruction (Marquer et al., 2014, 2017; Trondman et al., 2015) were used to evaluate  
544 other pollen-based reconstructions of Holocene tree-cover changes in Europe (Roberts et al., 2018) and scenarios of  
545 anthropogenic land-cover changes (ALCCs) (Kaplan et al., 2017) (see also section 1). The Trondman et al. (2015)  
546 reconstructions were used to create continuous spatial datasets of past land cover using spatial statistical modelling  
547 (Pirzamanbein et al., 2014, 2018, 2020).

548 Spatially explicit datasets/maps based on these second generation of REVEALS reconstructions are currently being produced  
549 within PAGES LandCover6k and used to evaluate and revise the HYDE (Klein Goldewijk et al., 2017) and KK10 (Kaplan et  
550 al., 2009) ALCC scenarios. Moreover, LandCover6k archaeology-based reconstructions of past land-use change (Morrison et  
551 al., 2021) will be integrated with the datasets of REVEALS land-cover. Besides the uses listed above, the second generation  
552 of REVEALS reconstruction for Europe offers great potential for use in a large range of studies on past European regional  
553 vegetation dynamics and changes in biodiversity over the Holocene ( Marquer et al., 2014, 2017) and the relationship between  
554 regional plant cover, land use, and climate over millennial and centennial time scales. Since the reconstructions are of regional  
555 plant cover they will have value in archaeological research when impacts are expected at the regional level (e.g. the impact of  
556 early mining (Schauer et al., 2019)). Archaeological questions and research programmes that require information on local  
557 vegetation cover will require the full application of the LRA (REVEALS and LOVE; Sugita, 2007a, b), such as the local  
558 vegetation estimates presented from Norway focussing on cultural landscape development (Mehl et al., 2015). The same  
559 approach of using the REVEALS results within the LOVE model is necessary for ecological questions that require local  
560 vegetation estimates (Cui et al., 2013, 2014; Sugita et al., 2010).

561 Several papers have discussed in depth the issues that need to be taken into account when interpreting REVEALS  
562 reconstructions of past plant cover, in particular Trondman et al. (2015) and Marquer et al. (2017). The interpretation in terms  
563 of human-induced vegetation change is one of the major challenges. The cover of open land (OL) may be used to assess  
564 landscape openness, but is not a precise measure of human disturbance, as OL will include plant taxa characterizing both  
565 naturally-open land and agricultural land that has been created by humans through the course of the Holocene with the

566 domestication of plants and livestock. Natural openness can occur in arctic and alpine areas, in wet regions, in river deltas and  
567 around large lakes, as well as in eastern steppe areas. It is a particular challenge in the Mediterranean region where natural  
568 vegetation openness represents a larger fraction of the land cover than in temperate or boreal Europe (Roberts et al., 2019).  
569 Agricultural Land (AL; Trondman et al., 2015 is the only PFT that includes cultivars; nevertheless, it is restricted to cereal  
570 cropping, and many other cultivated crop types that can be identified through pollen analysis do not yet have RPP values (e.g.  
571 *Linum usitatissimum* (common flax), *Cannabis* (hemp), *Fagopyrum* (buckwheat), beans, etc.). Moreover, the Cerealia-t. pollen  
572 morphological type includes pollen from wild species of Poaceae, especially when identification relies essentially on  
573 measurements of the pollen grain and its pore and does not consider exine structure and sculpture (Beug, 2004; Dickson, 1988).  
574 The maps presented and described in section 3 as an illustration of the results show similar changes in spatial distributions and  
575 quantitative cover of plant taxa and land-cover types through time, between 6000 BP and present, as the results published in  
576 Trondman et al., (2015). The much greater potential of the new REVEALS reconstruction resides in its larger spatial extent,  
577 covering not only boreal and temperate Europe but also southern and eastern Europe, and its contiguous time windows across  
578 the entire Holocene, from 11700 BP to present. The quality of results is also higher in a number of grid cells in comparison to  
579 Trondman et al (2015), where new pollen records have been included, which may in several cases decrease the standard error  
580 on the REVEALS estimates.

## 581 **5. Data availability**

582 All data files reported in this work, which were used for calculations, and figure production are available for public download  
583 at <https://doi.pangaea.de/10.1594/PANGAEA.937075> (Fyfe, Ralph M; Githumbi, Esther; Trondmann, Anna-Kari; Mazier,  
584 Florence; Nielsen, Anne Birgitte; Poska, Anneli; Sugita, Shinya; Woodbridge, Jessie; LandClimII contributors; Gaillard,  
585 Marie-José (2021): A full Holocene record of transient gridded vegetation cover in Europe. PANGAEA,). The data and the  
586 DOI number are subject to future updates and only refer to this version of the paper. The data available in Pangaea includes:  
587 1) REVEALS reconstructions and their associated SE for the 25 time windows; 2) Metadata of the 1128 pollen records used;  
588 3) LandClimII contributors listing the data contributors\collectors\databases. 4) The list of FSP and RPP values used for the  
589 reconstructions and 5) Grid cell quality information (in terms of available pollen data, which influences the result quality:  
590 mean REVEALS estimate of plant cover) for all grid cells. Pollen data were extracted from ALPADABA  
591 (<https://www.neotomadb.org/>), EMBSEC BIO (<https://research.reading.ac.uk/palaeoclimate/embsecbio/>), EPD  
592 (<http://www.europeanpollendatabase.net/index.php>), LandClimI, PALYCZ (<https://botany.natur.cuni.cz/palycz/>) and  
593 PALEOPYR (<http://paleopyr.univ-tlse2.fr/>).

594

## 595 **6. Code availability**

596 REVEALS was implemented using the REVEALS function within the LRA R-package (Abraham et al., 2014), available at  
597 <https://github.com/petrkunes/LRA>.

598 Example code for data preparation and implementation of REVEALS, using two grid cells from SW Britain, is available at  
599 <https://github.com/rmfyfe/landclimII>.

## 600 **7. Conclusions**

601 The application of the REVEALS model to 1128 pollen records distributed across Europe has produced the first full-Holocene  
602 estimates of vegetation cover for 31 plant taxa in  $1^\circ \times 1^\circ$  grid cells. These data are made available for use by the wider science  
603 community, including aggregation of results to PFTs and LCTs. The REVEALS model assumptions are clearly stated to allow  
604 interpretation and assessment of our results and several of the assumptions have been tested and validated. We can therefore  
605 use the land-cover reconstructions to test the role of climate and humans on Holocene plant cover at regional scales. The  
606 overview of land-cover change across Europe over the Holocene can be used to track the timing and rate of vegetation shifts.  
607 We can also determine the effect of human-induced changes in regional vegetation cover on climate, i.e. study land use as a  
608 climate forcing (Gaillard et al., 2010a, 2018; Harrison et al., 2020; Strandberg et al., 2014). Local reconstructions (LOVE) can  
609 be a complementary approach to archaeological surveys as fine-scale human use of the landscape cannot be distinguished  
610 using REVEALS (regional estimates). The LOVE model requires that regional plant cover is known: the REVEALS  
611 reconstructions are therefore needed for this purpose as well, and gridded reconstructions may be a way to perform LOVE  
612 reconstructions, although other strategies can be chosen (Cui et al., 2013; Mazier et al., 2015). Questions aiming to understand  
613 the degree of vegetation openness through the Holocene in Europe, or regarding changes in the relationship between summer-  
614 green and evergreen tree cover through time can now and in the future be answered and validated with fossil pollen data via  
615 the REVEALS approach. We expect that, in the future, improved REVEALS estimates, as more pollen records are  
616 incorporated, and work on RPPs develops.

## 617 Appendices

### 618 Appendix A - New RPP dataset for Europe

#### 619 A.1 New RPP synthesis for Europe

620 The most common method to estimate RPPs involves the application of the Extended R-Value (ERV) model on datasets of  
621 modern pollen assemblages and related vegetation cover. A summary of the ERV model and its assumptions, and an extensive  
622 description of standardised field methods for the purpose of RPP studies are found in Bunting et al. (2013b). Estimation of  
623 RPPs in Europe started with the studies by Sugita et al. (1999) and Broström et al. (2004) in southern Sweden, and Nielsen et  
624 al. (2004) in Denmark. The first tests of the RPP in pollen-based reconstructions of plant cover using the LRA's REVEALS  
625 (Regional Estimates of VEgetation Abundance from Large Sites) model (Sugita, 2007a) were published by Soepboer et al.  
626 (2007) in Switzerland and Hellman et al. (2008a and b) in South Sweden. Over the last 15 years, a large number of RPP studies  
627 have been undertaken in Europe North of the Alps, but it is only recently that RPP studies were initiated in the Mediterranean  
628 area (Grindean et al., 2019; Mazier et al., unpublished). Two earlier syntheses of RPPs in Europe were published by Broström  
629 et al. (2008) and Mazier et al. (2012). From 2012 onwards, these RPP values have been used in numerous applications of the  
630 LRA's two models REVEALS and LOVE (LOcal VEgetation Estimates) (Sugita, 2007a and b) to reconstruct regional and  
631 local plant cover in Europe (Cui et al., 2013; Fyfe et al., 2013; Marquer et al., 2020; Mazier et al., 2015; Nielsen et al., 2012;  
632 Nielsen and Odgaard, 2010; Trondman et al., 2015). Recently, Wiczorek and Herzschuh (2020) published a synthesis of the  
633 RPPs available for the northern Hemisphere; it includes new mean RPP values for Europe that were produced independently  
634 from the synthesis we present here.

635 Table A1 is the result of the new synthesis of RPPs available in Europe that we have performed for the REVEALS  
636 reconstruction presented in the paper. It includes RPPs for 39 plant taxa from studies in boreal and temperate Europe of which  
637 22 (Poaceae included) are herbs or low shrubs, and for 22 plant taxa from studies in the Mediterranean area. The two regions  
638 have RPP values for 7 plant taxa in common. These RPPs are compared to those from two syntheses published earlier, Mazier  
639 et al. (2012) and Wiczorek and Herzschuh (2020). The number of selected RPP values ( $n$ ) for Poaceae is larger than the total  
640 number of RPP ( $tn$ ), i.e.  $n = tn + 1$ . This is due to the fact that the study of Bunting et al. 2005 does not include a value for  
641 Poaceae and the RPP values are related to *Quercus* (Bunting et al., 2005); therefore, RPPs related to Poaceae were calculated  
642 by assuming the RPP value for *Quercus* (related to Poaceae;  $Quercus_{(Poaceae)}$ ) was the same in this study region than the mean  
643 of  $Quercus_{(Poaceae)}$  RPPs from all other available studies.

644 The ranking of RPPs (relative to Poaceae, RPP=1) for 23 tree taxa (M: Mediterranean taxa), from the largest (13.56) to the  
645 smallest (0.240), is as follows (Poaceae included for comparison): *Alnus*> evergreen *Quercus* t.(M)> *Abies alba*> *Pinus*>  
646 *Fagus sylvatica*> *Picea abies*> Ericaceae (M)> *Betula*> deciduous *Quercus* t.> *Carpinus betulus*> *Populus*> *Juniperus*>  
647 *Corylus avellana*> *Castanea sativa*> *Sambucus nigra*-t.> *Ulmus*> *Tilia*> *Salix*> *Fraxinus*> Poaceae (=1)> *Acer*> *Pistacia* (M)>  
648 *Phillyrea* (M)> *Carpinus orientalis* (M). All tree taxa have mean RPPs larger than 1 except *Acer* (0.8), *Pistacia* (0.755),  
649 *Phillyrea* (0.512) and *Carpinus orientalis* (0.240). The ranking of RPPs for 24 herb and low shrub taxa, from the largest (10.52)

650 to the smallest (0.10), is as follows: *Urtica*> Chenopodiaceae> *Secale*> *Artemisia*> Rubiaceae> *Rumex acetosa*-t.>  
651 *Filipendula*> *Plantago lanceolata*> *Trollius*> Ranunculaceae (M)> *Ranunculus acris*-t.> Cerealia-t.> *Potentilla*-t.> *Plantago*  
652 *media*> *Calluna vulgaris*> Poaceae (=1)> Cyperaceae> *Plantago montana*> Fabaceae (M)> Rosaceae (M)> Apiaceae>  
653 Compositae SF. Cichorioideae> *Empetrum*> *Leucanthemum (Anthemis)*-t.. Of the taxa with RPPs larger than 3, only six taxa  
654 are herbs while twelve are trees.

655 The two studies in the Mediterranean area provide single RPP values for 16 taxa, five herb taxa (Poaceae included) and 11 tree  
656 taxa of which six are sub-Mediterranean and/or Mediterranean, and three include both temperate and Mediterranean taxa  
657 (Cupressaceae, Ericaceae, *Fraxinus*) (Table B2). The RPP of herb taxa are significantly different between the study of  
658 Grindean et al. (2019) from the forest-steppe zone and our synthesis, except for *Artemisia* (5.89 and 3, 94, respectively). The  
659 RPP of *Corylus avellana* from the study of Mazier et al. (unpublished) (3.44) is double the mean RPP in our synthesis (1.71),  
660 and the mean RPP of deciduous *Quercus* t. in our synthesis (4.54) is four times larger than the RPP from the study of Grindean  
661 et al. (2019) (1.10).

662 **Table A1: New synthesis of European RPPs: mean RPPs with their SDs in brackets, and mean RPPs from the syntheses by Mazier**  
663 **et al. (2012) (St2 values) and Wieczorek and Herzsuh (2020), for comparison. This synthesis: values in bold are new mean RPPs**  
664 **compared to Mazier et al. (2012). The RPP values from studies in the Mediterranean area are indicated with “M” in the second**  
665 **column. The values in cells emphasized by a thick rectangle are the mean RPPs used in the new REVEALS reconstruction for**  
666 **Europe (this paper), values in bold are new values, values not in bold are the same values as in Mazier et al. (2012). The values of**  
667 **fall speed of pollen (FSP) are from Mazier et al. (2012) except those in italic, i.e. FSPs for Amaranthaceae/Chenopodiaceae, *Urtica***  
668 **and *Sambucus nigra*-t. (Abraham and Kozáková, 2012), and *Populus* (Wieczorek and Herzsuh, 2020) and the new FSPs for**  
669 **Mediterranean taxa. For the three syntheses, the number of selected RPP values (n) included in the calculation of the mean RPP**  
670 **estimate is indicated with the total number of available RPP values (tn) in brackets. The reason why the number of selected RPP**  
671 **values (n) for Poaceae is larger than the total number of RPP (tn) is provided in section A.1. Abbreviations: Comp. Compositae**  
672 **(=Asteraceae), Dec. deciduous, *Filipend Filipendula*, *Pot Potentilla*, SF. Subfamily, t. type, Symbols: \* Separate mean RPP values for**  
673 ***Calluna vulgaris*, *Empetrum*, and Ericaceae (*Calluna* and *Empetrum* excluded) in this synthesis, a single mean RPP values for all**  
674 **Ericales in Wieczorek and Herzsuh (2020), \*\* Separate mean RPP values for Cerealia type (*Secale* excluded) and *Secale* in this**  
675 **synthesis, a single mean RPP for all cereals in Wieczorek and Herzsuh (2020), \*\*\* Separate mean RPP values for Compositae SF**  
676 **Cichorioideae and *Leucanthemum (Anthemis)* type in this synthesis, a single mean RPP for all Asteraceae in Wieczorek and**  
677 **Herzsuh (2020). Note that there are no RPP for Asteraceae (Compositae SF Cichorioideae and *Leucanthemum (Anthemis)* type**  
678 **excluded) in our synthesis, ^ Separate mean RPP values for *Filipendula* and *Potentilla* type in this synthesis, a single mean RPP for**  
679 **all Rosaceae in Wieczorek and Herzsuh (2020); note that there are no RPP for Rosaceae (*Filipendula* and *Potentilla*-t. excluded)**  
680 **in our synthesis; moreover *Filipendula* and *Potentilla*-t. are classified as herbs, while Rosaceae is classified as tree in Wieczorek and**  
681 **Herzsuh (2020), ^^ Separate mean RPP values for *Plantago lanceolata*, *P. media* and *P. montana* in this synthesis, a single mean**  
682 **RPP for all Plantaginaceae in Wieczorek and Herzsuh (2020); note that there are no RPP for Plantaginaceae (*Plantago lanceolata*,**  
683 ***P. media* and *P. montana* excluded) in our synthesis, ^^ Separate mean RPP values for *Ranunculus acris* type and *Trollius* in this**  
684 **synthesis, a single mean RPP for all Ranunculaceae in Wieczorek and Herzsuh (2020); note that there are no RPP for**  
685 **Ranunculaceae (*Ranunculus acris*-t and *Trollius* excluded) in our synthesis.**



Study n (tn), FSP, RPP	This paper, synthesis			Mazier et al. 2012 St 3		Wieczorek & Herzsuh 2020 Europe version 2		
	n (tn)	FSP	RPP (SE)	n (tn)	RPP (SE)	n(tn)	RPP (SE)	Notes
<b>HERB TAXA</b>								
<b>Poaceae (Reference taxon)</b>	16(15)	0.035	<b>1.00 (0.00)</b>	9(8)	1.00 (0.00)	14(12)	1.00 (0.00)	
<b>Herb taxa</b>								
Amaranthaceae/Chenopodiaceae	1(1)	<b>0.019</b>	<b>4.280 (0.270)</b>	none	none	1(1)	<u>4.28 (0.27)</u>	Same value as in this synthesis
Apiaceae	1(1)	0.042	0.260 (0.010)	1(1)	0.26 (0.01)	3(3)	2.13 (0.41)	
Apiaceae	<b>M</b> 1(1)	0.042	5.910 (1.230)					
<i>Artemisia</i>	3(3)	0.025	<b>3.937 (0.146)</b>	1(1)	3.48 (0.20)	2(2)	4.33 (1.59)	
<i>Artemisia</i>	<b>M</b> 1(1)	0.014	5.890 (3.160)					
Comp. <i>Leucanth. (Anthemis)t.</i> ***	1(1)	0.029	0.100 (0.010)	1(1)	0.10 (0.01)			see Asteraceae all***
Comp. SF. Cichorioideae***	3(3)	0.051	0.160 (0.020)	3(3)	0.16 (0.02)	8(10)	0.22 (0.02)	<b>Asteraceae all***</b>
Comp. SF. Cichorioideae	<b>M</b> 1(1)	0.061	1.162 (0.075)					
Comp. (Asteroideae + Cichorioideae)	<b>M</b> 1(1)	0.029	0.160 (0.100)					
<i>Calluna vulgaris</i> *	2(4)	0.038	1.085 (0.029)	2(4)	1.09 (0.03)			see Ericales all*
Cerealia t.**	3(7)	0.060	<b>1.850 (0.380)</b>	2(4)	1.18 (0.04)	4(6)	2.36 (0.42)	<b>Cereals all**</b>
Cerealia t. ( <i>Triticum</i> ., <i>Secale</i> , <i>Zea</i> )	<b>M</b> 1(1)	0.060	0.220 (0.120)					
Cyperaceae	4(6)	0.035	<b>0.962 (0.050)</b>	4(6)	0.83 (0.04)	6(8)	0.56 (0.02)	
<i>Empetrum</i> *	1(2)	0.038	0.110 (0.030)	1(2)	0.11 (0.03)			see Ericales all*
Ericaceae*	1(1)	0.038	0.070 (0.040)	1(1)	0.07 (0.04)	7(9)	0.44 (0.02)	<b>Ericales all*</b>
Fabaceae	<b>M</b> 1(1)	0.021	0.400 (0.070)					
<i>Filipendula</i> ^	3(3)	0.006	<b>3.000 (0.285)</b>	2(3)	2.81 (0.43)	4(6)	0.97 (0.11)	<b>Rosaceae all ^</b>
<i>Plantago lanceolata</i> ^^	4(6)	0.029	<b>2.330 (0.201)</b>	3(4)	1.04 (0.09)	8(10)	2.49 (0.11)	<b>Plantaginaceae all^^</b>
<i>Plantago lanceolata</i>	<b>M</b> 1(1)	0.029	0.580 (0.320)					
<i>Plantago media</i> ^^	1(1)	0.024	1.270 (0.180)	1(1)	1.27 (0.18)			see Plantaginaceae all^^
<i>Plantago montana</i> ^^	1(1)	0.030	0.740 (0.130)	1(1)	0.74 (0.13)			see Plantaginaceae all^^
<i>Potentilla</i> t.^	2(3)	0.018	1.720 (0.200)	2(3)	1.72 (0.20)			see Rosaceae all^
Ranunculaceae	<b>M</b> 1(1)	0.020	2.038 (0.335)					
<i>Ranunculus acrist.</i> ^^^	2(2)	0.014	1.960 (0.360)	2(2)	1.96 (0.36)	3(5)	0.99 (0.12)	<b>Ranunculaceae all^^^</b>

Rosaceae ( <i>Filipend.</i> , <i>Pot. t.</i> , <i>Sanguisorba</i> )	<b>M</b>	1(1)	0.018	0.290 (0.120)		3.71			
Rubiaceae		2(3)	0.019	3.710 (0.340)	2(3)	(0.34)	3(5)	1.56 (012)	
Rubiaceae	<b>M</b>	1(1)	0.019	0.400 (0.070)					
<i>Rumex acetosat.</i>		3(4)	0.018	<b>3.020 (0.278)</b>	3(3)	0.85 (0.05)	3(4)	0.58 (0.03)	
<i>Secale**</i>		3(3)	0.060	<b>3.990 (0.320)</b>	1(1)	3.02 (0.05)			see Cereals all**
<i>Trollius^^^</i>		1(1)	0.013	2.290 (0.360)	1(1)	2.29 (0.36)			see Ranunculaceae all^^^
<i>Urtica</i>		1(1)	<b>0.007</b>	<b>10.520 (0.310)</b>	none	none	1(1)	<u>10.52 (0.31)</u>	Same value as in this synthesis
<b>TREE TAXA</b>									
<i>Abies alba</i>		2(2)	0.120	<b>6.875 (1.442)</b>	2(2)	6.88 (1.44)	2(2)	<u>6.88 (1.44)</u>	Same value as in this synthesis
<i>Acer</i>		2(2)	0.056	0.800 (0.230)	2(2)	0.80 (0.23)	3(3)	0.23 (0.04)	
<i>Acer</i>	<b>M</b>	1(1)	0.056	<b>0.300 (0.090)</b>					
<i>Alnus</i>		5(7)	0.021	<b>13.562 (0.293)</b>	3(3)	9.07 (0.10)	4(6)	8.49 (0.22)	
<i>Betula</i> (mainly <i>B. pubescens</i> , <i>B. pendula</i> )		7(9)	0.024	<b>5.106 (0.303)</b>	6(6)	3.99 (0.17)	6(8)	4.94 (0.44)	
<i>Buxus sempervirens</i>	<b>M</b>	1(1)	<b>0.032</b>	<b>1.890 (0.068)</b>					
<i>Carpinus betulus</i>		2(4)	0.042	<b>4.520 (0.425)</b>	2(2)	3.55 (0.43)	3(5)	3.09 (0.28)	
<i>Carpinus orientalis</i>	<b>M</b>	1(1)	0.042	<b>0.240 (0.070)</b>					
<i>Castanea sativa</i>	<b>M</b>	1(1)	<b>0.010</b>	<b>3.258 (0.059)</b>					
<i>Corylus avellana</i>		4(4)	0.025	<b>1.710 (0.100)</b>	3(3)	1.99 (0.20)	3(4)	1.05 (0.33)	
<i>Corylus avellana</i>	<b>M</b>	1(1)	0.025	<b>3.440 (0.890)</b>					
Cupressaceae ( <i>Juniperus</i> 3 species)	<b>M</b>	1(1)	<b>0.020</b>	<b>1.618 (0.161)</b>					See <i>Juniperus</i>
Ericaceae ( <i>Arbutus unedo</i> , <i>Erica</i> 3 species)	<b>M</b>	1(1)	<b>0.051</b>	<b>4.265 (0.094)</b>					
<i>Fagus sylvatica</i>		3(6)	0.057	<b>5.863 (0.176)</b>	4(4)	3.43 (0.09)	3(3)	2.35 (0.11)	
<i>Fraxinus excelsior</i>		5(6)	0.022	<b>1.044 (0.048)</b>	3(3)	1.03 (0.11)	5(5)	2.97 (0.25)	
<i>Fraxinus</i> ( <i>F. excelsior</i> , <i>F. ornus</i> )	<b>M</b>	1(1)	0.022	<b>2.990 (0.880)</b>					
<i>Juniperus communis</i>		1(2)	0.016	2.070 (0.040)	1(2)	2.07 (0.04)	1(1)	7.94 (1.28)	
<i>Phillyrea</i>	<b>M</b>	1(1)	<b>0.015</b>	<b>0.512 (0.076)</b>					
<i>Pistacia</i>	<b>M</b>	1(1)	<b>0.030</b>	<b>0.755 (0.201)</b>					
<i>Picea abies</i>		4(8)	0.056	<b>5.437 (0.097)</b>	4(6)	2.62 (0.12)	4(6)	1.65 (0.15)	
<i>Pinus</i> (mainly <i>P. sylvestris</i> )		6(9)	0.031	<b>6.058 (0.237)</b>	3(5)	6.38 (0.45)	4(6)	10.86 (0.80)	
<i>Populus</i>		1(1)	<b>0.025</b>	<b>2.660 (1.250)</b>	none	none	1(1)	3.42 (1.60)	

Dec. <i>Quercust.</i> (mainly <i>Q. robur</i> , <i>Q. petraea</i> )		6(8)	0.035	<b>4.537 (0.086)</b>	4(4)	5.83 (0.15)	5(7)	2.42 (0.10)	
Dec. <i>Quercust.</i> (mainly <i>Q. peduncularis</i> )	<b>M</b>	1(1)	<b>0.035</b>	<b>1.100 (0.350)</b>					
Evegreen <i>Quercust.</i> ( <i>Q. ilex</i> , <i>Q. coccifera</i> )	<b>M</b>	1(1)	<b>0.015</b>	<b>11.043 (0.261)</b>					
<i>Salix</i>		5(5)	0.022	<b>1.182 (0.077)</b>	3(4)	1.79 (0.16)	3(4)	0.39 (0.06)	
<i>Sambucus nigra</i> t.		1(1)	<b>0.013</b>	<b>1.300 (0.120)</b>	none	none	1(1)	<u>1.30 (0.12)</u>	Same value as in this synthesis
<i>Tilia</i>		4(5)	0.032	<b>1.210 (0.116)</b>	1(1)	0.80 (0.03)	3(4)	0.93 (0.09)	
<i>Ulmus</i>		1(2)	0.032	1.270 (0.050)	1(1)	1.27 (0.05)	none		

687

## 688 A.2 Comparison of the current synthesis with two previous syntheses (Table A1)

689 Of the 39 plant taxa for which we have a mean RPP in our new synthesis (New), 21 have a new mean RPP value compared to  
690 the earlier synthesis of Mazier et al. (2012) (Maz), 18 taxa have the same mean RPPs in both syntheses. There are three new  
691 taxa for which there were no RPP in Maz, i.e. Amaranthaceae/Chenopodiaceae, *Sambucus nigra*-t. and *Urtica*. The mean RPPs  
692 are comparable between the two syntheses New and Maz, except for *Plantago lanceolata* (2.33 in New/1.04 in Maz), *Alnus*  
693 (13.56/9.07), *Betula* (5.11/3.09), *Carpinus betulus* (4.52/3.55), *Fagus* (5.86/3.43), *Picea* (5.44/2.62) and *Quercus* (4.54/5.83).  
694 *Abies alba* has the same RPP in all three syntheses. Amaranthaceae/Chenopodiaceae, *Sambucus nigra*-t. and *Urtica* have the  
695 same single RPP values in the synthesis of Wieczorek and Herzsuh (2020) (W&H) and New. New and W&H also have  
696 comparable mean RPP values for *Artemisia*, Cereals (Cereals, *Secale* excluded in New, all Cereals in W&H), Compositae (SF  
697 Cichorioideae in N, all Compositae (=Asteraceae) in W&H), Cyperaceae, *Plantago* (*P. lanceolata* in New, all Plantaginaceae  
698 in W&H), *Betula*, *Corylus*, *Populus* and *Tilia*. There are relatively large differences in mean RPPs in W&H and New for 16  
699 plant taxa, although the ranking of the plant taxa in terms of their mean RPPs is almost the same. Mean RPP is larger in W&H  
700 than in New for Apiaceae (2.13/0.26), Ericales (0.44 in W&H) – *Empetrum* (0.11) and Ericaceae (0.07) in New, *Fraxinus*  
701 (2.97/1.04), *Juniperus* (7.94/2.07), *Pinus* (10.86/6.06). Mean RPP is smaller in W&H than in New for *Filipendula* (0.97/3.00),  
702 Rubiaceae (1.56/3.71), *Rumex acetosa* (0.58/2.02), *Acer* (0.23/0.80), *Alnus* (8.49/13.56), *Carpinus* (3.09/4.52), *Fagus*  
703 (2.35/5.86), *Picea* (1.65/5.44), *Quercus* (2.42/4.54) and *Salix* (0.39/1.18).

704 The larger differences between the mean RPPs in New and W&H than between New and Maz have not been examined in  
705 detail. It is due to a slightly different selection of studies, i.e. the study of Theuerkauf et al. (2013) is not included in W &H  
706 and we did not include in New (boreal and temperate Europe, Mediterranean area excluded) the studies of Bunting et al.  
707 (2013a), Kuneš et al. (2019) and Grindean et al. (2019). Another important influencing factor is the selection of RPP values  
708 for calculation of the mean RPP. Although the rules used to select RPP values are very similar between the syntheses, there  
709 are obvious differences between New and W&H that are sometimes very significant (e.g. *Juniperus*).

### 710 A.3 Comparison of the new synthesis with three additional individual studies (Table A2)

711 The RPPs from Twiddle et al. (2012) (Twi) for *Pinus*, *Betula* and *Calluna* are considerably larger than the mean RPPs in our  
712 synthesis (New). This is probably due to the assumption made on the RPP of *Picea* related to Poaceae. The RPP of *Picea*  
713 varies greatly between the selected studies in New, from 0.57 to 8.43 (eight values available). If we assumed that the RPP of  
714 *Picea* related to Poaceae in the study region of Twi was the mean RPP of the five smallest RPPs, i.e. 1.57, the RPP of the three  
715 taxa would be 4.8 for *Pinus*, 3.4 for *Betula*, and 3.3 for *Calluna*, which is more comparable to the mean RPPs in New.

716 Three taxa in Bunting et al. (2013a) (Bun) have a RPP comparable to the mean RPP in New, i.e. for Cyperaceae, *Ranunculus*  
717 *acris*-t., and *Rumex acetosa*-t. (*R. acetosa* in Bun). The other taxa have a RPP in Bun smaller than the mean RPP in New,  
718 except *Plantago maritima* that has a larger RPP (5.8) in Bun than the mean RPP for *P. lanceolata* in New.

719 Of nine taxa, three have a RPP in Kuneš et al. (2019) (Kun) that is comparable to the mean RPP in New, i.e. for *Plantago*  
720 *lanceolata*, *Ranunculus acris*-t. and *Rumex acetosa*-t.. The other six taxa have a RPP larger than the mean RPP in New  
721 (Compositae SF Cichorioideae, Cyperaceae and *Leucanthemum (Anthemis)*-t., or smaller (Amaranthaceae/Chenopodiaceae,  
722 Rubiaceae) to considerably smaller (*Urtica*). Of the 14 tree taxa, only four have a RPP in Kun comparable to the mean RPP in  
723 New, i.e. for *Corylus*, *Fraxinus*, *Salix*, and *Ulmus*. For the other 10 tree taxa, the RPP in K is much smaller than the mean RPP  
724 in N for *Abies alba*, *Alnus*, *Carpinus*, *Fagus*, *Picea*, *Pinus*, smaller for *Quercus*, and larger for *Acer* and *Tilia*.

725 Most of the RPP values of the three studies Twi, Bun and Kun are in the range of the values selected from the studies included  
726 in our synthesis (New) except for *Urtica*, *Abies alba*, *Carpinus*, and *Pinus* in Kun. The Lagrangian Stochastic Model is used  
727 in Kun instead of the Gaussian Plume Model in New, which may be one of the factors behind the lower RPPs in Kun, in  
728 particular (but not only) for taxa with heavy pollen grains.

729

730 Table A2: Comparison of the mean RPPs in this synthesis with the RPP estimates from Britain (Twiddle et al., 2012), Greenland  
731 (Bunting et al., 2013a) and Czech Republic (Kuneš et al., 2019). Explanations for symbols in the taxa list, see caption Table A1. The  
732 values in cells emphasized by a thick rectangle are the mean RPPs used in the new REVEALS reconstruction for Europe (this paper),  
733 values in bold are new values, values not in bold are the same values as in Mazier et al. (2012). Underlined values are values from  
734 the three published studies that are close to the values of the synthesis in this paper. Other symbols: + The original paper does not  
735 provide a RPP for Poaceae and values of standard deviations (SDs) for the RPPs. We extracted the RPP values related to *Picea* from  
736 Table 5 in Twiddle et al. (2012). RPPs related to Poaceae (1.00+) were then calculated by assuming that the RPP of *Picea* was equal  
737 to the mean RPP of *Picea* in Europe (this synthesis) (in bold). ++ The RPPs and their SDs are not listed in the original paper, we  
738 therefore extracted the values from Figure 4 in Bunting et al. (2013a) and the decimals are approximate. +++ Kuneš et al. (2019):  
739 we chose the RPP values that were considered best by the authors, i.e. using the lake dataset (pollen from lake sediment), ERV sub-  
740 model 1 and the Lagrangian Stochastic Model (for details, see Discussion section, this paper). # value for *Plantago maritima* and ##  
741 two values for *Rumex acetosa* and *Rumex acetosella*, respectively (Bunting et al., 2013a), for comparison with *Plantago* spp. and  
742 *Rumex acetosa-t.* (this paper). Underlined RPPs are close to mean RPPs (this synthesis).

743

Study	This paper synthesis RPP (SE)	Twiddle et al. (2012)+ RPP - ERV3 random GPM	Bunting et al. (2013)++ RPP (SE) - ERV1 GPM	Kunes et al (2019)+++ RPP (SE) - R ERV1 LSM
<b>Information on analysis</b>				
<b>HERB TAXA</b>				
<b>Poaceae (Reference taxon)</b>	1.000 (0.000)	1.00+	1.00 (0.00)	1.00 (0.00)
<b>Herb taxa</b>				
Amaranthaceae/Chenopodiaceae	<b>4.280 (0.270)</b>			1.58 (0.74)
<i>Calluna vulgaris</i> *	1.085 (0.029)	11.42		
Comp. <i>Leucanthemum</i> ( <i>Anthemis</i> )t.***	0.10 (0.01)			0.94 (0.43)
Comp. SF. Cichorioideae***	0.160 (0.020)			1.04 (0.64)
Cyperaceae	<b>0.962 (0.050)</b>		0.95 (0.05)	2.10 (0.88)
<i>Plantago lanceolata</i> ^^	<b>2.330 (0.201)</b>		5.8 (0.3)#	2.24 (0.71)
<i>Potentilla</i> t.^	1.720 (0.200)		0.4 (0.03)	
<i>Ranunculus acrist</i> .^^^	1.960 (0.360)		2.0 (0.1)	1.38 (1.13)
Rubiaceae	3.710 (0.340)			1.03 (0.74)
<i>Rumex acetosat</i> .	<b>3.020 (0.278)</b>		3.5 (0.3)/2.0 (0.1)##	1.94 (1.35)
<i>Urtica</i>	<b>10.520 (0.310)</b>			1.16 (0.52)
<b>TREE TAXA</b>				
<i>Abies alba</i>	6.875 (1.442)			1.08 (0.99)
<i>Acer</i>	0.800 (0.230)			1.25 (0.75)
<i>Alnus</i>	<b>13.562 (0.293)</b>			2.44 (0.73)
<i>Betula</i> (mainly <i>B. pubescens</i> , <i>B. pendula</i> )	<b>5.106 (0.303)</b>	13.16	3.75 (0.4)	2.53 (0.91)
<i>Carpinus betulus</i>	<b>4.520 (0.425)</b>			1.36 (0.36)
<i>Corylus avellana</i>	<b>1.710 (0.100)</b>			2.31 (1.13)
<i>Fagus sylvatica</i>	<b>5.863 (0.176)</b>			0.88 (0.25)
<i>Fraxinus excelsior</i>	<b>1.044 (0.048)</b>			0.79 (0.37)
<i>Picea abies</i>	<b>5.437 (0.097)</b>	5.44		2.39 (0.93)
<i>Pinus</i> (mainly <i>P. sylvestris</i> )	<b>6.058 (0.237)</b>	16.32		1.55 (0.44)
Dec. <i>Quercust.</i> (mainly <i>Q. robur</i> , <i>Q. petraea</i> )	<b>4.537 (0.086)</b>			2.08 (0.46)
<i>Salix</i>	<b>1.182 (0.077)</b>		0.7 (0.03)	1.43 (0.62)
<i>Tilia</i>	<b>1.210 (0.116)</b>			2.30 (1.24)
<i>Ulmus</i>	1.270 (0.050)			0.96 (0.77)

## 746 Appendix B - Selection of RPP values and calculation of the mean RPPs and their SDs

### 747 B.1 Methods

748 Tables B1 (Boreal and Temperate Europe) and B2 (Mediterranean Europe) list the RPP values from the 16 selected studies  
749 according to the information on models used provided in Appendix C (Table C1) with further explanations on selection of  
750 RPP studies. We followed similar procedures and rules as Mazier et al. (2012) and Li et al. (2018) to produce a new standard  
751 RPP dataset for Europe. We consider that there are still too few RPP values per taxon to disentangle variability in the RPP  
752 values for a particular taxon due to methodological issues, landscape characteristics, land use, or climate. We therefore use the  
753 mean of selected RPP values for each taxon in the new standard RPP dataset, following Broström et al. (2008) and Mazier et  
754 al. (2012). In boreal and temperate Europe, the number of RPP values per taxon varies between one and nine (*Betula*) (Table  
755 B1), and in Mediterranean Europe, there is only one value per taxon (Table B2). In general, all three sub-models of the ERV  
756 model were used in the RPP studies. We selected the RPP values obtained with the ERV sub-model considered by the authors  
757 to have provided the best results (following the approach of Li et al., 2018). This is usually evaluated from the shape of the  
758 curve of likelihood function scores (LFS), or log likelihood (LL) (Twiddle et al., 2012) and the LFS and LL values themselves.  
759 All RPPs selected for this synthesis are expressed relative to Poaceae (RPP=1). In studies that used another reference taxon  
760 and calculated a RPP for Poaceae, the RPPs were recalculated relative to Poaceae. In studies that did not include a RPP value  
761 for Poaceae, it was assumed that the reference taxon had a RPP related to Poaceae equal to the mean of the RPP values for that  
762 taxon in the other studies (Mazier et al., 2012). For simplicity, we used the value of *Quercus* (5.83) calculated by Mazier et al.  
763 (2012) for the study by Bunting et al. (2005) (*Quercus* as reference taxon, no RPP value for Poaceae). We could also have  
764 used the new mean RPP for *Quercus* (4.54) using our selected RPPs (five values, instead of three in Mazier et al. (2012)). The  
765 latter would not have changed our results significantly; the mean RPP for *Quercus* would have been 4.28 instead of 4.54 (Table  
766 A4). For the study by Baker et al. (2016), we used the RPP values obtained with Poaceae as the reference taxon, given that the  
767 RPPs relative to *Quercus* or *Pinus* were almost identical when ERV submodel 3 was used. The selection of RPP values in  
768 boreal and temperate Europe for the calculation of the mean RPP values of each taxon (values in bold and emphasized by a  
769 thick rectangle in Table B1, (A) and (B)) is based on the following rules:

- 770 1. We excluded the RPP values that were not significantly different from zero considering the lower bound of its SE,  
771 and values that were considered as uncertain by the authors of the original publications (e.g., *Vaccinium* for Finland  
772 (Räsänen et al., 2007), *Pinus* for Central Sweden (von Stedingk et al., 2008)). Moreover, some RPP values were  
773 excluded as they were assumed to be outliers or unreliable based on experts' knowledge on the plants involved, the  
774 pollen-vegetation dataset, and the field characteristics of the related studies. For example, the RPPs for Cyperaceae,  
775 *Potentilla-t* and Rubiaceae obtained in SW Norway (Hjelle, 1998) and those for *Salix* and *Calluna vulgaris* from  
776 Central Sweden (von Stedingk et al., 2008) were assumed to be too low compared to the values obtained in other  
777 study areas (Mazier et al., 2012).

778 2. (i) when five or more RPP estimates of pollen productivity ( $N \geq 5$ ) were available for a pollen type, the largest and the  
779 smallest RPP values (generally outlier values) were excluded, and the mean was calculated using the remaining three  
780 or more RPP estimates; (ii) when  $N=4$ , the most deviating value was excluded, and the mean calculated using the  
781 other three RPP values; (iii) when  $N=3$ , the mean was based on all values available except if one value was strongly  
782 deviating from the other two; and (iv) when  $N=2$ , the mean was based on the two values available; an exception is  
783 *Ulmus* for which we excluded the value from Germany (Theuerkauf et al. 2013) given that several of the RPPs in this  
784 study are considerably higher than most values in the other available studies, i.e. for *Betula* (18.7), *Quercus* (17.85)  
785 and *Tilia* (12.38). The latter values were also excluded from the mean RPP, as well as the unusually high values found  
786 by Baker et al. (2016) for *Betula* (13.94), *Pinus* (23.12) and *Quercus* (18.47). Baker et al. (2016) argue that the high  
787 RPP values might be characteristic of temperate deciduous forests that were little impacted by human activities. More  
788 studies in this type of wooded environments would be needed to confirm this assumption. In the absence of such  
789 studies we consider these values as outliers.

790 The SDs for the mean RPP values were calculated using the delta method (Stuart. and Ord., 1994), a mathematical solution to  
791 the problem of calculating the mean of individual SDs (see Li et al. 2020 for more details).



792 Table B1: Europe (Mediterranean area excluded): RPP estimates and their SDs (in brackets) with the total number of taxa per study  
793 indicated and in brackets the number of taxa with selected RPP estimates. (A) Studies using moss pollsters as pollen samples. (B)  
794 Studies using surface lake sediments as pollen samples. Values in bold emphasized by thick rectangle: selected RPP estimates to be  
795 included in the mean RPP values. Values in bold emphasized by thin rectangle: RPP estimates excluded because of a too large  
796 difference with the other available estimates and their mean (less than half or more than double the mean RPP). Values not  
797 emphasized by a rectangle: RPP estimates excluded due to its extreme high value compared to the other available estimates (much  
798 over double the mean of the other RPPs), i.e. from the study at Bialowice forest (Poland, Baker et al., 2016) for *Betula*, *Pinus* and  
799 *Quercus*, Central Sweden (von Stedingk et al., 2008) for *Pinus*, and Germany\*\*\*\* (Theuerkauf et al., 2013) for *Betula*, *Quercus*,  
800 *Tilia*, and *Ulmus*. Values in italic: RPP estimates excluded because  $SE \geq RPP$ . Abbreviations: t. type, C central, Comp. Compositae  
801 (= Asteraceae), ERV Extended R-Value model, Medit Mediterranean region, Rep Republic, S southern, SF. Subfamily. Symbols: #  
802 RPPs for herbs from Broström et al. (2004); RPPs for trees from Sugita et al. (1999) (reference taxon *Juniperus*), converted to  
803 Poaceae as reference taxon by Broström et al. (2004). ## Bunting et al. (2005), reference taxon *Quercus* and no RPP for Poaceae;  
804 RPPs relative to Poaceae calculated by Mazier et al. (2012) assuming that the RPP of *Quercus* relative to Poaceae is the same as the  
805 mean RPP of *Quercus* from three other studies in NW Europe. \* New RPPs from the Czech Republic (Abraham and Kozáková,  
806 2012). \*\* New RPPs from Poland. Poaceae as reference taxa (see text for more details). \*\*\* New RPPs from Germany (Matthias et  
807 al., 2012), reference taxon *Pinus*. RPPs converted to Poaceae as reference taxon. We selected the RPP estimates obtained with the  
808 dataset of vegetation cover including only the trees that had reached their flowering age (allFIDage) (for more information, see  
809 Matthias et al., 2012). \*\*\*\* New RPPs from Germany (Theuerkauf et al., 2013); in the original publication, the ERV analysis was  
810 performed with the Lagrangian Stochastic Model (LSM) for dispersal of pollen and with *Pinus* as reference taxon. For this synthesis,  
811 Martin Theuerkauf redid the analysis with the Gaussian Plume Model for dispersal of pollen (Parsons and Prentice, 1981; Prentice  
812 and Parsons, 1983) and with Poaceae as reference taxon.

813

Type of pollen sample	Moss polsters							
	Finland	C	S	Norway	England	Swiss	Czech Rep*	Poland*
	ERV 3	Sweden	Sweden#	ERV 1	##	Jura	ERV 1	*
<b>HERB TAXA</b>								
<b>Poaceae (Reference taxon)</b>	1.00 (0.00)	1.00 (0.00)	1.00 (0.00)	1.00 (0.00)	1.00 (0.00)	1.00 (0.00)	1.00 (0.00)	1.00 (0.00)
Amaranthaceae/Chenopodiaceae							<b>4.28 (0.27)</b>	
Apiaceae				<b>0.26 (0.009)</b>				
<i>Artemisia</i>							<b>2.77 (0.39)</b>	
<i>Calluna vulgaris</i>		<b>0.30 (0.03)</b>	<b>4.70 (0.69)</b>	<b>1.07 (0.03)</b>				
Cerealia t.			<b>3.20 (1.14)</b>				0.0462 (0.0018)	
Comp.				<b>0.10 (0.008)</b>				
<i>Leucanthemum(Anthemis) t.</i>			<b>0.24 (0.06)</b>	<b>0.06 (0.004)</b>				
Comp. SF. Cichorioideae								
Cyperaceae	0.002 (0.0022)	<b>0.89 (0.03)</b>	<b>1.00 (0.16)</b>	0.29 (0.01)			<b>0.73 (0.08)</b>	
<i>Empetrum</i>	<b>0.07 (0.06)</b>	<b>0.11 (0.03)</b>						
Ericaceae		<b>0.07 (0.04)</b>						
<i>Filipendula</i>			<b>2.48 (0.82)</b>	<b>3.39 (0.00)</b>				
<i>Plantago lanceolata</i>			12.76 (1.83)	<b>1.99 (0.04)</b>			<b>3.70 (0.77)</b>	
<i>Plantago media</i>							<b>1.27 (0.18)</b>	
<i>Plantago montana</i>							<b>0.74 (0.13)</b>	
<i>Potentillat.</i>			<b>2.47 (0.38)</b>	0.14 (0.005)			<b>0.96 (0.13)</b>	
<i>Ranunculus acrist.</i>			<b>3.85 (0.72)</b>	<b>0.07 (0.004)</b>				
Rubiaceae			<b>3.95 (0.59)</b>	0.42 (0.01)			<b>3.47 (0.35)</b>	
<i>Rumex acetosat.</i>			<b>4.74 (0.83)</b>	0.13 (0.004)				
<i>Secale</i>			<b>3.02 (0.05)</b>					
<i>Trollius</i>							<b>2.29 (0.36)</b>	
<i>Urtica</i>							<b>10.52 (0.31)</b>	
<i>Vaccinium</i>	0.01 (0.01)							

<b>TREE TAXA</b>								
<i>Abies</i>						<b>3.83</b> <b>(0.37)</b>		
<i>Acer</i>			<b>1.27</b> <b>(0.45)</b>			<b>0.32</b> <b>(0.10)</b>		
<i>Alnus</i>			<b>4.20</b> <b>(0.14)</b>		<b>8.74 (0.35)</b>		<b>2.56</b> <b>(0.32)</b>	<b>15.95</b> <b>(0.6622)</b>
<i>Betula</i>	<b>4.6 (0.70)</b>	<b>2.24 (0.20)</b>	<b>8.87</b> <b>(0.13)</b>		6.18 (0.35)			13.94 (0.2293)
<i>Carpinus</i>			<b>2.53</b> <b>(0.07)</b>					<b>4.48 (0.0301)</b>
<i>Corylus</i>			<b>1.40</b> <b>(0.04)</b>		<b>1.51 (0.06)</b>			<b>1.35 (0.0512)</b>
<i>Fagus</i>			<b>6.67</b> <b>(0.17)</b>			1.20 (0.16)		
<i>Fraxinus</i>			<b>0.67</b> <b>(0.03)</b>		<b>0.70 (0.06)</b>		<b>1.11</b> <b>(0.09)</b>	
<i>Juniperus</i>		0.11 (0.45)	<b>2.07</b> <b>(0.04)</b>					
<i>Picea</i>		<b>2.78 (0.21)</b>	<b>1.76</b> <b>(0.00)</b>			<b>8.43</b> <b>(0.30)</b>		
<i>Pinus</i>	<b>8.40</b> <b>(1.34)</b>	21.58 (2.87)	<b>5.66</b> <b>(0.00)</b>				<b>6.17</b> <b>(0.41)</b>	23.12 (0.2388)
Deciduous <i>Quercust.</i>			<b>7.53</b> <b>(0.08)</b>		<b>5.83</b> <b>(0.00)##</b>		<b>1.76</b> <b>(0.20)</b>	18.47 (0.1032)
<i>Salix</i>		<b>0.09 (0.03)</b>	<b>1.27</b> <b>(0.31)</b>		<b>1.05 (0.17)</b>		<b>1.19</b> <b>(0.12)</b>	
<i>Sambucus nigrat.</i>							<b>1.30</b> <b>(0.12)</b>	
<i>Tilia</i>			<b>0.80</b> <b>(0.03)</b>				<b>1.36</b> <b>(0.26)</b>	<b>0.98 (0.0263)</b>
<i>Ulmus</i>			<b>1.27</b> <b>(0.05)</b>					
Total number of taxa 39 (38)	6 (4)	10 (7)	26 (25)	12 (8)	7 (7)	11(10)	13(12)	8 (5)

816

Type of pollen sample Region ERV submodel	lake surface sediment				
	Estonia	Denmark	Swiss Plateau	Germany** *	Germany ****
	ERV 3	ERV 1		ERV 3	
<b>HERB TAXA</b>					
<b>Poaceae (Reference taxon)</b>	1.00 (0.00)	1.00 (0.00)	1.00 (0.00)	1.00 (0.00)	1.00 (0.00)
<i>Artemisia</i>	<b>3.48 (0.20)</b>				<b>5.56 (0.020)</b>
<i>Calluna vulgaris</i>		<b>1.10 (0.05)</b>	0.00076 (0.0019)		
Cerealia t.	<b>1.60 (0.07)</b>	<b>0.75 (0.04)</b>	<b>0.17 (0.03)</b>	9.00 (1.92)	0.08 (0.001)
Compositae <i>Leucanthemum</i> ( <i>Anthemis</i> ) t.			0.24 (0.15)		
Cyperaceae	<b>1.23 (0.09)</b>				
<i>Filipendula</i>	<b>3.13 (0.24)</b>				
<i>Plantago lanceolata</i>		<b>0.90 (0.23)</b>			<b>2.73 (0.043)</b>
<i>Rumex acetosa</i> t.		<b>1.56 (0.09)</b>			<b>2.76 (0.022)</b>
<i>Secale</i>				<b>4.08 (0.96)</b>	<b>4.87 (0.006)</b>
<b>TREE TAXA</b>					
			<b>9.92 (2.86)</b>		
<i>Alnus</i>	<b>13.93 (0.15)</b>		<b>2.42 (0.39)</b>	<b>15.51 (1.25)</b>	<b>13.68 (0.049)</b>
<i>Betula</i>	<b>1.81 (0.02)</b>		<b>4.56 (0.85)</b>	<b>9.62 (1.92)</b>	19.70 (0.117)
<i>Carpinus</i>			<b>2.58 (0.39)</b>	9.45 (0.51)	
<i>Corylus</i>			0.76 (0.17)		
<i>Fagus</i>		<b>5.09 (0.22)</b>	<b>1.39 (0.21)</b>	<b>5.83 (0.45)</b>	<b>9.63 (0.008)</b>
<i>Fraxinus</i>				6.74 (0.68)	<b>1.35 (0.012)</b>
<i>Juniperus</i>			<b>0.57 (0.16)</b>		
<i>Picea</i>	<b>4.73 (0.13)</b>	<b>1.19 (0.42)</b>	1.35 (0.45)	<b>1.58 (0.28)</b>	<b>5.81 (0.007)</b>
<i>Pinus</i>	<b>5.07 (0.06)</b>			<b>5.66 (0.00)</b>	<b>5.39 (0.222)</b>
<i>Populus</i>			<b>2.56 (0.39)</b>	<b>2.66 (1.25)</b>	
Deciduous <i>Quercust.</i>	<b>7.39 (0.20)</b>			<b>2.15 (0.17)</b>	17.85 (0.049)
<i>Salix</i>	<b>2.31 (0.08)</b>				
<i>Tilia</i>				<b>1.47 (0.23)</b>	12.38 (0.101)
<i>Ulmus</i>					11.51 (0.101)
Total number of taxa (selected values) 23 (22)	11 (11)	7 (7)	13 (9)	13 (10)	15 (11)

819 **Table B2: Mediterranean area: RPP estimates and their SDs from two available studies, and mean RPPs for northern and temperate**  
820 **Europe (Table A1, Appendix A), for comparison. RPPs and FSPs emphasized in bold are those used in the REVEALS reconstruction**  
821 **for Europe (this paper), single RPP values from the Mediterranean region within thick rectangles, and mean RPPs from Europe**  
822 **(Mediterranean region excluded) within thin rectangles. The plant taxa emphasized in bold are sub-Mediterranean and/or**  
823 **Mediterranean plant species and genera. FSP values: from Mazier et al. (2012) except (‘) new values from Mazier et al. (unpubl.),**  
824 **(‘’) value from Abraham and Kózáková (2012), (‘’’) value from (Commerford et al., 2013). \*, \*\*FSP from Mazier et al. (2012) used**  
825 **in the REVEALS reconstruction (this study) for Ericaceae (Medit)\* and evergreen *Quercus* t. \*\* instead of the new FSP values from**  
826 **Mazier et al. (unpubl.); for more explanations, see Discussion section, this paper. Abbreviations: Comp. Compositae (= Asteraceae),**  
827 **ERV Extended R-Value model, Medit Mediterranean region, SF. Subfamily.**

828

Region	France Medit. (ERV3)			Romania (ERV3)			Europe, Medit. excluded		
Study reference	Mazier et al. (unpubl.)			Grindean et al. (2019)			This paper (Tables A1)		
	RPP	SD	FSP	RPP	SD	FSP	RPP	SD	FSP
<b>HERB TAXA</b>									
<b>Poaceae (reference taxon)</b>	1.000	0.000	0.035	1.00	0.00	0.035	1.00	0.00	0.035
Apiaceae				5.91	1.23	0.042	0.26	0.01	0.042
<i>Artemisia</i>				5.89	3.16	0.014"	<b>3.937</b>	<b>0.146</b>	<b>0.014"</b>
Compositae (Asteroideae + Cichorioideae)				0.16	0.10	0.029			
Comp. SF. Asteroideae ( <i>Anthemis</i> t., <i>Leucanthemum</i> )							0.10	0.01	0.029
Comp. SF. Cichorioideae	1.162	0.675	0.061'				0.16	0.02	0.05
Cerealia (Cerealia t. + <i>Triticum</i> t. + <i>Secale</i> + <i>Zea</i> )				0.22	0.12	0.060			
Cerealia t. (Cerealia t., <i>Secale</i> excluded)							<b>1.85</b>	<b>0.38</b>	<b>0.060</b>
Cerealia - <i>Secale cereale</i>							<b>3.99</b>	<b>0.33</b>	<b>0.060</b>
Fabaceae				0.40	0.07	0.021'''			
<i>Plantago lanceolata</i>				0.58	0.32	0.029	<b>2.33</b>	<b>0.20</b>	<b>0.029</b>
Ranunculaceae	2.038	0.335	0.020'						
Ranunculaceae - <i>Ranunculus acris</i> t.							1.96	0.36	0.014
Ranunculaceae - <i>Trollius</i>							2.29	0.36	0.013
Rosaceae ( <i>Filipendula</i> , <i>Potentilla</i> t., <i>Sanguisorba</i> )				0.29	0.12	0.018			
Rosaceae - <i>Filipendula</i>							3.00	0.28	0.006
Rosaceae - <i>Potentilla</i> t.							1.72	0.20	0.018
Rubiaceae				0.40	0.07	0.019	3.71	0.34	0.019
<b>TREE/SHRUB TAXA</b>									
<i>Acer</i>				0.30	0.09	0.056	0.80	0.23	0.056
<b><i>Buxus sempervirens</i></b>	<b>1.890</b>	<b>0.068</b>	<b>0.032'</b>						
<i>Carpinus betulus</i>							<b>4.52</b>	<b>0.43</b>	<b>0.042</b>
<i>Carpinus orientalis</i>				<b>0.24</b>	<b>0.07</b>	<b>0.042</b>			
<i>Castanea sativa</i>	<b>3.258</b>	<b>0.059</b>	<b>0.010'</b>						
<i>Corylus avellana</i>	3.440	0.890	0.025				<b>1.71</b>	<b>0.10</b>	<b>0.025</b>
Cupressaceae ( <i>Juniperus communis</i> , <i>J. phoenicea</i> , <i>J. oxycedrus</i> )	1.618	0.161	0.020'						
Cupressaceae - <i>Juniperus communis</i>							<b>2.07</b>	<b>0.04</b>	<b>0.016</b>
Ericaceae ( <i>Arbutus unedo</i> , <i>Erica arborea</i> , <i>E. cinerea</i> , <i>E. multiflora</i> )	<b>4.265</b>	<b>0.094</b>	<b>0.051'</b>						

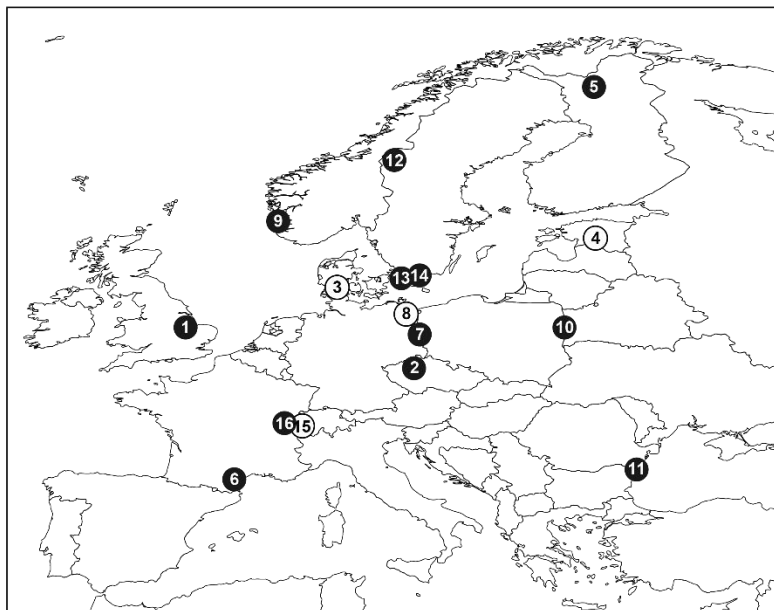
Ericaceae ( <i>Vaccinium</i> dominant, <i>Calluna</i> excluded)					0.07	0.04	<b>0.038*</b>
<i>Fraxinus excelsior</i>					<b>1.04</b>	<b>0.02</b>	<b>0.022</b>
<i>Fraxinus</i> ( <i>F. excelsior</i> , <i>F. ornus</i> )		2.99	0.88	0.022			
<i>Phillyrea</i>	<b>0.512</b>	<b>0.076</b>	<b>0.015'</b>				
<i>Pistacia</i>	<b>0.755</b>	<b>0.201</b>	<b>0.030'</b>				
Evergreen <i>Quercus</i> t. ( <i>Q. ilex</i> , <i>Q. coccifera</i> )	<b>11.04</b>	<b>3</b>	<b>0.261</b>	0.015'			
Deciduous <i>Quercus</i> t. ( <i>Q.</i> spp, <i>Q. peduncularis</i> dominant)					1.10	0.35	0.035
Deciduous <i>Quercus</i> t. ( <i>Q. petraea</i> + <i>Q. rubra</i> )					<b>4.54</b>	<b>0.09</b>	<b>0.035**</b>
Total number of taxa	11				13		

829

830 **Appendix C - Selection of RPP studies**

831 The synthesis of mean RPPs presented here was produced in 2018 and applied in REVEALS reconstructions 2018-2020. Of  
832 nineteen RPP studies available (in July 2021), we selected fifteen published between 1998 and 2018 and one unpublished  
833 study in 2018 (Grindean et al., 2019). The sixteen study regions are distributed in twelve European countries (Figure C1) and  
834 detailed in Table C1. Three studies are not included in our synthesis: Britain (Twiddle et al., 2012) because of the absence of  
835 Poaceae in the calculated RPPs, curves of likelihood function scores exhibiting departures from theoretically correct curves,  
836 and doubts expressed by the authors on the reliability of the values; Greenland (Bunting et al., 2013a) because this land area  
837 was not included in the REVEALS reconstruction of Holocene plant cover in Europe presented in this paper; and Czech  
838 Republic (Kuneš et al., 2019) because the study was not ready when we finalized our synthesis. However, we compare the  
839 RPP values from these three studies with the mean RPP values in this synthesis (Appendix A, Table A2).

840 All studies used the ERV model to calculate RPPs, and all but one study used modern pollen assemblages and vegetation; only  
841 Nielsen et al. (2004; Denmark) used historical pollen and vegetation data. Eleven studies used pollen assemblages from moss  
842 pollsters, five studies from lake sediments. Grindean et al. (2019; Romania) also used some pollen assemblages from surface



843

844 **Figure C1: Location of the selected studies of relative pollen productivities (RPP) in Europe. 1. Britain, (Bunting et al., 2005); 2.**  
845 **Czech Republic, (Abraham and Kozáková, 2012); 3. Denmark, (Nielsen, 2004); 4. Estonia, (Poska et al., 2011); 5. Finland, (Räsänen**  
846 **et al., 2007); 6. France, Mazier et al. unpublished; 7. Germany, (Matthias et al., 2012); 8. Germany, (Theuerkauf et al., 2013); 9.**  
847 **Norway, (Hjelle, 1998); 10. Poland, (Baker et al., 2016); 11. Romania, (Grindean et al., 2019); 12. Sweden, (von Stedingk et al., 2008);**  
848 **13. Sweden, (Sugita et al., 1999); 14. Sweden, (Broström et al., 2004); 15. Switzerland, (Soepboer et al., 2007); 16. Switzerland,**  
849 **(Mazier et al., 2008).**



850 soil samples. All studies used distance-weighted vegetation except two, Hjelle et al. (1998; SW Norway) and Sugita et al.  
851 (1999; S Sweden). The Gaussian Plume Model (GPM) was used for pollen dispersal and deposition to distance-weight  
852 vegetation, i.e. the Prentice's bog model (Parsons and Prentice, 1981; Prentice and Parsons, 1983) in studies using pollen from  
853 moss pollsters, and the Sugita's lake model (Sugita, 1993) in studies using pollen from lake sediments (see also caption of  
854 Table C1). In the case of the study by Theuerkauf et al. (2013), the published RPP values were calculated using the Lagrangian  
855 Stochastic Model. For the purpose of this synthesis, Theuerkauf recalculated the RPPs using the GPM bog model in the  
856 application of the ERV model. The distribution of sites for collection of pollen samples and vegetation data within the study  
857 regions is random or random stratified in seven of the eleven studies using moss pollsters; the five remaining studies used  
858 selected sites (or systematic distribution). Studies using lake sediments normally result in a systematic site distribution. Earlier  
859 studies (Broström et al., 2005; Twiddle et al., 2012) showed that random distribution of sites provided better estimates of  
860 "relevant source area of pollen" (RSAP; *sensu* Sugita, 1994) and thus of RPPs, given that the reliable RPPs are those obtained  
861 at the RSAP distance and beyond. Both studies indicated that systematic distribution of sites have the tendency to result in  
862 curves of likelihood function scores that do not follow the theoretical behaviour, i.e. an increase of the scores with distance  
863 until the values reach an asymptote. However, the difference in RPPs between systematic and random sampling is generally  
864 not very large. Nonetheless, systematic sampling may lead to uncertainty in terms of reliability of RPPs and random  
865 distribution of sites is recommended and has generally been used in studies using moss pollsters or soil samples published  
866 from 2008 and onwards.

867 **Table C1: Selection of studies for the synthesis of relative pollen productivity (RPP) estimates. Emphasized in bold: additional, new**  
868 **studies compared to the studies included in the synthesis of Mazier et al. (2012). Symbols: <sup>1</sup>L=lakes; M=moss pollsters; S=surface**  
869 **soil; <sup>2</sup>Other distance-weighting models were used in most studies, including the Gaussian Plume Model (GPM), 1/d, 1/d<sup>2</sup> (d=distance)**  
870 **and the Lagrangian Stochastic Model (LSM). The GPM is used in both the model developed for bogs (Parsons and Prentice, 1981;**  
871 **Prentice and Parsons, 1983) and lakes (Sugita, 1993). For this RPP synthesis, we chose the results from the analyses using GPM**  
872 **rather than 1/d or 1/d<sup>2</sup>. Note: In the study of Theuerkauf et al. (2013) the LSM was used. For this synthesis, Theuerkauf recalculated**  
873 **his RPPs using the lake model developed by Sugita (1993); <sup>3</sup>Number of plant taxa for which RPP was estimated, including the**  
874 **reference taxon. Note: In the study by Theuerkauf et al. (2013) RPPs were estimated for 17 taxa using LSM. The RPPs were**  
875 **recalculated using the lake model (Sugita, 1993) for 15 taxa (see note under <sup>2</sup> above) for this synthesis. In the study of Sugita et al.**  
876 **(1999) RPPs were calculated for 14 trees and 3 herbs. We used only the values for the 14 trees in this synthesis, following the syntheses**  
877 **by Broström et al. (2008) and Mazier et al. (2012); <sup>^</sup> Britain: the study includes two areas (a and b) in which RPP estimates were**  
878 **calculated for different sets of taxa and the two areas have different numbers of sites: a. Calthorpe (34), 5 taxa; b. Wheatfen (17),**  
879 **same 5 taxa and *Corylus* (6 taxa in total); <sup>^^</sup> random distribution restricted to areas of the study region with existing vegetation**  
880 **maps (therefore no sites outside these areas); i.e. study region including separate areas (Mazier et al., 2008). <sup>+</sup> Vegetation data from**  
881 **historical maps around 1800 CE; <sup>++</sup> lake sediments dated to ca. 1800; <sup>\*</sup> The reference taxon used in the original study is different**  
882 **from Poaceae. For this synthesis the RPPs were converted to values relative to Poaceae; <sup>\*\*</sup> The study of Bunting et al. (2005) does**  
883 **not include a RPP for Poaceae. In order to calculate the RPPs relative to Poaceae, it was assumed that the RPP of *Quercus* was equal**  
884 **to the mean of RPPs from three other studies in Europe (see Mazier et al., 2012 for details). Although we have included new RPP**  
885 **values for *Quercus* in this synthesis, we did not recalculate the RPPs from Bunting et al. (2005) with a new mean value for *Quercus*,**  
886 **but used the same values as in Mazier et al. (2012). For comparison, the mean value for *Quercus* using the RPPs of the additional**  
887 **studies included in this synthesis is 4.28 (instead of 5.83 in Mazier et al., 2012). This would imply slightly lower RPPs in Britain also**  
888 **for *Alnus*, *Betula*, *Corylus*, *Fraxinus* and *Salix*. # no distance weighting used for vegetation data because there was no information**  
889 **about vegetation with increasing distance from the pollen sample (Hjelle et al., 1998; Sugita et al., 1999). In the Swedish study,**  
890 **vegetation data within a 10<sup>2</sup> m<sup>2</sup> (herb taxa) and 10<sup>3</sup> m<sup>2</sup> quadrat (tree taxa) centred on the pollen sample was used (Sugita et al., 1999).**  
891

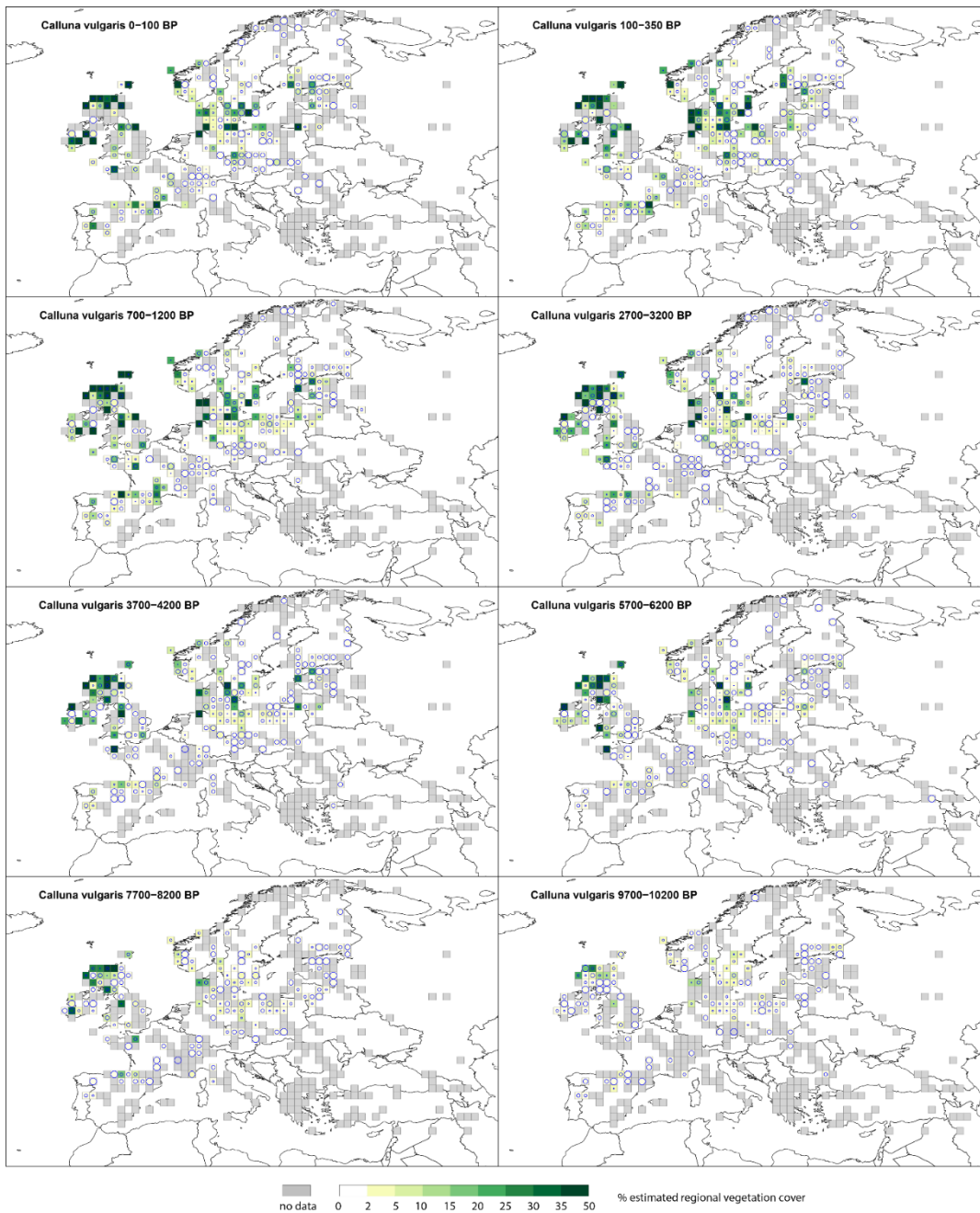
892

Country	Region	No sites	Site distrib.	Pollen sample <sup>1</sup>	ERV sub-model	Distance weighting model <sup>2</sup>	Reference taxon	No taxa <sup>3</sup>	Reference
Britain	East Anglian: Norfolk woodlands	(34 + 19) <sup>^</sup>	selected	M	1	GPM Prentice's bog	<i>Quercus</i> Poaceae**	6	Bunting et al. 2005
<b>Czech Republic</b>	<b>Central Bohemia: agricultural landscape</b>	54	stratified random	M	1	GPM Prentice's bog	Poaceae	13	<b>Abraham &amp; Kózáková 2012</b>
Denmark	Ancient agricultural landscape <sup>+</sup>	30	selected	L <sup>++</sup>	1	GPM Sugita's lake	Poaceae	7	Nielsen et al. 2004
Estonia	Hemiboreal forest zone: mixed woodland - agricultural landscape	40	selected	L	3	GPM Sugita's lake	Poaceae	10	Poska et al. 2011
Finland	N Finland	24	stratified random	M	3	GPM Prentice's bog	Poaceae	6	Räsänen et al. 2007
<b>France</b>	<b>Mediterranean region</b>	23	random	M	3	GPM Prentice's bog	Poaceae	11	<b>Mazier et al. unpubl.</b>
<b>Germany</b>	<b>Eastern Germany: Brandenburg, agricultural landscape</b>	49	selected	L	3	GPM Sugita's lake	<i>Pinus</i> Poaceae*	16	<b>Matthias et al. 2012</b>
	<b>NE Germany: agricultural landscape</b>	27	selected	L	3	LSM GPM Sugita's Lake <sup>2</sup>	<i>Pinus</i> Poaceae*	11 (15) <sup>3</sup>	<b>Theuerkauf et al. 2013</b>
Norway	SW Norway: Hordaland and Sogn og Fjordane, mown or grazed grass-land and heath	39	selected	M	1	None <sup>#</sup>	Poaceae	17	Hjelle 1998
<b>Poland</b>	<b>NE Poland: Bialowieza Forest</b>	18	stratified random	M	3	GPM Prentice's bog	Poaceae	8	<b>Baker et al. 2016</b>
<b>Romania</b>	<b>SE Romania: Forest-steppe region</b>	26	random	M & S	3	GPM Prentice's bog	Poaceae	13	<b>Grindean et al. 2019</b>
Sweden	West- Central Sweden: Forest-tundra ecotone	30	random	M	3	GPM Prentice's bog	Poaceae	10	von Stedingk et al. 2008
	S Sweden: ancient cultural landscapes	114	selected	M	3	None <sup>#</sup>	<i>Juniperus</i> Poaceae*	14 (17) <sup>3</sup>	Sugita et al. 1999
	S Sweden: unfertilized mown or grazed grasslands	42	selected	M	3	GPM Prentice's bog	Poaceae	11	Broström et al. 2004

Switzerland	Lowland: agricultural landscape	20	selected	L	3	GPM Prentice's bog	Poaceae	13	Soepboer et al. 2007
	Jura Mountain: pasture woodlands	20	(stratified) random^^	M	1	GPM Prentice's bog	Poaceae	11	Mazier et al. 2008

893

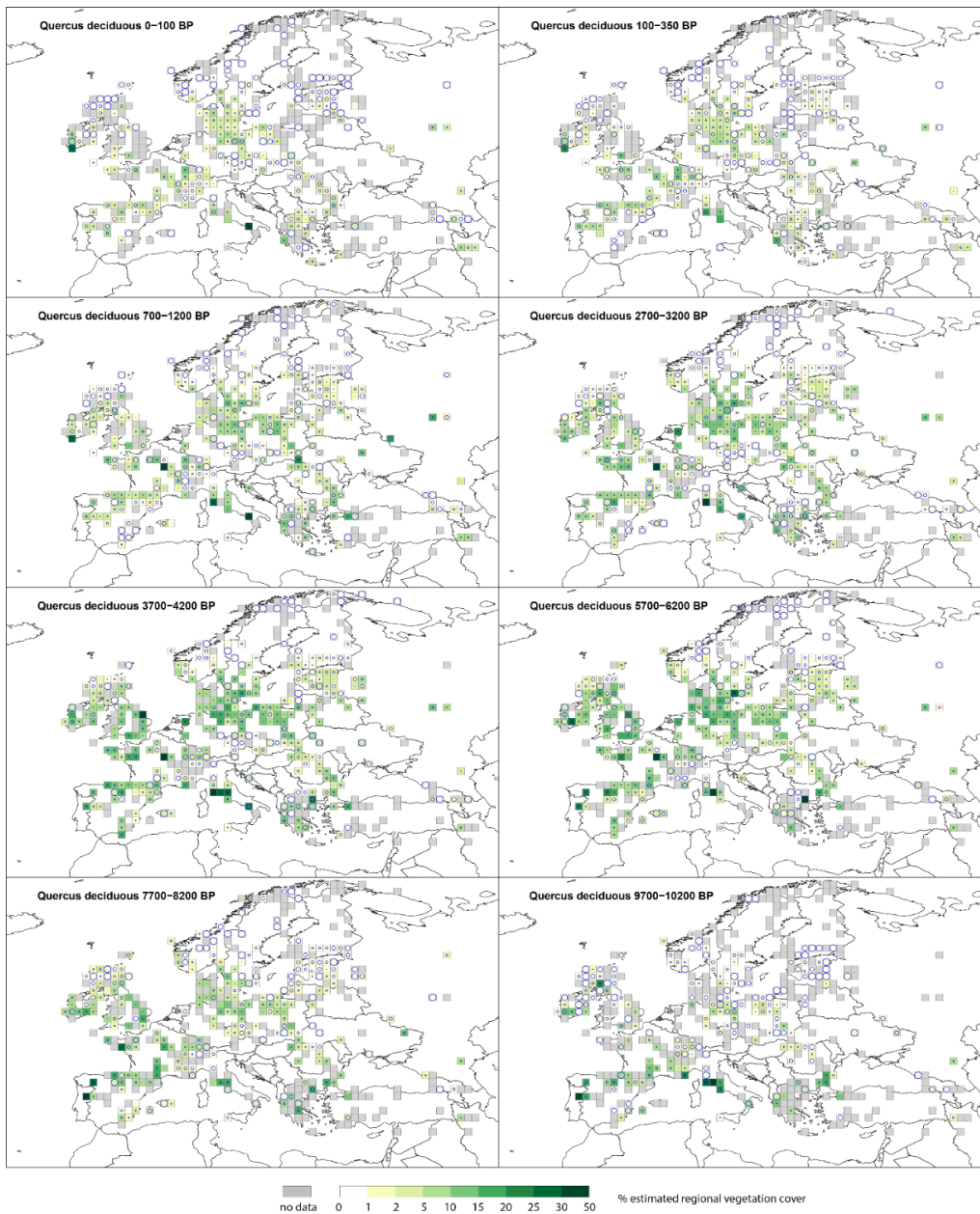
894 **Appendix D Maps of REVEALS cover for three plant taxa (*Calluna vulgaris*, deciduous *Quercus* type (t.) and evergreen**  
895 ***Quercus* t.)**



896

897 **Figure D1. Grid-based REVEALS estimates of *Calluna vulgaris* cover for eight Holocene time windows. Percentage cover in 2%**  
 898 **interval between 0 and 2%, 3% interval between 2 and 5%, 5% intervals between 5 – 35% and 15% interval between 35 and 50%.**  
 899 **Intervals represented by increasingly darker shades of green from 5-10%. Grey grid cells have no data (pollen) for *Calluna vulgaris***  
 900 **in the mapped time window. The circles represent the coefficient of variation (CV; the standard error divided by the REVEALS**  
 901 **estimate). When  $SE \geq REVEALS$  estimate, the circle fills the entire grid cell and the REVEALS estimate is not different from zero.**  
 902 **This occurs mainly where REVEALS estimates are low.**

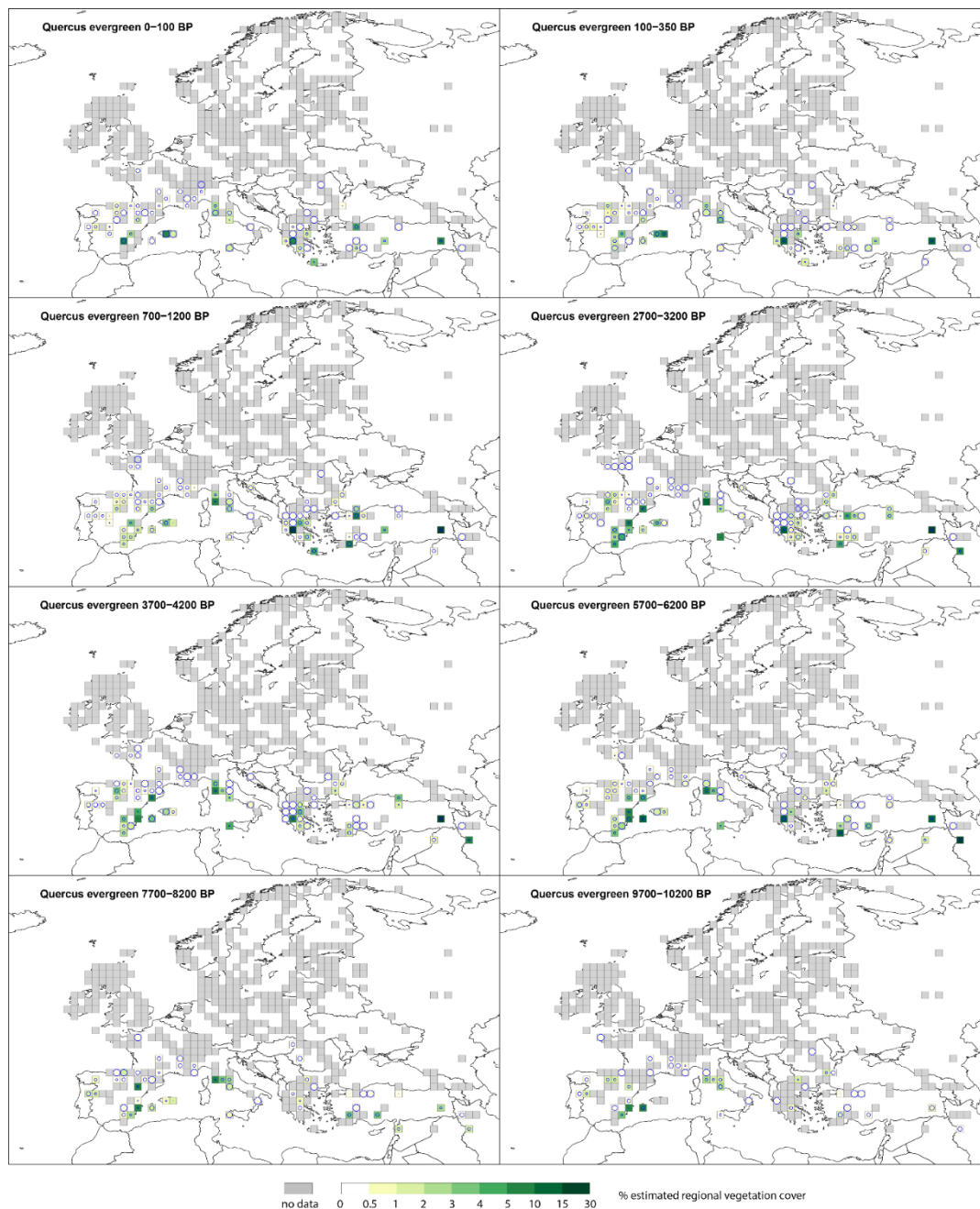
903



905

906

907 **Figure D2. Grid-based REVEALS estimates of deciduous *Quercus* cover in eight Holocene time windows. Percentage**  
 908 **cover in 1% interval between 0 and 2%, 3% interval between 2 and 5%, 5% intervals between 5 and 30% and 20%**  
 909 **interval between 30 and 50%. Intervals represented by increasingly darker shades of green from 2-5%. Grey grid**  
 910 **cells have no data (pollen) for *Calluna vulgaris* in the mapped time window. The circles represent the coefficient**  
 911 **of variation (CV; the standard error divided by the REVEALS estimate). When  $SE \geq$  REVEALS estimate, the circle**  
 912 **fills the entire grid cell and the REVEALS estimate is not different from zero. This occurs mainly where REVEALS**  
 913 **estimates are low.**



915

916 **Figure D3. Grid-based REVEALS estimates of evergreen *Quercus* cover for eight Holocene time windows. Percentage**  
 917 **cover in 0.5% intervals between 0 and 1%, 1% intervals between 1 and 5%, 5% intervals between 5 and 15% and 15%**  
 918 **interval between 15 and 30%. See caption of Figure A1 for more explanations. Intervals represented by increasingly**  
 919 **darker shades of green from 1-2%. Grey grid cells have no data (pollen) for *Calluna vulgaris* in the mapped time**  
 920 **window. The circles represent the coefficient of variation (CV; the standard error divided by the REVEALS**  
 921 **estimate). When  $SE \geq REVEALS$  estimate, the circle fills the entire grid cell and the REVEALS estimate is not**  
 922 **different from zero. This occurs mainly where REVEALS estimates are low.**

923 **+Team list**

924 Åkesson Christine (School of Geography & Sustainable Development, University of St. Andrews, UK), Balakauskas Lauras  
925 (Department of Geology and Mineralogy, Vilnius University, Vilnius, Lithuania), Batalova Vlada (Lomonosov Moscow State  
926 University, Department of Physical geography and Landscape science, Moscow, Russia), Birks H.J.B. (Department of  
927 Biological Sciences and Bjerknes Centre for Climate Research, University of Bergen, Norway), Bjune Anne. E. (Department  
928 of Biological Sciences and Bjerknes Centre for Climate Research, University of Bergen, Norway), Borisova Olga (Institute of  
929 Geography, Russian Academy of Sciences, Moscow, Russia), Bozilova Elissaveta (Department of Botany, Sofia University  
930 St. Kliment Ohridski, Sofia, Bulgaria), Burjachs Francesc (ICREA Barcelona, Catalonia, Spain; Rovira i Virgili University  
931 (URV), Tarragona, Catalonia, Spain; Institut Català de Paleoecologia Humana i Evolució Social (IPHES), Campus Sescelades  
932 URV, W3, 43007 Tarragona, Spain), Cheddadi Rachid (Institut des Sciences de l'Evolution de Montpellier, Université de  
933 Montpellier, CNRS-UM-IRD, Montpellier, France), Christiansen Jörg (Department of Palynology and Climate Dynamics,  
934 Georg-August University, Göttingen, Germany), David Remi (Archeosciences Laboratory, UMR 6566 CReAAH, CNRS,  
935 Rennes1 University, Rennes, France), de Klerk Pim (State Museum of Natural History, Karlsruhe, Germany), Di Rita Federico  
936 (Dipartimento di Biologia Ambientale, Università di Roma "La Sapienza", Piazzale Aldo Moro, 5, 00185, Roma, Italia),  
937 Dörfler Walter (Institute für Ur- und Frühgeschichte, Christian-Albrechts University, Kiel, Germany), Doyen Elise  
938 (Paleobotanisches Laboratoire, Bureau d'étude spécialisé en reconstitution des paléoenvironnements à partir de vestiges botaniques, 01300  
939 Nattages), Eastwood Warren (School of Geography, Earth and Environmental Sciences, University of Birmingham B15 2TT,  
940 UK), Etienne David (Savoie Mont Blanc University, Chambéry, France), Feeser Ingo (Institut für Ur- und Frühgeschichte,  
941 Christian-Albrechts University, Kiel, Germany), Filipova-Marinova Mariana (Museum of Natural History, Varna, Bulgaria),  
942 Fischer E. (Institute für Ur- und Frühgeschichte, Christian-Albrechts University, Kiel, Germany), Galop Didier (GEODE UMR  
943 5602, Toulouse University, Toulouse, France), Garcia Jose Sebastian Carrion (Departamento de Biología Vegetal, Facultad  
944 de Biología, Universidad de Murcia, 30100 Murcia, Spain), Gauthier Emilie (Laboratoire Chrono-Environnement, UMR 6249  
945 CNRS-Franche-Comté University, Besançon, France), Giesecke Thomas (Department of Physical Geography, Utrecht  
946 University, Utrecht, The Netherlands), Herking Christa (Institute of Botany and Landscape Ecology, EMAU, Greifswald,  
947 Germany), Herzschuh Ulrike (Alfred-Wegener-Institut Potsdam, Germany), Jouffroy-Bapicot Isabelle (Laboratoire Chrono-  
948 Environnement, UMR 6249 CNRS, Franche-Comté University, Besançon, France), Kasianova Alisa (Department of  
949 Palynology and Climate Dynamics, Georg-August-University, Göttingen, Germany), Kouli Katerina (Department of Geology  
950 and Geoenvironment, National and Kapodistrian University of Athens, Panepistimioupolis, 15784 Ilissia, Greece), Kuneš Petr  
951 (Department of Botany, Charles University, Prague, Czech Republic/Czech), Lagerås Per (The Archaeologists, National  
952 Historical Museums, Lund, Sweden), Latałowa Małgorzata (Department of Plant Ecology, University of Gdansk, Poland),  
953 Lechterbeck Jutta (State Office for Cultural Heritage Baden-Wuerttemberg, Germany), Leroyer Chantal (Archeosciences  
954 Laboratory, UMR 6566 CReAAH, CNRS, Rennes1 University, Rennes, France), Leydet Michelle (European Pollen Database,

955 IMBE, Aix-Marseille Université, Avignon Université, IRD, Aix-en-Provence, France), Lisystina Olga (Department of  
956 Geology, Tallinn University of Technology, 19086 Tallinn, Estonia), Lukanina Ekaterina (Department of Palynology and  
957 Climate Dynamics, Georg-August-University, Göttingen, Germany), Magyari Enikő (Department of Environmental and  
958 Landscape Geography, Eötvös Loránd University, Budapest, Hungary), Marguerie Dominique (UMR 6553 ECOBIO / Thème  
959 PaysaBio, Université de Rennes 1, 35042 RENNES Cedex France), Mariotti Lippi Marta (Dipartimento di Biologia,  
960 Università di Firenze, Via G. La Pira, 4, 50121 Firenze, Italy), Mensing Scott (Department of Geography, University of  
961 Nevada, Reno, NV 89557, USA), Mercuri Anna Maria (Laboratorio di Palinologia e Paleobotanica, Dipartimento di Scienze  
962 della Vita, Università di Modena e Reggio Emilia, Italy), Miebach Andrea (Steinmann Institute for Geology, Mineralogy, and  
963 Paleontology, University of Bonn, Bonn, Germany), Milburn Paula (College of Science and Engineering, University of  
964 Edinburgh, Edinburgh, Scotland), Miras Yannick (CNRS HNHP UMR 7194, Museum National d'Histoire Naturelle, Paris,  
965 France), Morales del Molino César (Alpine Pollen Database, Institute of Plant Sciences, Bern University, Switzerland),  
966 Mrotzek Almut (Institute of Botany and Landscape Ecology, EMAU ,Greifswald, Germany), Nosova Maria (Main Botanical  
967 Garden, Russian Academy of Sciences, Moscow, Russia), Odgaard Bent Vad (Department of Geoscience, Aarhus University,  
968 Denmark). Overballe-Petersen Mette (Forest & Landscape, Faculty of Life Sciences, University of Copenhagen,  
969 Frederiksberg, Denmark), Panajiotidis Sampson (Aristotle University of Thessaloniki, Department of Forestry and Natural  
970 Environment, PO Box: 270, GR54124 Thessaloniki, Greece), Pavlov Danail (Society of Innovative Ecologists of Bulgaria,  
971 Varna, Bulgaria), Persson Thomas<sup>†</sup> (Department of Geology, Lund University, Lund, Sweden), Pinke Zsolt (Department of  
972 Physical Geography, Eötvös Loránd University, Budapest, Hungary), Ruffaldi Pascale (Laboratoire Chrono-Environnement,  
973 UMR 6249 CNRS, Franche-Comté University, Besançon, France), Sapelko Tatyana (Institute of Limnology, Russian  
974 Academy of Sciences , St. Petersburg, Russia), Schmidt Monika (Department of Palynology and Climate Dynamics, Georg-  
975 August-University, Göttingen, Germany), Schult Manuela (Institute of Botany and Landscape Ecology, EMAU, Greifswald,  
976 Germany), ), Stivrins Normunds (Department of Geography, Faculty of Geography and Earth Sciences, University of Latvia,  
977 Jelgavas iela 1, Riga, 1004, Latvia), Tarasov Pavel E. (Institute of Geological Sciences, Free University of Berlin, Germany),  
978 Theuerkauf Martin (Institute of Botany and Landscape Ecology, EMAU Greifswald, 1748 Greiswald, Germany), Veski Siim  
979 (Department of Geology, Tallinn University of Technology, Tallinn, Estonia), Wick Lucia (IPNA, University of Basel, Basel,  
980 Switzerland), Wiethold Julian (INRAP, Direction interrégionale Grand-Est Nord, Laboratoire archéobotanique, Metz, France),  
981 Woldring Henk (Groningen Institute of Archaeology, University of Groningen, The Netherlands), Zernitskaya Valentina  
982 (Institute for Nature Management, National Academy of Sciences of Belarusk, Minsk, Republic of Belarus).

### 983 **Author Contribution**

984 MJG coordinated the study as part of LandClim II and PAGES LandCover6k, two research projects for which she is the overall  
985 coordinator and administrator. MJG, AKT, EG, FM, RF, ABN, AP and SS conceptualised the study and methodology. SS  
986 developed the REVEALS model and helped with all issues related to the application of the model and interpretation of results.



987 EG, AKT, RF, FM, ABN, and AP collected new pollen records from individual authors. JW provided part of the pollen records  
988 from the Mediterranean area (collected earlier for a separate project). LS, MS and ST provided unpublished pollen records.  
989 EG and AKT had the major responsibility of handling the pollen data files and collecting all related metadata. AKT collected  
990 new values of relative pollen productivity estimates (RPPs) in Europe. FM provided unpublished RPP values for the  
991 Mediterranean area. FM, JA, VL, LM, and NNC were all involved in the unpublished RPP study in southern France, and AF,  
992 RG, ABN and IT performed the RPP study in Romania. MJG performed the selection of RPP values for the new RPP synthesis  
993 used in this paper, EG made the calculations of mean RPPs, and MJG wrote Appendices A, B, and C, and prepared the Figures  
994 and Tables therein. RF performed the REVEALS model runs and created Figure 1 and the maps of REVEALS-based plant  
995 cover (Figures 2-6 and D1-D3). EG, RF and MJG designed the manuscript, EG prepared the first draft of the manuscript and  
996 all Tables, and the final manuscript for submission, RF and MJG wrote parts of the text and edited the full manuscript. All the  
997 co-authors, including the data contributors in the Team List (LandClim II data contributors), were involved in commenting  
998 and revising the manuscript.

#### 999 **Competing interests**

1000 The authors declare that they have no conflict of interest.

1001 **Figures entirely compiled by the manuscript authors:** Since such figures are part of the manuscript, they will receive the  
1002 same distribution licence as the entire manuscript, namely a CC BY License. No citation is needed and no reproduction rights  
1003 must be obtained.

## 1004 **Acknowledgements**

1005 This study was funded by a research project financed by the Swedish Research Council VR (Vetenskapsrådet) on  
1006 “Quantification of the bio-geophysical and biogeochemical forcings from anthropogenic de-forestation on regional Holocene  
1007 climate in Europe, LandClim II”. Financial support from the Linnaeus University’s Faculty of Health and Life Science is  
1008 acknowledged for Marie-José Gaillard, Anna-Kari Trondman, and Esther Githumbi. This is a contribution to the Swedish  
1009 Strategic Research Area (SRA) MERGE (Modelling the Regional and Global Earth system; [www.merge.lu.se](http://www.merge.lu.se)) and to the Past  
1010 Global Change (PAGES) project and its working group LandCover6k (<http://pastglobalchanges.org/landcover6k>) that in turn  
1011 received support from the Swiss National Science Foundation, the Swiss Academy of Sciences, the US National Science  
1012 Foundation, and the Chinese Academy of Sciences. Anneli Poska was supported by the ESF project number PRG323. We  
1013 thank Sandy Harrison (University of Reading, UK) for providing the pollen records from the EMBSeCBIO project. The work  
1014 of the data contributors to - and the database managers of ALPADABA (<https://www.neotomadb.org/>), EMBSeCBIO  
1015 (<https://research.reading.ac.uk/palaeoclimate/embsecbio/>), EPD (<http://www.europeanpollendatabase.net/index.php>),  
1016 LandClimI (Trondman et al., 2015), PALY CZ (<https://botany.natur.cuni.cz/palycz/>), and PALEOPYR ([http://paleopyr.univ-](http://paleopyr.univ-tlse2.fr/)  
1017 [tlse2.fr/](http://paleopyr.univ-tlse2.fr/)) is gratefully acknowledged.

## 1018 **References**

- 1019 Abraham, V. and Kozáková, R.: Relative pollen productivity estimates in the modern agricultural landscape of Central  
1020 Bohemia (Czech Republic), *Rev. Palaeobot. Palynol.*, 179, 1–12, doi:10.1016/j.revpalbo.2012.04.004, 2012.
- 1021 Abraham, V., Oušková, V. and Kuneš, P.: Present-Day Vegetation Helps Quantifying Past Land Cover in Selected Regions of  
1022 the Czech Republic, edited by B. Bond-Lamberty, *PLoS One*, 9(6), e100117, doi:10.1371/journal.pone.0100117, 2014.
- 1023 Andersen, S. T.: The relative pollen productivity and pollen representation of north European trees, and correction factors for  
1024 tree pollen spectra, *Danmarks Geol. Undersogelse II*, 96, 99, 1970.
- 1025 Baker, A. G., Zimny, M., Keczyński, A., Bhagwat, S. A., Willis, K. J. and Latałowa, M.: Pollen productivity estimates from  
1026 old-growth forest strongly differ from those obtained in cultural landscapes: Evidence from the Białowieża National Park,  
1027 *Poland, The Holocene*, 26(1), 80–92, doi:10.1177/0959683615596822, 2016.
- 1028 Barnosky, A. D., Hadly, E. A., Bascombe, J., Berlow, E. L., Brown, J. H., Fortelius, M., Getz, W. M., Harte, J., Hastings, A.,  
1029 Marquet, P. A., Martinez, N. D., Mooers, A., Roopnarine, P., Vermeij, G., Williams, J. W., Gillespie, R., Kitzes, J., Marshall,  
1030 C., Matzke, N., Mindell, D. P., Revilla, E. and Smith, A. B.: Approaching a state shift in Earth’s biosphere, *Nature*, 486(7401),  
1031 52–58, doi:10.1038/nature11018, 2012.
- 1032 Beug, H. J.: *Leitfaden der Pollenbestimmung für Mitteleuropa und angrenzende Gebiete (Guide to pollen determination for*  
1033 *Central Europe and neighboring areas).*, Verlag Dr. Friedrich Pfeil., 2004.
- 1034 Broström, A., Sugita, S. and Gaillard, M.-J.: Pollen productivity estimates for the reconstruction of past vegetation cover in  
1035 the cultural landscape of southern Sweden, *The Holocene*, 14(3), 368–381, doi:10.1191/0959683604hl713rp, 2004.

1036 Broström, A., Sugita, S., Gaillard, M.-J. and Pilesjö, P.: Estimating the spatial scale of pollen dispersal in the cultural landscape  
1037 of southern Sweden, *The Holocene*, 15(2), 252–262, doi:10.1191/0959683605hl790rp, 2005.

1038 Broström, A., Nielsen, A. B., Gaillard, M.-J., Hjelle, K., Mazier, F., Binney, H., Bunting, J., Fyfe, R., Meltsov, V., Poska, A.,  
1039 Räsänen, S., Soepboer, W., von Stedingk, H., Suutari, H. and Sugita, S.: Pollen productivity estimates of key European plant  
1040 taxa for quantitative reconstruction of past vegetation: a review, *Veg. Hist. Archaeobot.*, 17(5), 461–478, doi:10.1007/s00334-  
1041 008-0148-8, 2008.

1042 Bunting, M. J., Armitage, R., Binney, H. A. and Waller, M.: Estimates of ‘relative pollen productivity’ and ‘relevant source  
1043 area of pollen’ for major tree taxa in two Norfolk (UK) woodlands, *The Holocene*, 15(3), 459–465,  
1044 doi:10.1191/0959683605hl821rr, 2005.

1045 Bunting, M. J., Schofield, J. E. and Edwards, K. J.: Estimates of relative pollen productivity (RPP) for selected taxa from  
1046 southern Greenland: A pragmatic solution, *Rev. Palaeobot. Palynol.*, 190, 66–74, doi:10.1016/j.revpalbo.2012.11.003, 2013a.

1047 Bunting, M. J., Farrell, M., Broström, A., Hjelle, K. L., Mazier, F., Middleton, R., Nielsen, A. B., Rushton, E., Shaw, H. and  
1048 Twiddle, C. L.: Palynological perspectives on vegetation survey: a critical step for model-based reconstruction of Quaternary  
1049 land cover, *Quat. Sci. Rev.*, 82, 41–55, doi:10.1016/j.quascirev.2013.10.006, 2013b.

1050 Commerford, J. L., McLauchlan, K. K. and Sugita, S.: Calibrating Vegetation Cover and Grassland Pollen Assemblages in the  
1051 Flint Hills of Kansas, USA, *Am. J. Plant Sci.*, 04(07), 1–10, doi:10.4236/ajps.2013.47A1001, 2013.

1052 Cui, Q.-Y., Gaillard, M.-J., Lemdahl, G., Sugita, S., Greisman, A., Jacobson, G. L. and Olsson, F.: The role of tree composition  
1053 in Holocene fire history of the hemiboreal and southern boreal zones of southern Sweden, as revealed by the application of the  
1054 Landscape Reconstruction Algorithm: Implications for biodiversity and climate-change issues, *The Holocene*, 23(12), 1747–  
1055 1763, doi:10.1177/0959683613505339, 2013.

1056 Cui, Q., Gaillard, M., Lemdahl, G., Stenberg, L., Sugita, S. and Zernova, G.: Historical land-use and landscape change in  
1057 southern Sweden and implications for present and future biodiversity, *Ecol. Evol.*, 4(18), 3555–3570, doi:10.1002/ece3.1198,  
1058 2014.

1059 Davis, B. A. S., Collins, P. M. and Kaplan, J. O.: The age and post-glacial development of the modern European vegetation: a  
1060 plant functional approach based on pollen data, *Veg. Hist. Archaeobot.*, 24(2), 303–317, doi:10.1007/s00334-014-0476-9,  
1061 2015.

1062 Davis, M. B.: On the theory of pollen analysis, *Am. J. Sci.*, 261(10), 897–912, doi:10.2475/ajs.261.10.897, 1963.

1063 Dawson, A., Cao, X., Chaput, M., Hopla, E., Li, F., Edwards, M., Fyfe, R., Gajewski, K., Goring, S. J., Herzsuh, U., Mazier,  
1064 F., Sugita, S., Williams, J. W., Xu, Q. and Gaillard, M.-J.: Finding the magnitude of human-induced Northern Hemisphere  
1065 land-cover transformation between 6 and 0.2 ka BP, *Past Glob. Chang. Mag.*, 26(1), 34–35, doi:10.22498/pages.26.1.34, 2018.

1066 Dickson, C.: Distinguishing cereal from wild grass pollen: some limitations, *Circaea*, 5, 67–71, 1988.

1067 Downs, P. W. and Piégay, H.: Catchment-scale cumulative impact of human activities on river channels in the late  
1068 Anthropocene: implications, limitations, prospect, *Geomorphology*, 338, 88–104, doi:10.1016/j.geomorph.2019.03.021, 2019.

1069 Edwards, K. J., Fyfe, R. and Jackson, S. T.: The first 100 years of pollen analysis, *Nat. Plants*, 3(2), 17001,

1070 doi:10.1038/nplants.2017.1, 2017.

1071 Ellis, E. C.: Ecology in an anthropogenic biosphere, *Ecol. Monogr.*, 85(3), 287–331, doi:10.1890/14-2274.1, 2015.

1072 Feurdean, A., Vanni re, B., Finsinger, W., Warren, D., Connor, S. C., Forrest, M., Liakka, J., Panait, A., Werner, C., Andri ,

1073 M., Bobek, P., Carter, V. A., Davis, B., Diaconu, A.-C., Dietze, E., Feeser, I., Florescu, G., Ga ka, M., Giesecke, T., Jahns, S.,

1074 Jamrichova, E., Kajuka o, K., Kaplan, J., Karpi nska-Ko aczek, M., Ko aczek, P., Kune , P., Kupriyanov, D., Lamentowicz,

1075 M., Lemmen, C., Magyari, E. K., Marcisz, K., Marinova, E., Niamir, A., Novenko, E., Obremaska, M., P dziszewska, A.,

1076 Pfeiffer, M., Poska, A., R sch, M., S owi nski, M., Stan ikait , M., Szal, M., Święta-Musznicka, J., Tan au, I., Theuerkauf, M.,

1077 Tonkov, S., Valk , O., Vassiljev, J., Veski, S., Vincze, I., Wacnik, A., Wiethold, J. and Hickler, T.: Fire hazard modulation by

1078 long-term dynamics in land cover and dominant forest type in eastern and central Europe, *Biogeosciences*, 17(5), 1213–1230,

1079 doi:10.5194/bg-17-1213-2020, 2020.

1080 Foley, J. A.: Global Consequences of Land Use, *Science* (80-. ), 309(5734), 570–574, doi:10.1126/science.1111772, 2005.

1081 Fyfe, R., de Beaulieu, J.-L., Binney, H., Bradshaw, R. H. W., Brewer, S., Le Flao, A., Finsinger, W., Gaillard, M.-J., Giesecke,

1082 T., Gil-Romera, G., Grimm, E. C., Huntley, B., Kunes, P., K hl, N., Leydet, M., Lotter, A. F., Tarasov, P. E. and Tonkov, S.:  
1083 The European Pollen Database: past efforts and current activities, *Veg. Hist. Archaeobot.*, 18(5), 417–424,

1084 doi:10.1007/s00334-009-0215-9, 2009.

1085 Fyfe, R., Roberts, N. and Woodbridge, J.: A pollen-based pseudobiomisation approach to anthropogenic land-cover change,

1086 *The Holocene*, 20(7), 1165–1171, doi:10.1177/0959683610369509, 2010.

1087 Fyfe, R., Twiddle, C., Sugita, S., Gaillard, M. J., Barratt, P., Caseldine, C. J., Dodson, J., Edwards, K. J., Farrell, M., Froyd,

1088 C., Grant, M. J., Huckerby, E., Innes, J. B., Shaw, H. and Waller, M.: The Holocene vegetation cover of Britain and Ireland:  
1089 Overcoming problems of scale and discerning patterns of openness, *Quat. Sci. Rev.*, 73, 132–148,

1090 doi:10.1016/j.quascirev.2013.05.014, 2013.

1091 Fyfe, R. M., Woodbridge, J. and Roberts, N.: From forest to farmland: pollen-inferred land cover change across Europe using  
1092 the pseudobiomization approach, *Glob. Chang. Biol.*, 21(3), 1197–1212, doi:10.1111/gcb.12776, 2015.

1093 Fyfe, R. M., Woodbridge, J. and Roberts, C. N.: Trajectories of change in Mediterranean Holocene vegetation through  
1094 classification of pollen data, *Veg. Hist. Archaeobot.*, 27(2), 351–364, doi:10.1007/s00334-017-0657-4, 2018.

1095 Fyfe, R. M., Githumbi, E., Trondmann, A.-K., Mazier, F., Nielsen, A. B., Poska, A., Sugita, S., Woodbridge, J., Contributors,

1096 L. and Gaillard, M.-J.: A full Holocene record of transient gridded vegetation cover in Europe, *Pangaea*,

1097 doi:https://doi.pangaea.de/10.1594/PANGAEA.931856, 2021.

1098 Gaillard, M.-J., Sugita, S., Bunting, M. J., Middleton, R., Brostr m, A., Caseldine, C., Giesecke, T., Hellman, S. E. V., Hicks,

1099 S., Hjelle, K., Langdon, C., Nielsen, A.-B., Poska, A., von Stedingk, H. and Veski, S.: The use of modelling and simulation  
1100 approach in reconstructing past landscapes from fossil pollen data: a review and results from the POLLANDCAL network,

1101 *Veg. Hist. Archaeobot.*, 17(5), 419–443, doi:10.1007/s00334-008-0169-3, 2008.

1102 Gaillard, M.-J., Sugita, S., Mazier, F., Trondman, A.-K., Brostr m, A., Hickler, T., Kaplan, J. O., Kjellstr m, E., Kokfelt, U.,

1103 Kune , P., Lemmen, C., Miller, P., Olofsson, J., Poska, A., Rundgren, M., Smith, B., Strandberg, G., Fyfe, R., Nielsen, A. B.,

1104 Alenius, T., Balakauskas, L., Barnekow, L., Birks, H. J. B. B., Bjune, A., Björkman, L., Giesecke, T., Hjelle, K., Kalnina, L.,  
1105 Kangur, M., van der Knaap, W. O., Koff, T., Lagerås, P., Latałowa, M., Leydet, M., Lechterbeck, J., Lindbladh, M., Odgaard,  
1106 B., Peglar, S., Segerström, U., von Stedingk, H. and Seppä, H.: Holocene land-cover reconstructions for studies on land cover-  
1107 climate feedbacks, *Clim. Past*, 6(4), 483–499, doi:10.5194/cp-6-483-2010, 2010a.

1108 Gaillard, M.-J., Kleinen, T., Samuelsson, P., Nielsen, A. B., Bergh, J., Kaplan, J. O., Poska, A., Sandström, C., Strandberg,  
1109 G., Trondman, A.-K. and Wramneby, A.: Second Assessment of Climate Change for the Baltic Sea Basin, edited by The  
1110 BACC II Author Team, Springer International Publishing, Cham., 2015.

1111 Gaillard, M. J., Sugita, S., Rundgren, M., Smith, B., Mazier, F., Trondman, A.-K., Fyfe, R., Kokfelt, U., Nielsen, A.-B.,  
1112 Strandberg, G. and Team, L. members: Pollen-inferred quantitative reconstructions of Holocene land-cover in NW Europe for  
1113 the evaluation of past climate-vegetation feedbacks - The Swedish LANDCLIM project and the NordForsk LANDCLIM  
1114 network, *Geophys. Res. Abstr.*, 12(April 2010), 3–4, 2010b.

1115 Gaillard, M. J., Morrison, K. D., Madella, M. and Whitehouse, N.: Editorial: Past land-use and land-cover change: the  
1116 challenge of quantification at the subcontinental to global scales, *Past Glob. Chang. Mag.*, 26(1), 3–3,  
1117 doi:10.22498/pages.26.1.3, 2018.

1118 Giesecke, T., Davis, B., Brewer, S., Finsinger, W., Wolters, S., Blaauw, M., de Beaulieu, J.-L., Binney, H., Fyfe, R. M.,  
1119 Gaillard, M.-J., Gil-Romera, G., van der Knaap, W. O., Kuneš, P., Kühl, N., van Leeuwen, J. F. N. N., Leydet, M., Lotter, A.  
1120 F., Ortu, E., Semmler, M. and Bradshaw, R. H. W. W.: Towards mapping the late Quaternary vegetation change of Europe,  
1121 *Veg. Hist. Archaeobot.*, 23(1), 75–86, doi:10.1007/s00334-012-0390-y, 2014.

1122 Gilgen, A., Wilkenskjeld, S., Kaplan, J. O., Kühn, T. and Lohmann, U.: Effects of land use and anthropogenic aerosol  
1123 emissions in the Roman Empire, *Clim. Past*, 15(5), 1885–1911, doi:10.5194/cp-15-1885-2019, 2019.

1124 Githumbi, E., Fyfe, R., Kjellström, E., Lindström, J., Lu, Z., Mazier, F., Nielsen, A. B., Poska, A., Smith, B., Strandberg, G.,  
1125 Sugita, S., Zhang, Q. and Gaillard, M.-J.: Holocene quantitative pollen-based vegetation reconstructions in Europe for climate  
1126 modelling: LandClim II, in INQUA 2019: Life on the Edge, Dublin. [online] Available from:  
1127 [https://portal.research.lu.se/portal/en/publications/holocene-quantitative-pollenbased-vegetation-reconstructions-in-europe-](https://portal.research.lu.se/portal/en/publications/holocene-quantitative-pollenbased-vegetation-reconstructions-in-europe-for-climate-modelling-landclim-ii(46cc8471-f51c-4117-a7c6-ccff00638e82)/export.html)  
1128 [for-climate-modelling-landclim-ii\(46cc8471-f51c-4117-a7c6-ccff00638e82\)/export.html](https://portal.research.lu.se/portal/en/publications/holocene-quantitative-pollenbased-vegetation-reconstructions-in-europe-for-climate-modelling-landclim-ii(46cc8471-f51c-4117-a7c6-ccff00638e82)/export.html) (Accessed 9 August 2021), 2019.

1129 Gregory, P.: Spores: their properties and sedimentation in still air. *Microbiology of the atmosphere. A plant science*  
1130 *monograph*, 1973.

1131 Grindean, R., Nielsen, A. B., Tanțău, I. and Feurdean, A.: Relative pollen productivity estimates in the forest steppe landscape  
1132 of southeastern Romania, *Rev. Palaeobot. Palynol.*, 264, 54–63, doi:10.1016/j.revpalbo.2019.02.007, 2019.

1133 Guiry, E., Beglane, F., Szpak, P., Schulting, R., McCormick, F. and Richards, M. P.: Anthropogenic changes to the Holocene  
1134 nitrogen cycle in Ireland, *Sci. Adv.*, 4(6), eaas9383, doi:10.1126/sciadv.aas9383, 2018.

1135 Harrison, S. P., Gaillard, M. J., Stocker, B. D., Vander Linden, M., Klein Goldewijk, K., Boles, O., Braconnot, P., Dawson,  
1136 A., Fluet-Chouinard, E., Kaplan, J. O., Kastner, T., Pausata, F. S. R., Robinson, E., Whitehouse, N. J., Madella, M. and  
1137 Morrison, K. D.: Development and testing scenarios for implementing land use and land cover changes during the Holocene

1138 in Earth system model experiments, *Geosci. Model Dev.*, 13(2), 805–824, doi:10.5194/gmd-13-805-2020, 2020.

1139 He, F., Vavrus, S. J., Kutzbach, J. E., Ruddiman, W. F., Kaplan, J. O. and Krumhardt, K. M.: Simulating global and local  
1140 surface temperature changes due to Holocene anthropogenic land cover change, *Geophys. Res. Lett.*, 41(2), 623–631,  
1141 doi:10.1002/2013GL058085, 2014.

1142 Hellman, S., Gaillard, M.-J., Broström, A. and Sugita, S.: The REVEALS model, a new tool to estimate past regional plant  
1143 abundance from pollen data in large lakes: validation in southern Sweden, *J. Quat. Sci.*, 23(1), 21–42, doi:10.1002/jqs.1126,  
1144 2008a.

1145 Hellman, S. E. V., Gaillard, M., Broström, A. and Sugita, S.: Effects of the sampling design and selection of parameter values  
1146 on pollen-based quantitative reconstructions of regional vegetation: a case study in southern Sweden using the REVEALS  
1147 model, *Veg. Hist. Archaeobot.*, 17(5), 445–459, doi:10.1007/s00334-008-0149-7, 2008b.

1148 Hibbard, K., Janetos, A., van Vuuren, D. P., Pongratz, J., Rose, S. K., Betts, R., Herold, M. and Feddema, J. J.: Research  
1149 priorities in land use and land-cover change for the Earth system and integrated assessment modelling, *Int. J. Climatol.*, 30(13),  
1150 2118–2128, doi:10.1002/joc.2150, 2010.

1151 Hjelle, K. L.: Herb pollen representation in surface moss samples from mown meadows and pastures in western Norway, *Veg.*  
1152 *Hist. Archaeobot.*, 7(2), 79–96, doi:10.1007/BF01373926, 1998.

1153 Hofman-Kamińska, E., Bocherens, H., Drucker, D. G., Fyfe, R. M., Gumiński, W., Makowiecki, D., Pacher, M., Piličiauskienė,  
1154 G., Samojlik, T., Woodbridge, J. and Kowalczyk, R.: Adapt or die—Response of large herbivores to environmental changes  
1155 in Europe during the Holocene, *Glob. Chang. Biol.*, 25(9), 2915–2930, doi:10.1111/gcb.14733, 2019.

1156 Huntley, B.: European vegetation history: Palaeovegetation maps from pollen data - 13 000 yr BP to present, *J. Quat. Sci.*,  
1157 5(2), 103–122, doi:10.1002/jqs.3390050203, 1990.

1158 Kaplan, J., Krumhardt, K., Gaillard, M.-J., Sugita, S., Trondman, A.-K., Fyfe, R., Marquer, L., Mazier, F. and Nielsen, A.:  
1159 Constraining the Deforestation History of Europe: Evaluation of Historical Land Use Scenarios with Pollen-Based Land Cover  
1160 Reconstructions, *Land*, 6(4), 91, doi:10.3390/land6040091, 2017.

1161 Kaplan, J. O., Krumhardt, K. M. and Zimmermann, N.: The prehistoric and preindustrial deforestation of Europe, *Quat. Sci.*  
1162 *Rev.*, 28(27–28), 3016–3034, doi:10.1016/j.quascirev.2009.09.028, 2009.

1163 Kaplan, J. O., Krumhardt, K. M., Ellis, E. C., Ruddiman, W. F., Lemmen, C. and Goldewijk, K. K.: Holocene carbon emissions  
1164 as a result of anthropogenic land cover change, *The Holocene*, 21(5), 775–791, doi:10.1177/0959683610386983, 2011.

1165 Klein Goldewijk, K., Beusen, A., Doelman, J. and Stehfest, E.: Anthropogenic land use estimates for the Holocene – HYDE  
1166 3.2, *Earth Syst. Sci. Data*, 9(2), 927–953, doi:10.5194/essd-9-927-2017, 2017.

1167 Kuneš, P., Abraham, V., Kovářik, O., Kopecký, M., Břízová, E., Dudová, L., Jankovská, V., Knipping, M., Kozšková, R.,  
1168 Nováková, K., Petr, L., Pokorný, P., Roszková, A., Rybničková, E., Svobodová-Svitavská, H. and Wacnik, A.: Czech  
1169 quaternary palynological Database - Palycz: review and basic statistics of the data, *Preslia*, 81(3), 209–238, 2009.

1170 Kuneš, P., Abraham, V., Werchan, B., Plesková, Z., Fajmon, K., Jamrichová, E. and Roleček, J.: Relative pollen productivity  
1171 estimates for vegetation reconstruction in central-eastern Europe inferred at local and regional scales, *The Holocene*, 29(11),

1172 1708–1719, doi:10.1177/0959683619862026, 2019.

1173 Lerigoleur, E., Mazier, F., Jégou, L., Perret, M. and Galop, D.: PALEOPYR: un système d'information pour la gestion et  
1174 l'exploitation de données palaeoenvironnementales sur le massif nord-pyrénéen. *Ingénierie des Systèmes d'Information* 3.  
1175 [online] Available from: <http://paleopyr.univ-tlse2.fr/%0A>, 2015.

1176 Li, F., Gaillard, M.-J., Xu, Q., Bunting, M. J., Li, Y., Li, J., Mu, H., Lu, J., Zhang, P., Zhang, S., Cui, Q., Zhang, Y. and Shen,  
1177 W.: A Review of Relative Pollen Productivity Estimates From Temperate China for Pollen-Based Quantitative Reconstruction  
1178 of Past Plant Cover, *Front. Plant Sci.*, 9(September), doi:10.3389/fpls.2018.01214, 2018.

1179 Li, F., Gaillard, M.-J., Cao, X., Herzsuh, U., Sugita, S., Tarasov, P. E., Wagner, M., Xu, Q., Ni, J., Wang, W., Zhao, Y., An,  
1180 C., Beusen, A. H. W., Chen, F., Feng, Z., Goldewijk, C. G. M. K., Huang, X., Li, Y., Li, Y., Liu, H., Sun, A., Yao, Y., Zheng,  
1181 Z. and Jia, X.: Towards quantification of Holocene anthropogenic land-cover change in temperate China: A review in the light  
1182 of pollen-based REVEALS reconstructions of regional plant cover, *Earth-Science Rev.*, 203(February), 103119,  
1183 doi:10.1016/j.earscirev.2020.103119, 2020.

1184 Marinova, E., Harrison, S. P., Bragg, F., Connor, S., Laet, V., Leroy, S. A. G., Mudie, P., Atanassova, J., Bozilova, E., Caner,  
1185 H., Cordova, C., Djamali, M., Filipova-Marinova, M., Gerasimenko, N., Jahns, S., Kouli, K., Kotthoff, U., Kvavadze, E.,  
1186 Lazarova, M., Novenko, E., Ramezani, E., Röpke, A., Shumilovskikh, L., Tanțău, I. and Tonkov, S.: Pollen-derived biomes  
1187 in the Eastern Mediterranean–Black Sea–Caspian–Corridor, *J. Biogeogr.*, 45(2), 484–499, doi:10.1111/jbi.13128, 2018.

1188 Marquer, L., Gaillard, M.-J., Sugita, S., Trondman, A.-K., Mazier, F., Nielsen, A. B., Fyfe, R., Odgaard, B. V., Alenius, T.,  
1189 Birks, H. J. B., Bjune, A. E., Christiansen, J., Dodson, J., Edwards, K. J., Giesecke, T., Herzsuh, U., Kangur, M., Lorenz,  
1190 S., Poska, A., Schult, M. and Seppä, H.: Holocene changes in vegetation composition in northern Europe: why quantitative  
1191 pollen-based vegetation reconstructions matter, *Quat. Sci. Rev.*, 90, 199–216, doi:10.1016/j.quascirev.2014.02.013, 2014.

1192 Marquer, L., Gaillard, M.-J., Sugita, S., Poska, A., Trondman, A.-K., Mazier, F., Nielsen, A. B., Fyfe, R., Jönsson, A. M.,  
1193 Smith, B., Kaplan, J. O., Alenius, T., Birks, H. J. B. J. B., Bjune, A. E., Christiansen, J., Dodson, J., Edwards, K. J., Giesecke,  
1194 T., Herzsuh, U., Kangur, M., Koff, T., Latałowa, M., Lechterbeck, J., Olofsson, J. and Seppä, H.: Quantifying the effects of  
1195 land use and climate on Holocene vegetation in Europe, *Quat. Sci. Rev.*, 171, 20–37, doi:10.1016/j.quascirev.2017.07.001,  
1196 2017.

1197 Marquer, L., Mazier, F., Sugita, S., Galop, D., Houet, T., Faure, E., Gaillard, M.-J., Haunold, S., de Munnik, N., Simonneau,  
1198 A., De Vleeschouwer, F. and Le Roux, G.: Pollen-based reconstruction of Holocene land-cover in mountain regions:  
1199 Evaluation of the Landscape Reconstruction Algorithm in the Vicdessos valley, northern Pyrenees, France, *Quat. Sci. Rev.*,  
1200 228, 106049, doi:10.1016/j.quascirev.2019.106049, 2020.

1201 Matthias, I., Nielsen, A. B. and Giesecke, T.: Evaluating the effect of flowering age and forest structure on pollen productivity  
1202 estimates, *Veg. Hist. Archaeobot.*, 21(6), 471–484, doi:10.1007/s00334-012-0373-z, 2012.

1203 Mazier, F., Broström, A., Gaillard, M.-J., Sugita, S., Vittoz, P. and Buttler, A.: Pollen productivity estimates and relevant  
1204 source area of pollen for selected plant taxa in a pasture woodland landscape of the Jura Mountains (Switzerland), *Veg. Hist.*  
1205 *Archaeobot.*, 17(5), 479–495, doi:10.1007/s00334-008-0143-0, 2008.

1206 Mazier, F., Gaillard, M. J., Kunes, P., Sugita, S., Trondman, A.-K. and Brostrom, A.: Testing the effect of site selection and  
1207 parameter setting on REVEALS-model estimates of plant abundance using th Czech Quaternary Palynological database  
1208 Testing the effect of site selection and parameter setting on REVEALS-model estimates of plant abunda, *Rev. Palaeobot.*  
1209 *Palynol.*, 187, 38–49 [online] Available from: <https://halshs.archives-ouvertes.fr/halshs-00959845>, 2012.

1210 Mazier, F., Broström, A., Bragée, P., Fredh, D., Stenberg, L., Thiere, G., Sugita, S. and Hammarlund, D.: Two hundred years  
1211 of land-use change in the South Swedish Uplands: comparison of historical map-based estimates with a pollen-based  
1212 reconstruction using the landscape reconstruction algorithm, *Veg. Hist. Archaeobot.*, 24(5), 555–570, doi:10.1007/s00334-  
1213 015-0516-0, 2015.

1214 McLauchlan, K. K., Williams, J. J., Craine, J. M. and Jeffers, E. S.: Changes in global nitrogen cycling during the Holocene  
1215 epoch, *Nature*, 495(7441), 352–355, doi:10.1038/nature11916, 2013.

1216 Mehl, I. K., Overland, A., Berge, J. and Hjelle, K. L.: Cultural landscape development on a west–east gradient in western  
1217 Norway – potential of the Landscape Reconstruction Algorithm (LRA), *J. Archaeol. Sci.*, 61, 1–16,  
1218 doi:10.1016/j.jas.2015.04.015, 2015.

1219 Morrison, K. D., Hammer, E., Boles, O., Madella, M., Whitehouse, N., Gaillard, M.-J., Bates, J., Vander Linden, M., Merlo,  
1220 S., Yao, A., Popova, L., Hill, A. C., Antolin, F., Bauer, A., Biagetti, S., Bishop, R. R., Buckland, P., Cruz, P., Dreslerová, D.,  
1221 Dusseldorp, G., Ellis, E., Filipovic, D., Foster, T., Hannaford, M. J., Harrison, S. P., Hazarika, M., Herold, H., Hilpert, J.,  
1222 Kaplan, J. O., Kay, A., Klein Goldewijk, K., Kolář, J., Kyazike, E., Laabs, J., Lancelotti, C., Lane, P., Lawrence, D., Lewis,  
1223 K., Lombardo, U., Lucarini, G., Arroyo-Kalin, M., Marchant, R., Mayle, F., McClatchie, M., McLeester, M., Mooney, S.,  
1224 Moskal-del Hoyo, M., Navarrete, V., Ndiema, E., Góes Neves, E., Nowak, M., Out, W. A., Petrie, C., Phelps, L. N., Pinke, Z.,  
1225 Rostain, S., Russell, T., Sluyter, A., Styring, A. K., Tamanaha, E., Thomas, E., Veerasamy, S., Welton, L. and Zanon, M.:  
1226 Mapping past human land use using archaeological data: A new classification for global land use synthesis and data  
1227 harmonization, edited by J. Freeman, *PLoS One*, 16(4), e0246662, doi:10.1371/journal.pone.0246662, 2021.

1228 Nielsen, A. B.: Modelling pollen sedimentation in Danish lakes at c.ad 1800: an attempt to validate the POLLSCAPE model,  
1229 *J. Biogeogr.*, 31(10), 1693–1709, doi:10.1111/j.1365-2699.2004.01080.x, 2004.

1230 Nielsen, A. B. and Odgaard, B. V.: Quantitative landscape dynamics in Denmark through the last three millennia based on the  
1231 Landscape Reconstruction Algorithm approach, *Veg. Hist. Archaeobot.*, 19(4), 375–387, doi:10.1007/s00334-010-0249-z,  
1232 2010.

1233 Nielsen, A. B., Giesecke, T., Theuerkauf, M., Feeser, I., Behre, K.-E., Beug, H.-J., Chen, S.-H., Christiansen, J., Dörfler, W.,  
1234 Endtmann, E., Jahns, S., de Klerk, P., Kühl, N., Latałowa, M., Odgaard, B. V., Rasmussen, P., Stockholm, J. R., Voigt, R.,  
1235 Wiethold, J. and Wolters, S.: Quantitative reconstructions of changes in regional openness in north-central Europe reveal new  
1236 insights into old questions, *Quat. Sci. Rev.*, 47, 131–149, doi:10.1016/j.quascirev.2012.05.011, 2012.

1237 Nosova, M. B., Novenko, E. Y., Severova, E. E. and Volkova, O. A.: Vegetation and climate changes within and around the  
1238 Polistovo-Lovatskaya mire system (Pskov Oblast, north-western Russia) during the past 10,500 years, *Veg. Hist. Archaeobot.*,  
1239 28(2), 123–140, doi:10.1007/s00334-018-0693-8, 2018.



1240 Palmisano, A., Woodbridge, J., Roberts, C. N., Bevan, A., Fyfe, R., Shennan, S., Cheddadi, R., Greenberg, R., Kaniewski, D.,  
1241 Langgut, D., Leroy, S. A. G., Litt, T. and Miebach, A.: Holocene landscape dynamics and long-term population trends in the  
1242 Levant, *The Holocene*, 29(5), 708–727, doi:10.1177/0959683619826642, 2019.

1243 Parsons, R. W. and Prentice, I. C.: Statistical approaches to R-values and the pollen—vegetation relationship, *Rev. Palaeobot.*  
1244 *Palynol.*, 32(2–3), 127–152, doi:10.1016/0034-6667(81)90001-4, 1981.

1245 Pinhasi, R., Fort, J. and Ammerman, A. J.: Tracing the origin and spread of agriculture in Europe, *PLoS Biol.*, 3(12), 1–9,  
1246 doi:10.1371/journal.pbio.0030410, 2005.

1247 Pirzamanbein, B., Lindström, J., Poska, A., Sugita, S., Trondman, A.-K., Fyfe, R., Mazier, F., Nielsen, A. B., Kaplan, J. O.,  
1248 Bjune, A. E., Birks, H. J. B., Giesecke, T., Kangur, M., Latałowa, M., Marquer, L., Smith, B. and Gaillard, M.-J.: Creating  
1249 spatially continuous maps of past land cover from point estimates: A new statistical approach applied to pollen data, *Ecol.*  
1250 *Complex.*, 20, 127–141, doi:10.1016/j.ecocom.2014.09.005, 2014.

1251 Pirzamanbein, B., Lindström, J., Poska, A. and Gaillard, M. J.: Modelling Spatial Compositional Data: Reconstructions of past  
1252 land cover and uncertainties, *Spat. Stat.*, 24, 14–31, doi:10.1016/j.spasta.2018.03.005, 2018.

1253 Pirzamanbein, B., Poska, A. and Lindström, J.: Bayesian Reconstruction of Past Land Cover From Pollen Data: Model  
1254 Robustness and Sensitivity to Auxiliary Variables, *Earth Sp. Sci.*, 7(1), doi:10.1029/2018EA000547, 2020.

1255 Poska, A., Meltsov, V., Sugita, S. and Vassiljev, J.: Relative pollen productivity estimates of major anemophilous taxa and  
1256 relevant source area of pollen in a cultural landscape of the hemi-boreal forest zone (Estonia), *Rev. Palaeobot. Palynol.*, 167(1–  
1257 2), 30–39, doi:10.1016/j.revpalbo.2011.07.001, 2011.

1258 Prentice, C.: Records of vegetation in time and space: the principles of pollen analysis, in *Vegetation history*, pp. 17–42,  
1259 Springer Netherlands, Dordrecht., 1988.

1260 Prentice, C., Guiot, J., Huntley, B., Jolly, D. and Cheddadi, R.: Reconstructing biomes from palaeoecological data: a general  
1261 method and its application to European pollen data at 0 and 6 ka, *Clim. Dyn.*, 12(3), 185–194, doi:10.1007/BF00211617, 1996.

1262 Prentice, I. C.: Pollen Representation, Source Area, and Basin Size: Toward a Unified Theory of Pollen Analysis, *Quat. Res.*,  
1263 23(1), 76–86, doi:10.1016/0033-5894(85)90073-0, 1985.

1264 Prentice, I. C. and Parsons, R. W. A.: Maximum Likelihood Linear Calibration of Pollen Spectra in Terms of Forest  
1265 Composition, *Biometrics*, 39(4), 1051–1057, doi:10.2307/2531338, 1983.

1266 Prentice, I. C. and Webb III, T.: BIOME 6000: reconstructing global mid-Holocene vegetation patterns from palaeoecological  
1267 records, *J. Biogeogr.*, 25(6), 997–1005, doi:10.1046/j.1365-2699.1998.00235.x, 1998.

1268 Räsänen, S., Suutari, H. and Nielsen, A. B.: A step further towards quantitative reconstruction of past vegetation in  
1269 Fennoscandian boreal forests: Pollen productivity estimates for six dominant taxa, *Rev. Palaeobot. Palynol.*, 146(1–4), 208–  
1270 220, doi:10.1016/j.revpalbo.2007.04.004, 2007.

1271 Roberts, C. N., Woodbridge, J., Palmisano, A., Bevan, A., Fyfe, R. and Shennan, S.: Mediterranean landscape change during  
1272 the Holocene: Synthesis, comparison and regional trends in population, land cover and climate, *The Holocene*, 29(5), 923–  
1273 937, doi:10.1177/0959683619826697, 2019.

1274 Roberts, N., Fyfe, R. M., Woodbridge, J., Gaillard, M.-J., Davis, B. A. S. S., Kaplan, J. O., Marquer, L., Mazier, F., Nielsen,  
1275 A. B., Sugita, S., Trondman, A.-K. and Leydet, M.: Europe's lost forests: a pollen-based synthesis for the last 11,000 years,  
1276 *Sci. Rep.*, 8(1), 716, doi:10.1038/s41598-017-18646-7, 2018.

1277 Ruddiman, W. F.: The Anthropogenic Greenhouse Era Began Thousands of Years Ago, *Clim. Change*, 61(3), 261–293,  
1278 doi:10.1023/B:CLIM.0000004577.17928.fa, 2003.

1279 Ruddiman, W. F., Fuller, D. Q., Kutzbach, J. E., Tzedakis, P. C., Kaplan, J. O., Ellis, E. C., Vavrus, S. J., Roberts, C. N., Fyfe,  
1280 R., He, F., Lemmen, C. and Woodbridge, J.: Late Holocene climate: Natural or anthropogenic?, *Rev. Geophys.*, 54(1), 93–  
1281 118, doi:10.1002/2015RG000503, 2016.

1282 Schauer, P., Shennan, S., Bevan, A., Cook, G., Edinborough, K., Fyfe, R., Kerig, T. and Parker Pearson, M.: Supply and  
1283 demand in prehistory? Economics of Neolithic mining in northwest Europe, *J. Anthropol. Archaeol.*, 54, 149–160,  
1284 doi:10.1016/j.jaa.2019.03.001, 2019.

1285 Shennan, S.: *The First Farmers of Europe An Evolutionary Perspective*, Cambridge University Press, Cambridge. [online]  
1286 Available from: [https://www-cambridge-org.proxy.lnu.se/se/academic/subjects/archaeology/archaeology-europe-and-near-](https://www-cambridge-org.proxy.lnu.se/se/academic/subjects/archaeology/archaeology-europe-and-near-and-middle-east/first-farmers-europe-evolutionary-perspective?format=HB&isbn=9781108422925)  
1287 [and-middle-east/first-farmers-europe-evolutionary-perspective?format=HB&isbn=9781108422925](https://www-cambridge-org.proxy.lnu.se/se/academic/subjects/archaeology/archaeology-europe-and-near-and-middle-east/first-farmers-europe-evolutionary-perspective?format=HB&isbn=9781108422925), 2018.

1288 Smith, P., Davis, S. J., Creutzig, F., Fuss, S., Minx, J., Gabrielle, B., Kato, E., Jackson, R. B., Cowie, A., Kriegler, E., van  
1289 Vuuren, D. P., Rogelj, J., Ciais, P., Milne, J., Canadell, J. G., McCollum, D., Peters, G., Andrew, R., Krey, V., Shrestha, G.,  
1290 Friedlingstein, P., Gasser, T., Grübler, A., Heidug, W. K., Jonas, M., Jones, C. D., Kraxner, F., Littleton, E., Lowe, J., Moreira,  
1291 J. R., Nakicenovic, N., Obersteiner, M., Patwardhan, A., Rogner, M., Rubin, E., Sharifi, A., Torvanger, A., Yamagata, Y.,  
1292 Edmonds, J. and Yongsung, C.: Biophysical and economic limits to negative CO<sub>2</sub> emissions, *Nat. Clim. Chang.*, 6(1), 42–50,  
1293 doi:10.1038/nclimate2870, 2016.

1294 Soepboer, W., Sugita, S., Lotter, A. F., van Leeuwen, J. F. N. and van der Knaap, W. O.: Pollen productivity estimates for  
1295 quantitative reconstruction of vegetation cover on the Swiss Plateau, *The Holocene*, 17(1), 65–77,  
1296 doi:10.1177/0959683607073279, 2007.

1297 Soepboer, W., Sugita, S. and Lotter, A. F.: Regional vegetation-cover changes on the Swiss Plateau during the past two  
1298 millennia: A pollen-based reconstruction using the REVEALS model, *Quat. Sci. Rev.*, 29(3–4), 472–483,  
1299 doi:10.1016/j.quascirev.2009.09.027, 2010.

1300 von Stedingk, H., Fyfe, R. M. and Allard, A.: Pollen productivity estimates from the forest—tundra ecotone in west-central  
1301 Sweden: implications for vegetation reconstruction at the limits of the boreal forest, *The Holocene*, 18(2), 323–332,  
1302 doi:10.1177/0959683607086769, 2008.

1303 Stephens, L., Fuller, D., Boivin, N., Rick, T., Gauthier, N., Kay, A., Marwick, B., Armstrong, C. G., Barton, C. M., Denham,  
1304 T., Douglass, K., Driver, J., Janz, L., Roberts, P., Rogers, J. D., Thakar, H., Altaweel, M., Johnson, A. L., Sampietro Vattuone,  
1305 M. M., Aldenderfer, M., Archila, S., Artioli, G., Bale, M. T., Beach, T., Borrell, F., Braje, T., Buckland, P. I., Jiménez Cano,  
1306 N. G., Capriles, J. M., Diez Castillo, A., Çilingiroğlu, Ç., Negus Cleary, M., Conolly, J., Coutros, P. R., Covey, R. A.,  
1307 Cremaschi, M., Crowther, A., Der, L., di Lernia, S., Doershuk, J. F., Doolittle, W. E., Edwards, K. J., Erlandson, J. M., Evans,

1308 D., Fairbairn, A., Faulkner, P., Feinman, G., Fernandes, R., Fitzpatrick, S. M., Fyfe, R., Garcea, E., Goldstein, S., Goodman,  
1309 R. C., Dalpoim Guedes, J., Herrmann, J., Hiscock, P., Hommel, P., Horsburgh, K. A., Hritz, C., Ives, J. W., Junno, A., Kahn,  
1310 J. G., Kaufman, B., Kearns, C., Kidder, T. R., Lanoë, F., Lawrence, D., Lee, G.-A., Levin, M. J., Lindsoug, H. B., López-  
1311 Sáez, J. A., Macrae, S., Marchant, R., Marston, J. M., McClure, S., McCoy, M. D., Miller, A. V., Morrison, M., Motuzaite  
1312 Matuzeviciute, G., Müller, J., Nayak, A., Noerwidi, S., Peres, T. M., Peterson, C. E., Proctor, L., Randall, A. R., Renette, S.,  
1313 Robbins Schug, G., Ryzewski, K., Saini, R., Scheinsohn, V., Schmidt, P., Sebillaud, P., Seitsonen, O., Simpson, I. A.,  
1314 Sołtysiak, A., Speakman, R. J., Spengler, R. N., Steffen, M. L., et al.: Archaeological assessment reveals Earth's early  
1315 transformation through land use, *Science* (80-. ), 365(6456), 897–902, doi:10.1126/science.aax1192, 2019.

1316 Strandberg, G., Kjellström, E., Poska, A., Wagner, S., Gaillard, M.-J., Trondman, A.-K., Mauri, A., Davis, B. A. S. S., Kaplan,  
1317 J. O., Birks, H. J. B. B., Bjune, A. E., Fyfe, R., Giesecke, T., Kalnina, L., Kangur, M., van der Knaap, W. O., Kokfelt, U.,  
1318 Kuneš, P., Latašová, M., Marquer, L., Mazier, F., Nielsen, A. B., Smith, B., Seppä, H. and Sugita, S.: Regional climate  
1319 model simulations for Europe at 6 and 0.2 k BP: sensitivity to changes in anthropogenic deforestation, *Clim. Past*, 10(2), 661–  
1320 680, doi:10.5194/cp-10-661-2014, 2014.

1321 Stuart, A. and Ord, J. K.: *Kendall's advanced theory of statistics*, *Distrib. theory*, 1 [online] Available from:  
1322 <https://ci.nii.ac.jp/naid/10004597057> (Accessed 2 July 2021), 1994.

1323 Sugita, S.: A Model of Pollen Source Area for an Entire Lake Surface, *Quat. Res.*, 39(2), 239–244,  
1324 doi:10.1006/qres.1993.1027, 1993.

1325 Sugita, S.: Theory of quantitative reconstruction of vegetation I: pollen from large sites REVEALS regional vegetation  
1326 composition, *The Holocene*, 17(2), 229–241, doi:10.1177/0959683607075837, 2007a.

1327 Sugita, S.: Theory of quantitative reconstruction of vegetation II: all you need is LOVE, *The Holocene*, 17(2), 243–257,  
1328 doi:10.1177/0959683607075838, 2007b.

1329 Sugita, S., Gaillard, M.-J. and Broström, A.: Landscape openness and pollen records: a simulation approach, *The Holocene*,  
1330 9(4), 409–421, doi:10.1191/095968399666429937, 1999.

1331 Sugita, S., Parshall, T., Calcote, R. and Walker, K.: Testing the Landscape Reconstruction Algorithm for spatially explicit  
1332 reconstruction of vegetation in northern Michigan and Wisconsin, *Quat. Res.*, 74(2), 289–300,  
1333 doi:10.1016/j.yqres.2010.07.008, 2010.

1334 Sun, A., Luo, Y., Wu, H., Chen, X., Li, Q., Yu, Y., Sun, X. and Guo, Z.: An updated biomization scheme and vegetation  
1335 reconstruction based on a synthesis of modern and mid-Holocene pollen data in China, *Glob. Planet. Change*, 192(May 2019),  
1336 103178, doi:10.1016/j.gloplacha.2020.103178, 2020.

1337 Sutton, O. .: *Micrometeorology*, *Q. J. R. Meteorol. Soc.*, 79(341), 457–457, doi:10.1002/qj.49707934125, 1953.

1338 Theuerkauf, M., Kuparinen, A. and Joosten, H.: Pollen productivity estimates strongly depend on assumed pollen dispersal,  
1339 *The Holocene*, 23(1), 14–24, doi:10.1177/0959683612450194, 2012.

1340 Theuerkauf, M., Couwenberg, J., Kuparinen, A. and Liebscher, V.: A matter of dispersal: REVEALSinR introduces state-of-  
1341 the-art dispersal models to quantitative vegetation reconstruction, *Veg. Hist. Archaeobot.*, 25(6), doi:10.1007/s00334-016-

1342 0572-0, 2016.

1343 Trondman, A.-K., Gaillard, M.-J., Sugita, S., Björkman, L., Greisman, A., Hultberg, T., Lagerås, P., Lindbladh, M. and Mazier,  
1344 F.: Are pollen records from small sites appropriate for REVEALS model-based quantitative reconstructions of past regional  
1345 vegetation? An empirical test in southern Sweden, *Veg. Hist. Archaeobot.*, 25(2), 131–151, doi:10.1007/s00334-015-0536-9,  
1346 2016.

1347 Trondman, A. K., Gaillard, M. J., Mazier, F., Sugita, S., Fyfe, R., Nielsen, A. B., Twiddle, C., Barratt, P., Birks, H. J. B.,  
1348 Bjune, A. E., Björkman, L., Broström, A., Caseldine, C., David, R., Dodson, J., Dörfler, W., Fischer, E., van Geel, B., Giesecke,  
1349 T., Hultberg, T., Kalnina, L., Kangur, M., van der Knaap, P., Koff, T., Kuneš, P., Lagerås, P., Latalowa, M., Lechterbeck, J.,  
1350 Leroyer, C., Leydet, M., Lindbladh, M., Marquer, L., Mitchell, F. J. G., Odgaard, B. V., Peglar, S. M., Persson, T., Poska, A.,  
1351 Rösch, M., Seppä, H., Veski, S. and Wick, L.: Pollen-based quantitative reconstructions of Holocene regional vegetation cover  
1352 (plant-functional types and land-cover types) in Europe suitable for climate modelling, *Glob. Chang. Biol.*, 21(2), 676–697,  
1353 doi:10.1111/gcb.12737, 2015.

1354 Twiddle, C. L., Jones, R. T., Caseldine, C. J. and Sugita, S.: Pollen productivity estimates for a pine woodland in eastern  
1355 Scotland: The influence of sampling design and vegetation patterning, *Rev. Palaeobot. Palynol.*, 174, 67–78,  
1356 doi:10.1016/j.revpalbo.2011.12.006, 2012.

1357 de Vareilles, A., Pelling, R., Woodbridge, J. and Fyfe, R.: Archaeology and agriculture: plants, people, and past land-use,  
1358 *Trends Ecol. Evol.*, 36(10), 943–954, doi:10.1016/j.tree.2021.06.003, 2021.

1359 Wiczorek, M. and Herzschuh, U.: Compilation of relative pollen productivity (RPP) estimates and taxonomically harmonised  
1360 RPP datasets for single continents and Northern Hemisphere extratropics, *Earth Syst. Sci. Data*, 12(4), 3515–3528,  
1361 doi:10.5194/essd-12-3515-2020, 2020.

1362 Wolf, A., Callaghan, T. V. and Larson, K.: Future changes in vegetation and ecosystem function of the Barents Region, *Clim.*  
1363 *Change*, 87(1–2), 51–73, doi:10.1007/s10584-007-9342-4, 2008.

1364 Woodbridge, J., Fyfe, R. M. and Roberts, N.: A comparison of remotely sensed and pollen-based approaches to mapping  
1365 Europe’s land cover, edited by M. Bush, *J. Biogeogr.*, 41(11), 2080–2092, doi:10.1111/jbi.12353, 2014.

1366 Woodbridge, J., Fyfe, R., Roberts, C., Trondman, A., Mazier, F. and Davis, B.: European forest cover since the start of  
1367 Neolithic agriculture: a critical comparison of pollen-based reconstructions, *Past Glob. Chang. Mag.*, 26(1), 10–11,  
1368 doi:10.22498/pages.26.1.10, 2018.

1369 Zanon, M., Davis, B. A. S. S., Marquer, L., Brewer, S. and Kaplan, J. O.: European Forest Cover During the Past 12,000  
1370 Years: A Palynological Reconstruction Based on Modern Analogs and Remote Sensing, *Front. Plant Sci.*, 9(March), 1–25,  
1371 doi:10.3389/fpls.2018.00253, 2018.

1372